NOTE: Half of Appendix A and all of Appendices B through E are missing

GEOLOGIC INVESTIGATION OF THE APACHE ORO MINING CLAIMS, LOST BASIN RANGE, MOHAVE COUNTY, ARIZONA

by

Alfred J. Deaderick

Submitted in Partial Fulfillment
Of the Requirements for the Degree of
Master of Science in Geology

New Mexico Institute of Mining and Technology

Socorro, New Mexico

May, 1980

ABSTRACT

The Apache Oro mining claims are in the central and southern portions of the Lost Basin Range in northwestern Arizona. This investigation studied the mineralization potential and association between gold-bearing quartz-carbonate-sulfide veins and adjacent placer gold deposits of Tertiary age; alteration zoning has led some investigators to postulate a porphyry copper deposit at depth in the central part of the claims.

Within the mapped area four Precambrian metamorphic rock units crop out along the axis of the range. Deformed Tertiary volcanic sediments are faulted against the southeastern flank and late Tertiary Muddy Creek fm. fills structural basins adjacent to the range. The Precambrian complex has undergone three recognizable periods of deformation: The "Mazatzal Revolution" (Wilson, 1939) of folding and regional metamorphism; the Nevadian orogeny of faulting and shearing resulting in major N.-trending fault structures; and late Cenozoic Basin and Range block faulting which developed the present physiographic features of the range and adjacent areas. The volcanic sediments were strongly deformed during the last period of deformation while the Muddy Creek fm. is only slightly tilted and faulted.

Late Cretaceous (?) vein mineralization in the metamorphic complex follows major N.-trending fault fissures developing occasional irregular ore shoots. Brecciation along the veins is attributed to late Cenozoic faulting along previous zones of weakness. The placer gold deposits are found in the Muddy Creek fanglomerate and represent paleo-placers rather than modern stream deposits. Evidence suggests the source area for the placer gold is west-southwest of the Lost Basin Range and not in the

adjacent mineralized veins. Rock types, mineralization, and alteration in the Precambrian complex does not substantiate a potential porphyry copper deposit at depth in the study area.

Hydrothermal alteration is restricted to the immediate vicinity of mineralized veins and consists of phyllic $\pm$ argillic and/or weak propylitic assemblages. A zone of retrograde metamorphism follows a major fault structure containing the principal mineralization and has modified the observable hydrothermal alteration. Field evidence does not suggest a through-going major vein system; instead sporadic, weak mineralization with localized ore shoots is present. Supergene enrichment of the vein gold within the oxidized-brecciated vein structures could have economic potential. The best mining potential of the placer gold is along Quaternary arroyos as a result of reworking and concentration of gold due to recent erosion of both the paleo-placer and the adjacent vein mineralization.

ACKNOWLEDGMENTS

The author would like to express his sincere appreciation to Dr. Clay T. Smith for serving as academic advisor, and for his unlimited support and recommendations during the preparation of this research report. Special thanks go to Dr. Kent Condie for his suggestions, advice and assistance on the Precambrian complex.

Resources International Corporation provided financial support and geochemical data, as well as geochemical analyses of samples collected for this report which are gratefully acknowledged.

Particular gratitude is due Warren Mallory, whose information and maps were essential to the project. Mr. John C. Antweiler of the U. S. Geological Survey generously shared photos, maps and data; Max Troyer visited the claims and gave field assistance and information.

Appreciation is expressed to the U. S. National Park Service for permission to work and collect samples within the Lake Mead National Recreation Area; to Marx Brook for the use of a camper trailer; also to Evert Putnam for access onto his mining claims.

The author wishes to acknowledge the assistance of Lynn Brandvold of the New Mexico Bureau of Mines for her advice and use of the geochemical labs. Also, appreciation is extended to the faculty at New Mexico Tech. for their many helpful suggestions and use of laboratory facilities.

Special thanks are extended to the author's wife, Katie, for her assistance in the completion of this report, and to Dan Simpson for assisting me in the field.

TABLE OF CONTENTS

TABLE OF CONTENTS (Cont.)

TABLE OF CONTENTS (Cont.)

TABLE OF CONTENTS (Cont.)

LIST OF FIGURES

LIST OF FIGURES (cont.)

LIST OF FIGURES (cont.)

LIST OF TABLES

LIST OF PLATES

INTRODUCTION

PURPOSE OF STUDY

The Lost Basin mining district is situated along a north trending mountain range of altered and mineralized rock in part concealed by an onlap of alluvial gravels. Mining in the area was predominantly oriented towards the placer deposits; however, small scale mining operations are evident on lode claims throughout the region. Earlier studies conducted by Apache Oro Company emphasized the Lost Basin property's potential as a minable placer deposit and a porphyry copper prospect. Based on a lease with Apache Oro Company, Resources International Corp. has continued with the evaluation of the district. The purpose of this investigation was to determine if the geology, structure, and vein mineralization of the area indicate a possible porphyry copper deposit at depth and if the vein mineralization could represent a source for the placer minerals. The association of vein and placer deposits with a porphyry copper deposit on this property could have strong enconomic potential.

METHOD OF STUDY

The Lost Basin mining district covers an area of approximately 20 square miles. Within this area, a rectangular block of altered and mineralized rock comprising about $4\frac{1}{2}$ square miles was mapped on a scale of 1:6000 between June 1977 and January 1979. The geology and structure of the area were delineated; geochemical and petrologic techniques aided in determining lithologies, zones of alteration, degrees of metamorphism and extent of mineralization.

One hundred twenty petrographic thin sections were prepared; they were examined and described using a Zeiss petrographic microscope. Twenty-six samples of mineralized rock were analyzed for elements of economic importance. Analyses were run on a Perkin-Elmer model 403 atomic absorption spectrophotometer, operated by Resources International Corp. In addition, Resources International Corp. provided geochemical assays on samples from 54 shallow drill holes within the mapped area. This information was compiled into a Fortran program at the New Mexico Institute of Mining and Technology computer facility to study statistical parameters as well as estimating feasibility of outlining ore horizons if present.

Finally, 5 samples of heavy mineral concentrates were studied to establish a provenance for the placer deposits. Elemental identifications were done by emission spectrographic analysis; mineral percentages were estimated by grain population counts using a Zeiss petrographic microscope mounted with a mechanical stage.

LOCATION AND ACCESSIBILITY

The Lost Basin mining district is located in the northern portion of Mohave County in northwest Arizona. The property is just east of the White Hills, 5 to 8 miles west of the Grand Wash Cliffs and about 7 miles south of the eastern portion of Lake Mead. The district is contained within Townships 29 and 30 North, and Ranges 17 and 18 West. The mapped area is limited to sections 4, 5, 8, 9, 16, 17, 20 and 21 of T.29N., R.17W.; sections 5 and 8 are within the Lake Mead National Recreation Area.

The property can be reached from Kingman, Arizona by driving about 40 miles north on U.S. Highway 93 and turning right at the Dolan Springs-Pierce Ferry junction, halfway between Kingman and Boulder City, Nevada. Following the paved road 31 miles northeast, drive through Dolan Springs, heading towards the Pierce Ferry anchorage. The Apache Oro claims are 2 miles west of the paved road between Lake Mead City and Meadview Village. Access to the mapped area is by a number of unimproved dirt trails following drainages from the eastern slopes of the Lost Basin Range into Grapevine Wash (Figure 1).

HISTORY OF THE LOST BASIN DISTRICT

In a preliminary report on the mineral deposits of Mohave County, Arizona, Schrader (1909) stated that the initial discovery of the Lost Basin district could have been as early as 1886. He mentioned that the interest in the area was focused on two sets of quartz veins containing gold and copper. However, he noted that nothing more than surface prospecting was ever done due to the remoteness of the area and lack of readily available water. The earliest mention of any placer deposits for this district was made by Wilson (1933) in a report on Arizona gold placers. In his report, Wilson gave short descriptions of the King Tut placers, on the east flank and the Gold Basin placers on the southwest flank of the Lost Basin Range. He considered 1931 as the earliest known discovery date for the King Tut deposits and 1932 for the Gold Basin deposits.

Between 1933 and 1960, there has been no other mention of any further mining developments or detailed investigations for this area. In 1960, Warren M. Mallory (president of Apache Oro Co.) was directed to this area to evaluate it as an "outstanding" gold mining prospect. After initial investigations, Mr. Mallory purchased $3\frac{1}{4}$ sections of mining claims for further evaluation. From 1961 to 1968, Apache Oro Co. continued their acquisition of available mining claims and by 1969, they had filed 92 unpatented placer claims and 174 unpatented lode claims in the Lost Basin mining district (Mallory, 1974a, and oral commun., 1979).

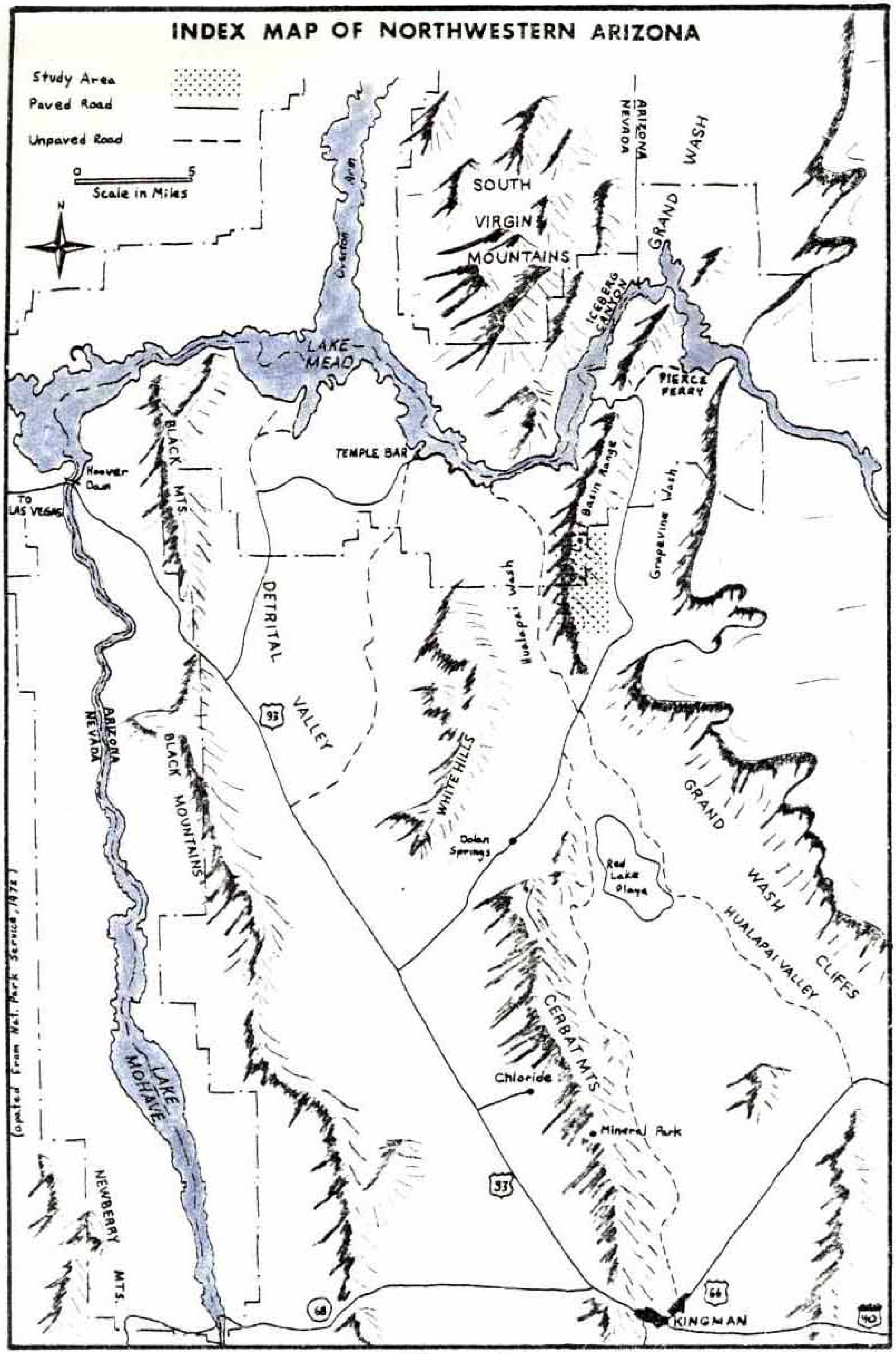
INDEX MAP OF NORTHWESTERN ARIZONA
Study Area
Paved Road
Unpaved Road
0
5
Scale in Miles
N
Overton Arm
LAKE MEAD
SOUTH VIRGIN MOUNTAINS
ARIZONA
NEVADA
GRAND WASH
ICEBERG CANYON
PIERCE FERRY
TEMPLE BAR
Hoover Dam
TO LAS VEGAS
BLACK MTS.
Lost Basin Range
Grapevine Wash
Hualapai Wash
DETRITAL VALLEY
93
BLACK MOUNTAINS
WHITE HILLS
Dolan Springs
Red Lake Playa
GRAND WASH CLIFFS
HUALAPAI VALLEY
CERBAT MTS
Chloride
Mineral Park
LAKE MOHAVE
NEWBERRY MTS.
68
66
40
KINGMAN
(adapted from Nat. Park Service, 1972)

Figure I.

The most recent development occurred in May 1976 when Resources International Corp. leased the mineral rights from the Apache Oro Co. to continue in the exploration and development of these claims. Their participation in the area includes: a drilling program of shallow test holes to evaluate mineralization, an experimental cyanide heap-leaching facility to extract the placer gold, and feasibility studies of the placer deposits utilizing conventional mechanical placering techniques.

PREVIOUS WORK IN THE LOST BASIN RANGE

The earliest geologic work pertaining to the Lost Basin mining district was by Schrader (1909) in his report on the mineral deposits of Mohave County, Arizona. He gave a brief description of the Precambrian complex and discussed the field relationships of the mineralized veins. He noted two distinct sets of structurally controlled veins characterized by the mineral zonation of gold and copper.

Wilson (1933) provided the earliest description and summary of the gold placer deposits in this district. He reported that the loose alluvial fill confined to arroyo-bottoms contained rich gold-bearing gravels and pointed out that the underlying caliche-cemented gravels were also gold-bearing but were not tested.

Stratigraphic correlation of the pediment gravels bounding Grapevine Wash on the west was included in a Ph.D. thesis submitted by Lucchitta (1966) to Pennsylvania State University. He described the Cenozoic stratigraphy between the Lost Basin Range and the Grand Wash Cliffs, and correlated the sedimentary facies over the entire region. Lucchitta (1966) summarized the Cenozoic geologic history for the immediate area. The development of the present physiographic boundary between the Basin-Range and the Colorado Plateau provinces in northwest Arizona and southern

Nevada is closely related to the Cenozoic history.

The initial evaluation of the Lost Basin property by Mallory (1972, 1974a) included geochemical sampling and plotting the distribution of mineralized veins throughout the Lost Basin district. An aeromagnetic and radiometric survey was flown by Heinrichs Geoexploration Co. (1967) and was supplemented by 7 preliminary induced polarization profiles. The results of the geophysical surveys indicated a broad magnetic low in the vicinity of possible porphyry copper mineralization (Mallory, 1971a, 1971b). Apache Oro Co. concluded that the results of the geochemical and geophysical surveys provided sufficient evidence to warrant further investigations (Mallory, 1974b).

Based on field observations and geochemical analyses, Post (1970) summarized Mallory's observations and reported the presence of anomalous values of certain elements commonly associated with porphyry copper deposits. In his synopsis of the Lost Basin prospect, Post mentioned several factors supportive of the property's potential for such a deposit.

Trites (1974) reported on the mineralization in the Ford mine and the immediate vicinity of section 33, T.30N., R.17W., less than one mile to the northwest of this study area. He concluded the remaining potential of commercial grade mineralization in the mine was minimal but encouraged further exploration for wider fault zones with greater lateral extent.

An investigation overlapping the northern boundary of this study area was done by Krish (1974) as a master's thesis at the Colorado School of Mines. The study compared two producing copper deposits with the Lost Basin property and another prospect. He utilized trace element distributions to establish levels of surface erosion based on the porphyry copper model described by Lowell and Guilbert (1970). Krish concluded that his results implied a porphyry Cu target at depth, but it's location would be to one side of the model that he developed.

Regional mapping of the Lost Basin Range was conducted by Blacet (1975) during an investigation for the U. S. Geological Survey of the 15 minute Garnet Mountain quadrangle, Mohave County, Arizona (Figure 2). An earlier report from the Heavy Metals program of the U. S. Geological Survey (1968) gave a brief description of the placer gold deposits of Gold Basin and Lost Basin. Blacet (1969) briefly summarized his evaluation of the placer deposits and recognized two types of lode deposits: one as gold-bearing quartz-carbonate-sulfide veins and the second as gold-bearing medium-grained porphyritic leucosyenite pipes.

Preliminary spectrochemical analyses of placer and lode golds from Lost Basin were completed by Antweiler and Sutton (1970) for a progress report on gold compositions. They were developing analytical techniques to evaluate the amount of silver and trace elements within gold as identification signatures of gold sources. Recent investigations by Antweiler and Campbell (1979) have discriminated between placer and lode gold in the Lost Basin gold samples.

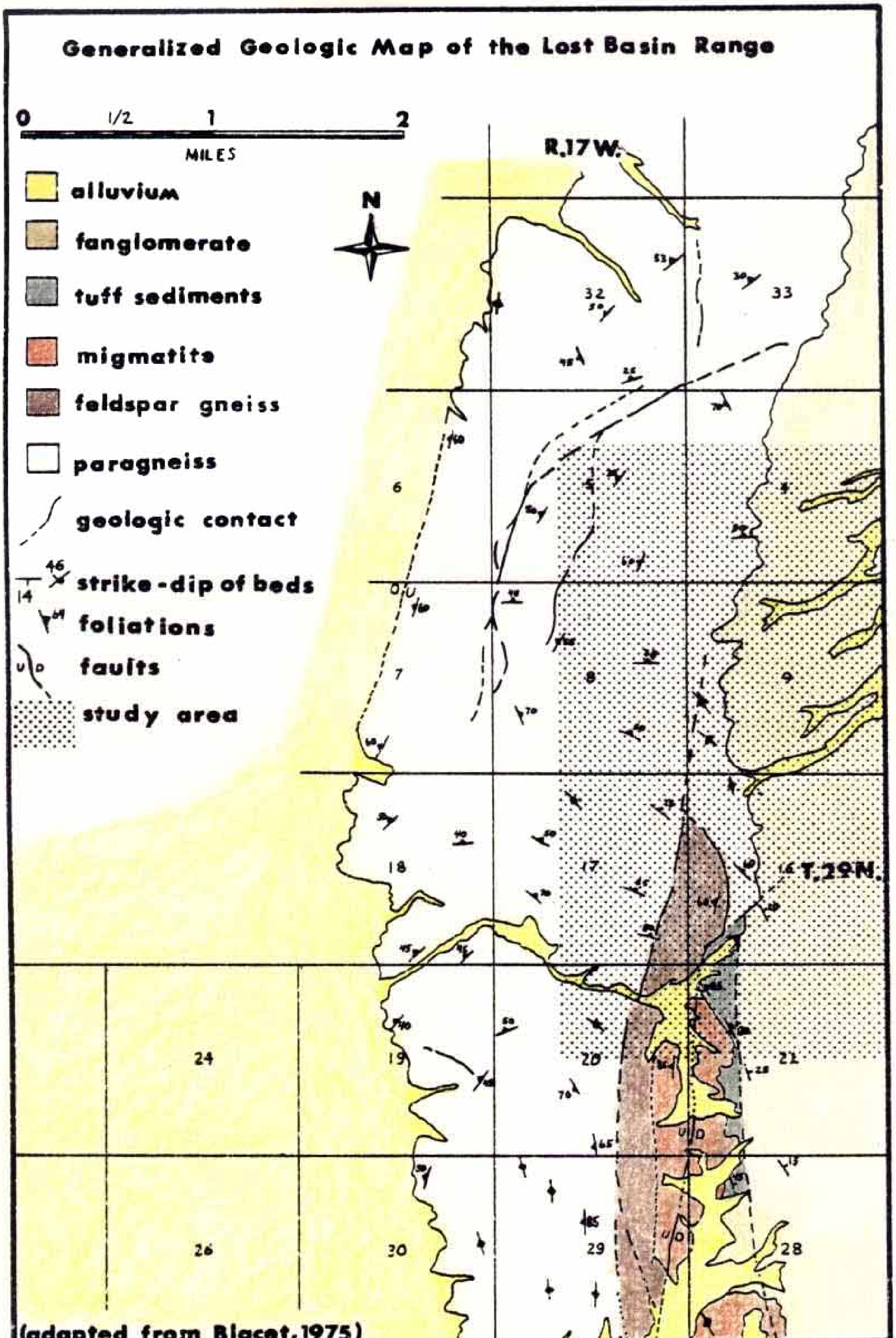
Generalized Geologic Map of the Lost Basin Range
0 1/2 1 2
MILES
alluvium
fanglomerate
tuff sediments
migmatite
feldspar gneiss
paragneiss
geologic contact
strike-dip of beds
foliations
faults
study area
N
R.17W.
T.29N.
32
33
6
7
8
9
17
18
19
20
21
24
26
28
29
30
(adapted from Blacet, 1975)

Figure 2.

GEOGRAPHY OF THE AREA

CLIMATE AND VEGETATION

The climate and vegetation of the Lost Basin mining district are characteristic of the Mohave Desert. The "desert shrub community" is the most predominant vegetation of the valley floors and along gravel slopes up to about 6,000 feet elevation. The most abundant plants include Joshua tree, Mohave yucca, creosote bush and a large variety of cacti. A "transzonal community" occupies major drainages where moisture is contained beneath the gravel wash bottoms. Honey mesquite, saltbush and desert willow are typical of this community (Nat. Park Service, 1972).

Weather during the summer months is generally hot and dry with daylight temperatures ranging from 70°F. to above 110°F. on occasions. Infrequent summer cloudbursts contribute marginal precipitation during these months. Winter months are typically cool and mild during the day but cold at night, seldom below 32°F. for any prolonged period. Precipitation for the area is usually between 5" to 7" annually, with the majority of it as rain and sporadic sleet storms during the winter months.

PHYSIOGRAPHY AND TOPOGRAPHY

The north trending Lost Basin Range is located along the northeastern boundary of the Basin and Range physiographic province in Arizona. To the east, the southwestern portion of the Colorado Plateau terminates abruptly along the Grand Wash Cliffs which are a west-facing, north-trending scarp about 110 miles long. In between the Lost Basin Range and the cliffs is the "Grand Wash Trough" which includes the Grapevine drainage. The trough is an elongate depression of regional extent, several thousand feet lower than the scarp and contains a thick sequence of Cenozoic sediments (Lucchitta, 1966).

Due west of the Lost Basin Range are the White Hills separated by the Hualapai drainage and on the south are the Cerbat Mountains. To the north, in Nevada, are the South Virgin Mountains isolated by Lake Mead and the Colorado River which flows westward across topographic structures of the region.

The topography of the area ranges between 2,000 feet above sea level along Hualapai Wash to about 5,000 feet along the Grand Wash Cliffs. Within the Lost Basin Range, the highest point is Pai Peak at 4,685 feet elevation just south of this study area. The lowest elevation is along the 2,800 foot topographic contour representing the approximate contact between the western fault scarp of the range and the downdropped Hualapai basin.

The Lost Basin Range is a rugged, strongly dissected chain of ridges and peaks about 20 miles in length and 4 miles wide. The eastern limb of the range has 250 feet of moderate relief consisting of rolling hills and ridges with a pronounced pediment surface sloping east away from the mountain crest. The pediment surface is called Grapevine Mesa and partially conceals the range's eastern flank. The western limb has 1,400 feet of relief in steep mountainous terrain.

The drainages in the Lost Basin Range are fed by ephemeral streams that flow into Grapevine and Hualapai Washes. The eastern braided drainages cut the pediment surface while the western drainages, at lower elevations, have a dendritic pattern strongly incised in the mountain core. Headward erosion by some of the western drainages have breached the drainage divide locally and will eventually capture the eastern drainages.

Informal names of physiographic places within this study area have been used and the reader is referred to Plate II to become acquainted with the location for these local names. Also note that previous use in the literature of the name "Infernal Mountains" was in reference to the Lost Basin Range.

GENERAL GEOLOGY OF MAPPED AREA

STRATIGRAPHY

General

Descriptions of the Precambrian rocks in the region were published by Longwell (1936, 1963), Schrader (1908, 1909, 1917) and Thomas (1949, 1953). Summaries by Post (1970), Krish (1974) and Blacet (1975) of the Precambrian suite of the Lost Basin Range resemble many of the rock types described by Dings (1950, 1951) and Eidel, Frost, and Clippinger (1968) from the Cerbat Mountain complex.

Cambrian-Permian sedimentary rocks comprise the Grand Wash Cliffs and Shivwits Plateau to the east. Outcrops at the extreme northeastern end of the Lost Basin Range contain sedimentary rocks of early to middle Paleozoic age, yet south of a line extending eastward from the mouth of Hualapai Wash across the Lost Basin Range to the base of the Grand Wash Cliffs Paleozoic-Mesozoic sediments are missing. Few examples of this rock sequence crop out anywhere to the south and west in Mohave County (Lucchitta, 1966).

Cenozoic rocks of late Tertiary-Quaternary age are widely distributed throughout the area and they overlie the Precambrian rocks with marked unconformity. Lucchitta (1966) notes that some of the older Cenozoic rocks are preserved only as scattered remnants. The mappable units used in this report consist of four members of a Precambrian complex and three Cenozoic sedimentary units (see Plate I). Precambrian units 1, 2 and 3 represent distinct lithologic divisions of Blacet's (1975) regional paragneiss unit and Precambrian unit 4 corresponds to his migmatite unit. The Cenozoic units are the same as those recognized by Blacet (1975) except the legend symbols for the Tertiary units were changed to agree more closely with the lithologies described.

Precambrian Units

Migmatitic Gneiss ($p\mathrm{C}_1$) - The migmatitic gneiss unit is an undifferentiated assemblage of thin-bedded amphibolite facies metasediments which is correlated with Krish's $p\mathrm{C}_1$ unit (1974). Distribution of the unit is limited to the northern portion of the mapped area; it crops out in parts of sections 4, 5, 8 and 9 of T.29N., R.17W. This unit is the oldest member of the Precambrian complex in this study and its foliation trends in two dominant directions: N.40°E., and N.30°W.; dips range from 30° to 65° to the north. The contact with the overlying unit ($p\mathrm{C}_2$) is gradational over a 30 foot width and is marked by:

1) a strong decrease in the number of mica-garnet schist layers and an absence of sillimanite schist layers;
2) the disappearance of the dominant migmatitic gneisses which are characterized by ptygmatic folding of compositional layers; and
3) a change in thickness, abundance and lateral extent of amphibolites and associated pegmatites.

The dominant lithologic unit is a light to dark grey, fine- to medium-grained granite gneiss composed primarily of quartz, orthoclase and microcline with minor amounts of plagioclase, chloritic-biotite and garnet. Large scale asymmetric ptygmatic folding is well-developed and leucocratic layers average 3-6 cm thick. Petrographic analyses reveal a weak to moderate development of gneissic-lepidoblastic textures intermixed with occasional decussate-granoblastic textures. Alterations include mild selective argillic alteration of plagioclase, moderate chloritic alteration and bleaching of biotite, and limited replacement of biotite by sericite (samples A.D. 84-87; Appendix A; Plate II)*.

Interbedded with the main unit are abundant thin bedded garnet-biotite to garnet-biotite-sillimanite schists with occasional chlorite-biotite schists. These layers have a strong schistose-lepidoblastic texture and are composed of garnet, biotite and sillimanite with minor percentages of chlorite, quartz and feldspars. The alteration products include chlorite, sericite and magnetite reflecting breakdown of the biotite. A major petrographic feature is the development of prominent kelyphitic rims on the garnets (samples A.D. 8, 71, 88; Appendix A).

Thin to moderately-thick beds of amphibolite and amphibole gneiss are irregularly distributed and often discontinuous in this unit. Their mineralogy is mainly hornblende, biotite, plagioclase and minor quartz. Well-developed textures range from gneissic-granoblastic to nematoblastic and only a mild chloritic stage of alteration is present (samples A.D. 76, 90a; Appendix A). Commonly associated with the amphibolite layers are pegmatites of various sizes and shapes that are concordant with the strike of the foliation. Examination of thin sections from a few amphibolites exhibited a poorly-developed relict diabasic intersertal igneous texture which has had superimposed on it a decussate-nematoblastic texture due to regional metamorphism (samples A.D. 81, 89, 90b, 101; Appendix A). Of particular interest is sample A.D. 101 (Figure 3) which contained an amphibole that was tentatively identified as pargasite or cummingtonite and has been extensively altered and replaced by a calcite matrix, yet none of the adjacent rocks were subject to this type of alteration.

---

* Detailed petrographic descriptions of samples mentioned are contained in Appendix A in numeric order and the specific location of the samples is plotted on Plate II.

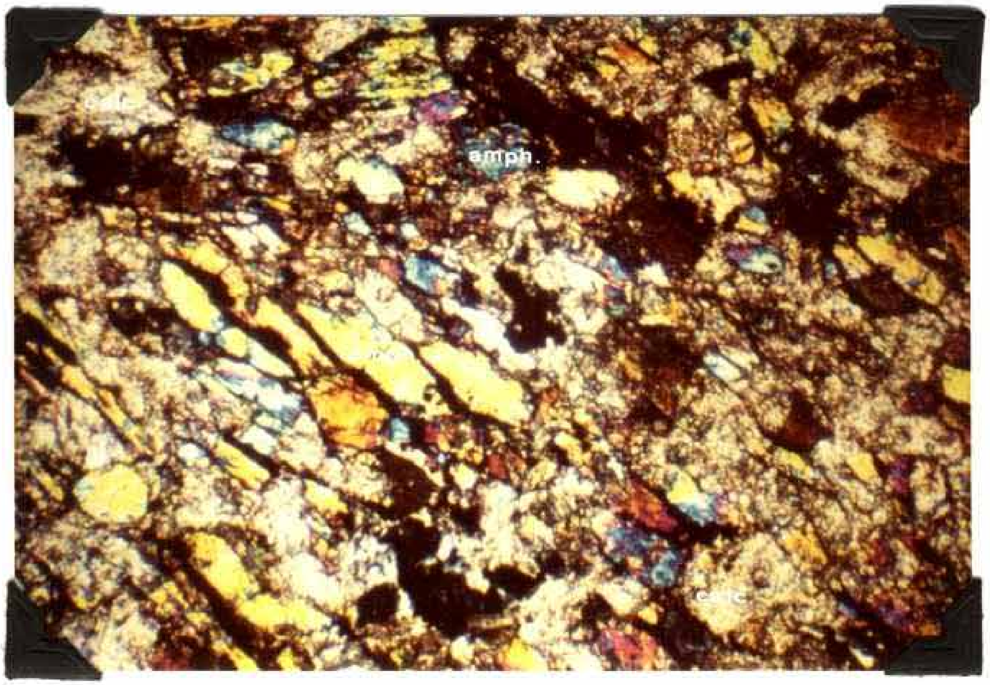

Figure 3. Photomicrograph of hydrothermally (?) altered amphibolite in the migmatitic gneiss unit ($P\epsilon_1$). The amphibole (amph.), tentatively identified as pargasite or cummingtonite, is replaced by a calcite (calc.) matrix. Note the relict metamorphic fabric masked by a mosaic texture in the matrix. Field of view 2.0 x 1.45 mm with crossed nicols, (sample A.D. 101; Appendix A).

Based on field observations and petrographic evaluations, the author prefers a Precambrian age for these dike-like features and had been unable to confirm any post-Precambrian andesitic dike features in the area of section 4 as reported by Krish (1974).

The composition of the pegmatites ranges from granite and quartz monzonite to granodiorite and the textures are phaneritic-pegmatitic with occasional porphyroblasts of garnet. Early stages of cataclastic to mylonitic texture are restricted to the pegmatites (samples A.D. 70, 74, 80, 100; Appendix A). In hand specimen, the texture is a "flow-banding" of fine grain, granular quartz and feldspar enveloping porphyroclasts (augen) of quartz and microcline.

Two rock types that have been observed only within the p€$_1$ unit are a calc-silicate gneiss (sample A.D. 83; Appendix A) and a magnetite-bearing quartzite (sample A.D. 73; Appendix A). The calc-silicate gneiss is confined to the top of a knoll just north of the Copper Blowout quarry (see Plate II). It is composed of actinolite-tremolite, garnet, epidote, calcite and quartz with minor orthoclase, sphene and apatite. This zone has been extensively altered hydrothermally but still shows a weak metamorphic fabric masked by the interlocking mosaic texture of the alteration suite (Figure 4). Such a localized lithology may represent a lime-rich facies within the original sedimentary sequence.

The magnetite-bearing quartzite is 5 to 10 feet thick, dark hematitic-red to limonitic-brown in color and is an extremely resistant marker bed in the field but was too small to map on the scale used. It contains mostly polycrystalline quartz interbedded with very thin discontinuous bands of magnetite weathering to limonite. A pronounced granulose-granoblastic texture is superimposed over a relict sedimentary texture (Figure 5). This quartzite resembles a thin mineralized layer containing

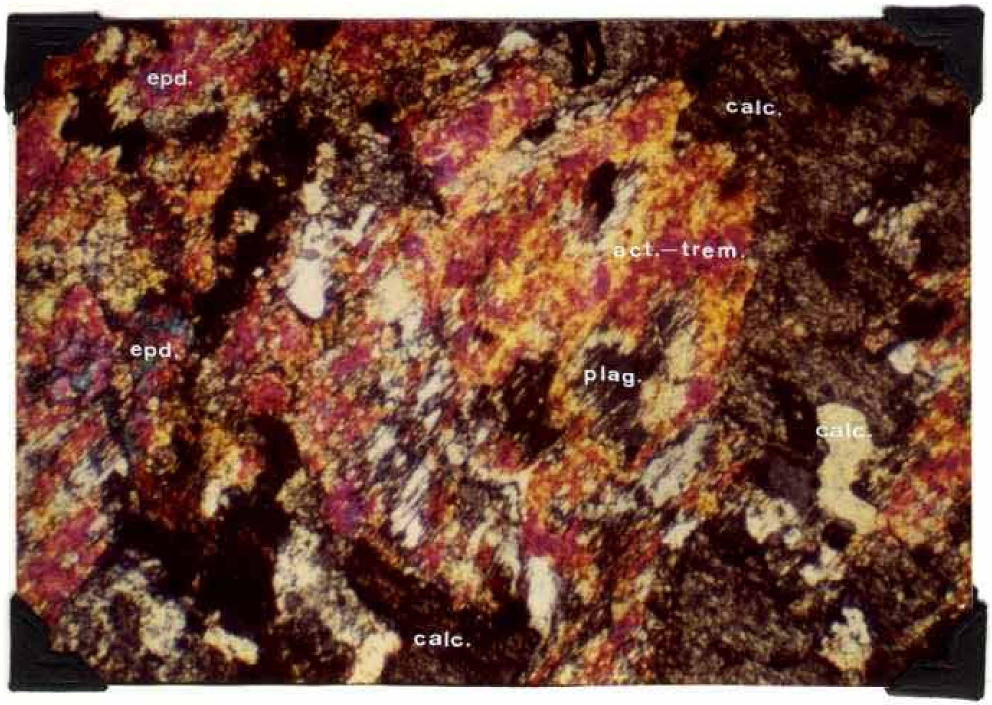

Figure 4. Photomicrograph of hydrothermally altered calc-silicate gneiss in the migmatitic gneiss unit ($P\mathrm{C}_1$). Remnant plagioclase (plag.) replaced by actinolite-tremolite (act.-trem.) which is altering to epidote (epd.). Note the interlocking mosaic texture of the calcite (calc.) matrix at extinction. Field of view 2.0 x 1.45 mm with crossed nicols, (sample A.D. 83; Appendix A).

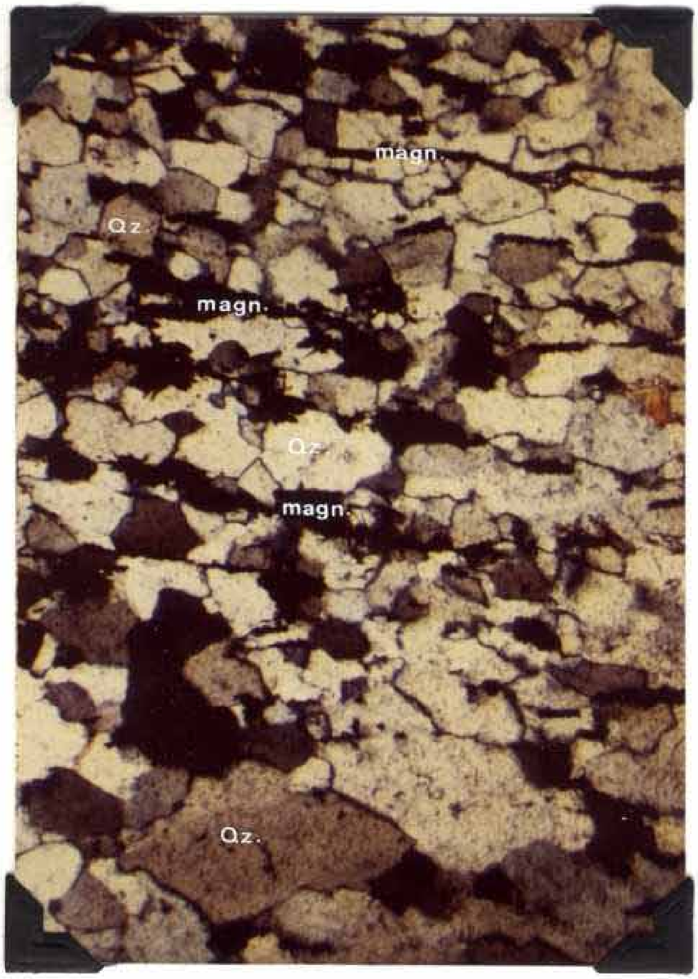

Figure 5. Photomicrograph of magnetite-bearing quartzite in the migmatitic gneiss unit (P€$_1$). Granoblastic quartz (Qz.) grains interlayered with oxidized magnetite (magn.). Note the relict sedimentary texture of parallel and graded (?) bedding. Field of view 2.0 x 1.45 mm with crossed nicols, (sample A.D. 73; Appendix A).

primary sulfides exposed in many of the prospect holes surrounding the Copper Blowout ridge (see Plate II), and appears strata-bound within the $P\epsilon_1$ unit.

Paragneiss Complex ($P\epsilon_2$) - The paragneiss complex is an undifferentiated assemblage of metasediments essentially corresponding to the $P\epsilon_2$ member described by Krish (1974). This sequence consists of alternating very thin-to thick-interbedded lithologies of considerable lateral extent and compositional variation. This metamorphic complex apparently overlies the $P\epsilon_1$ unit along the western and southern margins forming the crest of the range in the southern half of section 8, T.29N., R.17W. The paragneiss complex ($P\epsilon_2$) constitutes the entire Altered Valley, and terminates at the southern end of the Wall Street area as a result of major fault displacement. The offset extension continues further to the southwest along the western flank of the Migmatite Valley (see Plate II).

The paragneiss complex ($P\epsilon_2$) assemblage has been extensively altered from the Copper Blowout quarry south into the Migmatite Valley (see Plate I). The alteration and replacement is pervasive, increasing eastward from the ridge crest across the valley and appearing to continue under the fanglomerate. The alteration has obscured many of the original lithologies in the valley and obliterated a majority of the trends and attitudes that project southeast into the valley from the mountain crest to the west. Strong tectonic activity in this unit is evident from the extent of brecciation observed (samples A.D. 6, 16e, 24, 29f, 30, 58, 64, 65, 69; Appendix A; Plate I).

The general trend of the foliation in $P\epsilon_2$ along the mountain crest and to the west varies from N.10°E. to N.60°W., with dips from 30° to 60° northwest and north. Foliations from the mountain crest eastward into the

Altered Valley are discontinuous and diverse. The contact relationship with the next youngest member ($P\epsilon_3$) is recognized by:

1) changes in the dominant lithologies of the two units;
2) a contrast between the interbedded heterogeneous lithologies of $P\epsilon_2$ and the massive, homogeneous leucocratic patterns of $P\epsilon_3$;
3) the presence of ptygmatic folding and/or metamorphic deformational features in $P\epsilon_3$;
4) the contrast between sharp lithologic boundaries in $P\epsilon_2$ and gradational lithologic boundaries in $P\epsilon_3$; and
5) the greater abundance of pegmatite dikes and sills in $P\epsilon_2$.

Two distinct lithologic units dominate the Paragneiss Complex ($P\epsilon_2$). A sequence of granite to granodiorite gneisses is interbedded with amphibolite, gneissic amphibolite, and amphibole schists. The gneisses are composed primarily of quartz, potash-feldspar, plagioclase and biotite with variable amounts of cordierite, garnet, and magnetite. The textures are mostly gneissic-granoblastic with occasional lepidoblastic zones due to an increase in micas. Petrographic analyses demonstrated the pervasive nature of the alteration suites and that alteration intensifies when traversing eastward from the mountain crest into the Altered Valley. Argillic alteration of feldspars varies from slight to intense and selective alteration of plagioclase over potash-feldspar is common. Chloritic alteration of biotite is most common and pronounced while weak, sporadic sericitization is present. Only minor amounts of feldspar are replaced by either epidote or clinozoisite but such samples were in the immediate vicinity of known hydrothermal mineralization (samples A.D. 1, 3, 4, 15, 25, 29d, 59, 63, 103; Appendix A).

The amphibolites, gneissic amphibolites and amphibole schists range from 2 to 40 feet thick with moderately developed, continuous gneissic banding, 2 to 4 cm wide, from the separation of the leucocratic and melanocratic zones. The mineralogy consists of hornblende, plagioclase, biotite and minor quartz with lesser amounts of orthoclase and magnetite. Textures are from gneissic-nematoblastic to schistose-nematoblastic with minor gneissic-granoblastic layers confined to leucocratic zones. Chloritic alteration of hornblende and biotite is intense while moderate argillic alteration of feldspars and hornblende is common. Sericite and epidote, more common within the amphibolitic suites, partially replaces both plagioclase and hornblende (samples A.D. 2, 10, 13, 16b, 16d, 29c, 32; Appendix A).

Less common lithologies include biotite-cordierite, garnet-muscovite-biotite and garnet-biotite schists. In hand specimen, these rocks are well-foliated, moderately-crenulated, dark green-black to mottled grey-brown, fine- to medium-grained with slightly oxidized weathered surfaces. The schists are principally biotite, chlorite and quartz with variable amounts of garnet, cordierite and muscovite. A prominent schistose-lepidoblastic texture is prevalent and chloritic alteration is the most dominant (samples A.D. 7, 16c, 66; Appendix A).

As with the migmatitic gneiss unit (PЄ$_1$), a group of pegmatites intrudes PЄ$_2$ but the pegmatite bodies are considerably thicker and the contacts with amphibolites are more conformable than in PЄ$_1$. The pegmatites are massive, continuous and concordant with foliation. However, on the western flank of the range, several of the intrusive bodies do display local discordant trends to the regional metamorphic fabric (Figure 15, page 45). The pegmatites range from granite to granodiorite in composition, with a majority representing the latter end member (samples A.D. 5, 14, 16a, 29a, 29b, 29e; Appendix A).

The best development of cataclastic to mylonitic textures is observed in the $P\epsilon_2$ unit due to the abundance of pegmatites and the extent of structural deformation preserved in this unit. The stages of development for these textures are illustrated in Figures 17, 18, 19 and 20(pages 49-52); details are discussed under description of pegmatites (page 47), (samples A.D. 11, 26, 31, 33, 60, 61a, 61b, 62, 72, 75, 97, 102; Appendix A).

The only post-Precambrian igneous activity observed in the study area crops out in this paragneiss unit. Two small dikes, one in the Altered Valley (samples A.D. 9, 68; Appendix A) and one in Wall Street (samples A.D. 56a, 96a, 96b; Appendix A) were examined in thin-section revealing relict igneous diabasic intersertal textures masked by alteration but lacking any superimposed metamorphic fabric (Figures 13, 14; pages 40, 41).

Granodiorite Gneiss Complex ($P\epsilon_3$) - The Granodiorite Gneiss Complex ($P\epsilon_3$) is a thick, massive, homogeneous gneissic complex cropping out along the southern and western boundaries of the study area. It represents the second youngest Precambrian member and is very resistant, incorporating the major peaks in the southern portion of the mapped area (see Figure 6) and Pai Peak, highest point in the Lost Basin Range. Abundant outcrops occur in section 17, the west-central portion of section 16, and small areas of sections 8 and 20 of T.29N., R.17W. The general trend of the foliation is N.65°W., dipping 50° to 85°N.E., but local deviations in a fault block in section 16 vary from N.10°W. to N.40°E. dipping 45° to 60°W. to N.W.

The contact relationship between $P\epsilon_2$ and $P\epsilon_3$ has already been defined and $P\epsilon_3$ is faulted against the migmatite unit ($P\epsilon_4$). $P\epsilon_3$ could correspond to the quartz-feldspar gneiss ($P\epsilon_3$) used by Krish (1974).

The bulk composition of the $P\epsilon_3$ grades from quartz monzonite to granodiorite and consists primarily of quartz, plagioclase, potash-

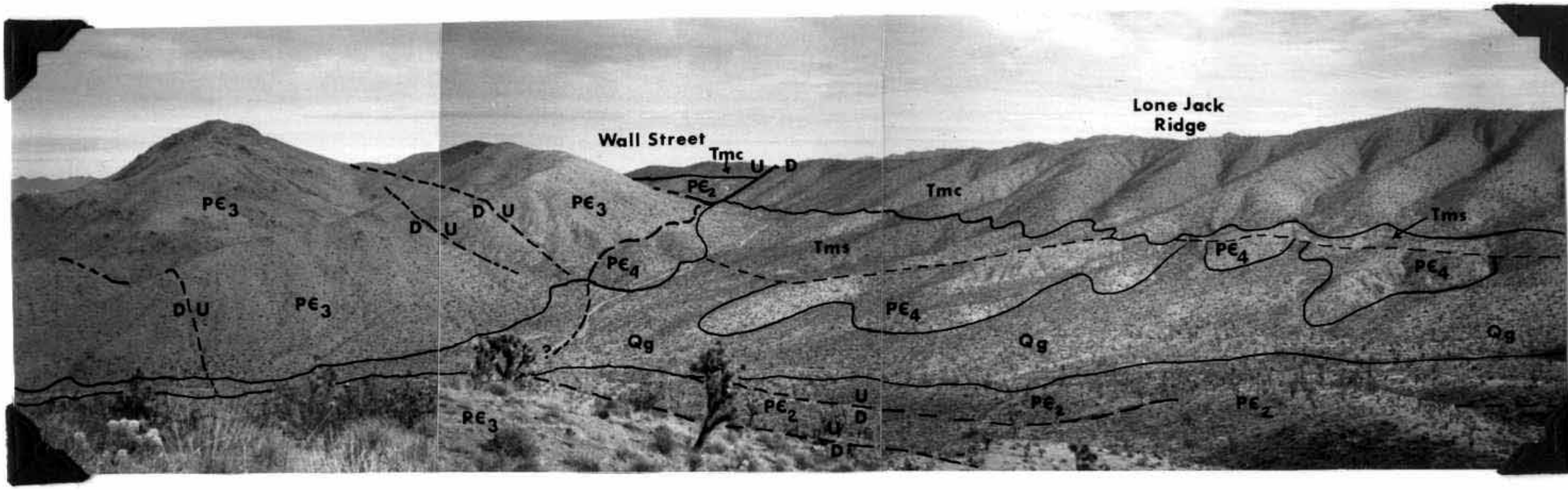

Figure 6. Panoramic view of the northern portion of Migmatite Valley looking northeast towards the southern extent of Wall Street. Note the abrupt termination of $P\epsilon_2$ unit and the thickness of the Tmc unit on the upthrown block compared with that on the downthrown block. (Photos taken from the southwestern border of mapped area).

feldspar, and chloritic biotite with minor amounts of chlorite, garnet, magnetite and hornblende (samples A.D. 17, 20, 27, 45b, 45c, 48, 50, 51; Appendix A). Minor thin layers of gneissic amphibolite, chlorite-biotite schist and scattered pegmatites constitute the remaining lithologies observed within this unit (samples A.D. 19, 22, 53; Appendix A).

In hand specimen, the gneisses of $p\epsilon_3$ are dark pink-grey to light grey-green, fine- to medium-grained with gradational boundaries and stained with desert varnish (Mn and Fe oxides). Discontinuous gneissic banding, 2 to 4 cm wide, is moderately developed within the leucocratic layers. Strong ptygmatic folding occurs with the axial planes of the folding irregular and divergent. A granulose to weak gneissic-granoblastic texture is prevalent in thin section and weak argillic to phyllic (eg. sericite) alteration pervades the plagioclase. Propylitic alteration is confined to samples taken in the vicinity of localized hydrothermal mineralization and is superimposed over the basic regional alteration suite. The propylitic alteration consists of limited replacement of plagioclase and hornblende by epidote, calcite, chlorite-sericite and minor secondary quartz.

Granite Migmatite Complex ($p\epsilon_4$) - The granitic migmatite complex is the youngest member of the Precambrian rocks mapped in this study and corresponds to the migmatite unit described by Blacet (1975). This migmatite complex is located in the northern portion of the Migmatite Valley and resembles an intrusive body contained within the paragneiss complex ($p\epsilon_2$). Outcrops in the mapped area are restricted to denuded knolls and arroyos in the S.W. $\frac{1}{4}$ of the S.W. $\frac{1}{4}$ of section 16 and the W. $\frac{1}{4}$ of section 21 T.29N., R.17W. (Figure 6). Exposures of $p\epsilon_4$ are partially obscured by colluvium derived from Lone Jack ridge as a result of headward erosion of the western drainages into the Tertiary sediments. The northern extent of $p\epsilon_4$ is marked by a low-angle normal (?) fault adjacent to $P\epsilon_3$ and the western boundary is covered by recent alluvium. The eastern border is an irregular non-conformity beneath the deformed Tertiary sediments (Tms). Post (1970) noted that in sections 4 and 28 of T.28N., R.17W. (south of mapped area) there was a contact between the Tertiary sediments and the Precambrian rocks that indicated the depositional surface must have been of "considerable local relief". The migmatite unit continues south along the Migmatite Valley floor and is eventually covered by Quaternary gravels before reaching the southern end of Lone Jack ridge.

$P\epsilon_4$ contains two distinct facies. First is a peripheral schistose zone dominated by a sillimanite-biotite migmatite, characterized by a well developed lepidoblastic texture with contorted and tightly crenulate foliations (Figure 7). It is composed primarily of sillimanite and magnetite replacing biotite with minor amounts of quartz, orthoclase and cordierite. This zone contains abundant leucocratic veinlets exhibiting metamorphic structures ranging from irregular ptygmatic folds with divergent axial planes to boudins of granitic migmatite aligned with the deformed trend in foliation. Argillic alteration of feldspars within this zone is recognizable only in thin section (samples A.D. 38, 46b; Appendix A).

The second facies is a granitic migmatite core with a weak gneissic fabric near the contact with the outer schistose zone. The contact is gradational. The "granite" is medium pink to light red-brown, phaneritic (medium- to coarse-grained and less than 1% porphyritic, locally), homogeneous, equigranular with a microscopic hypautomorphic texture. Three phases were observed in the field: a finer-grained "granite" marginal to the "schist" facies, a coarser-grained core, and late aplite dikelets (with garnet), 5 to 15 cm wide, injected randomly into the main granitic zone (samples A.D. 98a-c; Appendix A). The mineralogy consists of quartz,

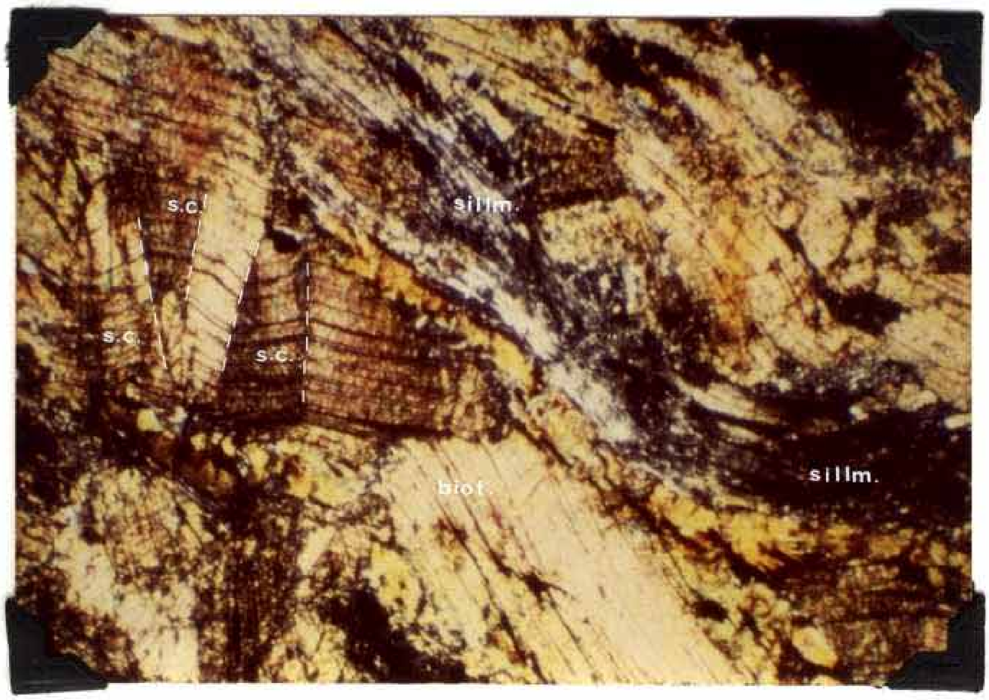

Figure 7. Photomicrograph of biotite migmatite zone in the granitic migmatite complex ($P\epsilon_4$). The biotite (biot.) is being replaced by fibrous sillimanite (sillm.). Note how the biotite is brittle, deformed and subject to slip cleavages (s.c.). Field of view 2.0 x 1.45 mm with crossed nicols, (sample A.D. 38; Appendix A).

microcline, orthoclase, plagioclase and biotite with variable amounts of muscovite, chlorite and garnet. Petrographic analyses showed no pervasive alteration; argillic alteration of the more calcium-rich plagioclase and limited oxidation of chloritic biotite are present.

Several discordant intrusive pegmatite dikes cut P€$_4$, but the author does not consider them as "differentiates" of the granitic migmatite because of:

1) textural and compositional differences with the granitic migmatite (samples 39, 42, 46a, 91; Appendix A);
2) apparent trends in the field coincide with the general trend of a majority of pegmatites throughout the Precambrian complex;
3) textural and compositional similarities with a majority of pegmatites elsewhere in the complex;
4) degree and extent of argillic alteration in the pegmatites are greater than in the granitic migmatite.

Therefore, the granitic migmatite is considered the youngest Precambrian unit mapped in the area but older than the intrusive pegmatites within the complex.

Cenozoic Units

Mudflows and Rhyolitic Sediments (Tms) - The Tms unit in the mapped area is limited to the S.W. $\frac{1}{4}$ of section 16 and N.W. $\frac{1}{4}$ of section 21 T.29N., R.17W. within the northern part of the Migmatite Valley (Figure 6). Outcrops are restricted to arroyos with an occasional resistant layer projecting from the valley floor (Figure 8). The mudflows and tuffaceous sediments are deposited unconformably on the granitic migmatite (P€$_4$) and are overlain unconformably by the Muddy Creek fm. (Tmc). The upper contact of Tms is characterized by a distinct lithologic contrast and a sharp angular

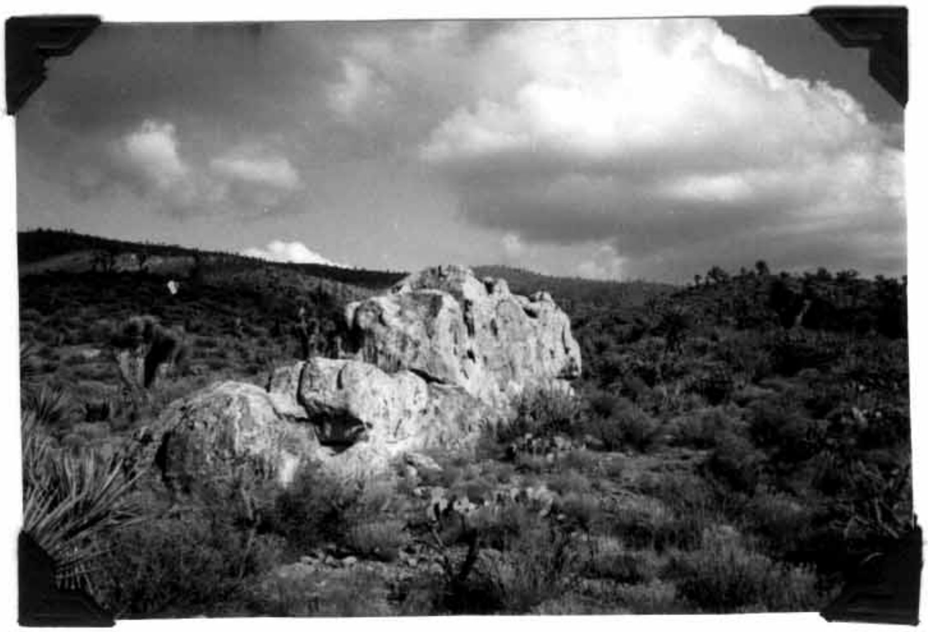

Figure 8. Tuffaceous sandstone member of the Tms unit in an isoclinal fold (syncline) exhibiting a near vertical attitude, within the northern portion of the Migmatite Valley. (Stratigraphic unit 2 from the stratigraphic section B-B'; see Plate II; Appendix B).

unconformity. The Tms was considered by Lucchitta (1966) to be the lower portion of the Muddy Creek fm. It has been mapped by Blacet (1975) as tuffaceous sediments (Ts) and correlated with the Mt. Davis volcanics of Miocene age (12-15 m.y.).

The mudflow-rhyolitic sediments sequence is steeply dipping and the strike length of the unit is deformed concavely to the east (see Plate I). Strikes range from N.45^{o}W. to N.30^{o}E. with dips between 75^{o}E. to 90^{o} but not overturned as mapped by Blacet (1975). The author observed several internal structures that indicated the top and bottom of individual layers and established the upright attitude of the unit (Figures 10 and 11). Approximately 350 feet of exposed sediments were measured and the descriptions are in stratigraphic sections A-A' and B-B' (Appendix B; Plate II). However, the extent of outcrops observed in the field suggested a possible thickness for this unit of 800 to 1,000 feet; it appears to continue unconformably under the younger fanglomerate (Tmc).

The Tms consists of tuffaceous (rhyolitic) sandstones interbedded with tuffaceous mudflows. In hand specimen, the sandstone members are light grey-white to buff, coarse- to fine-grained, moderately friable, thin-bedded (5-60 cm thick) to very thin-bedded (1-5 cm thick) and horizontally stratified (McKee and Weir, 1953). Sets of strata are well developed with normal and reverse graded bedding with a slabby to flaggy property. The origin of the reverse graded bedding in these layers could be attributed to mechanisms described by Duffield and Bacon (1978). The coset unit varies in thickness from $1\frac{1}{2}$ to 30 feet and is moderately resistant to weathering. It exhibits an abrupt change in character and composition from the adjacent mudflows (Figure 9). The sandstones are planar and tabular in shape. The lower contact commonly represents nonerosional deposition upon weathered surfaces of the mudflows (Figure 11). Petro-

Figure 9. Contact between a tuffaceous mudflow member (3) and a tuffaceous sandstone member (4) of the Tms unit. Note the vertical attitude of the beds and a regolith consisting of predominantly porphyritic granite clasts weathering directly out of the mudflow members, (Stratigraphic units 3-4 from the stratigraphic section B-B'; see Plate II; Appendix B).

Figure 10. Sharp undulatory contact between a fine grained tuffaceous sandstone member (14) and a tuffaceous mudflow member (15) of the Tms unit. Note the clasts within the mudflow are matrix supported. Stratigraphic top of sequence is at top of photo, (Stratigraphic units 14-15 from the stratigraphic section B-B'; see Plate II; Appendix B).

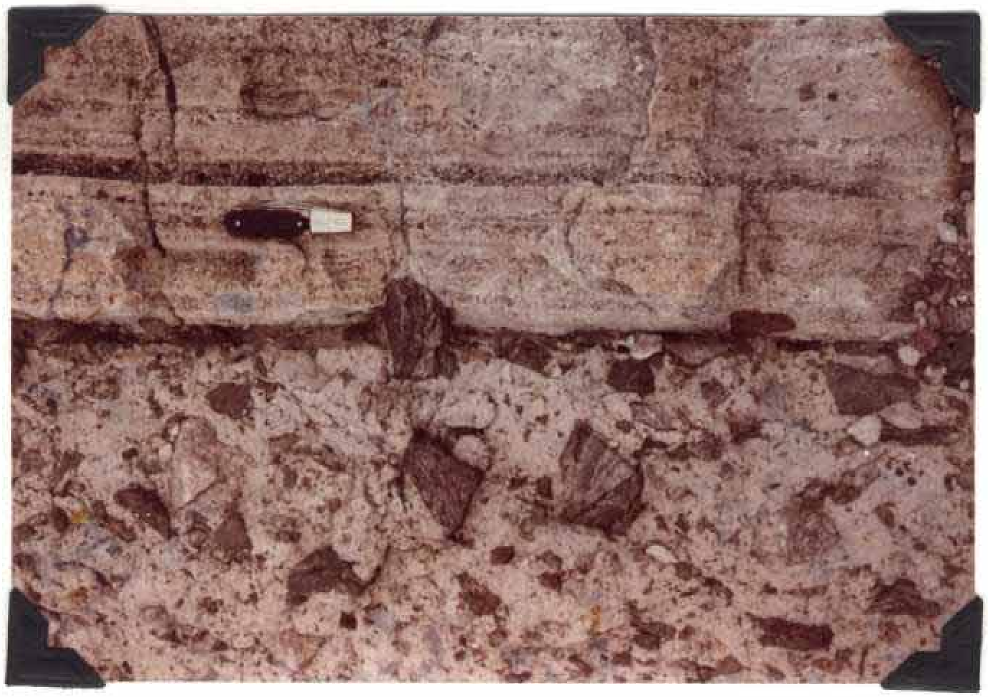

Figure 11. Contact relationship between a tuffaceous mudflow member (3) and tuffaceous sandstone (4) of the Tms unit. Granitic clasts armor top of mudflow; reflective of a weathered surface. The tuffaceous sandstone is very thin bedded with moderately developed normal and reverse graded beds. Note the deformed beds of sandstone draped over the protruding granitic clast and the clasts are matrix supported within the mudflow. Stratigraphic top of sequence is at top of photo, (Stratigraphic units 3-4 from the stratigraphic section B-B'; see Plate II; Appendix B).

graphic analyses indicate a composition for the volcanic constituents ranging from rhyolite to latite; however, two samples (A.D. 40, 99; Appendix A) are andesitic tuffs. The sandstones are primarily composed of pumice and glass fragments in a glass shard matrix. Minor amounts (less than 15%) of crystal and lithic fragments are present consisting mostly of feldspar, plagioclase, biotite, quartz and hornblende. Alteration is limited to moderate devitrification of the volcanic matrix and traces of calcite or Fe_2O_3. No welding, compaction or collapsing of pumice fragments were observed and most samples are moderately mature texturally and mineralogically (samples A.D. 41a-b, 46c, 93, 94; Appendix A).

The andesitic tuff layers are dark grey to yellow-brown, massive, and homogeneous in hand specimen. Sample A.D. 40 is moderately resistant, lacking internal structures while sample A.D. 99 is extremely friable and weathers to an oxidized yellow-brown knobby soil (see stratigraphic section A-A'; Plate II). In thin section, both samples show extensive devitrification and oxidation with abundant calcite and ferrigenous cements.

The tuffaceous mudflows are monolithologic breccias containing clasts of coarse porphyritic granite (40-50%) with lesser amounts of granitic migmatite (20-30%). The mudflows are grey-brown, massive, structureless and tabular in shape. A fine grained volcanic matrix supports angular clasts that range in size from pebbles to cobbles with occasional boulders (1-2 feet in diameter). Individual layers vary from 5-30 feet thick, are non-resistant and weather to a conspicuous, homogeneous regolith. This is due to the removal of matrix and surface accumulation of the weathered-out clasts. The upper contacts (Figure 11) are sharp and commonly armored with clasts. Deposition by tuffaceous sandstone members exhibited deformed strata draped over the irregular surfaces. The lower contact of the mudflows commonly displayed a sharp undulatory boundary, indicating an erosional deposition on top of the sandstones (Figure 10). In thin section the volcanic matrix is texturally and mineralogically immature. It is comprised of nearly devitrified glass shards and pumice fragments supporting clastic non-volcanic debris (less than 30%). The clastic constituents include crystal fragments of plagioclase, biotite, quartz and opaques mixed with lithic fragments of pegmatite, amphibolite and gneiss (sample A.D. 46d; Appendix A; see Figure 12). Petrographic examination of the porphyritic granite clasts (samples A.D. 34, 35, 47; Appendix A) shows enough dissimilarity from the granitic migmatite ($P\epsilon_4$) described earlier, to suggest a more distant source area for the porphyritic clasts. Outcrops of such a coarse porphyritic granite have not been observed in the mapped area or elsewhere within the Precambrian complex of the Lost Basin Range.

Fanglomerate (Tmc) - The fanglomerate represents the youngest Tertiary sediments in the mapped area and correlates with the Muddy Creek formation, described by Longwell (1928); similar fanglomerates are attributed to the Cenozoic deposition of basin fills on a regional scale (Longwell, 1936, 1963). The eastern 1/3 of the mapped area consists entirely of Muddy Creek fm. which flanks the eastern portion of the Lost Basin Range and across which is cut Grapevine Mesa. The average strike is between N.10°W. and N.5°E. with dips of 15° to 30°E. The northern 3/4 of the fanglomerates are in unconformable depositional contact with the Precambrian complex (predominantly $P\epsilon_1$ and $P\epsilon_2$) while the southern 1/4 is in unconformable depositional contact with the Tertiary mudflow-rhyolitic sediments (Tms) and the granitic migmatite unit ($P\epsilon_4$). The thickest sequence of fanglomerate comprises Lone Jack Ridge and at least

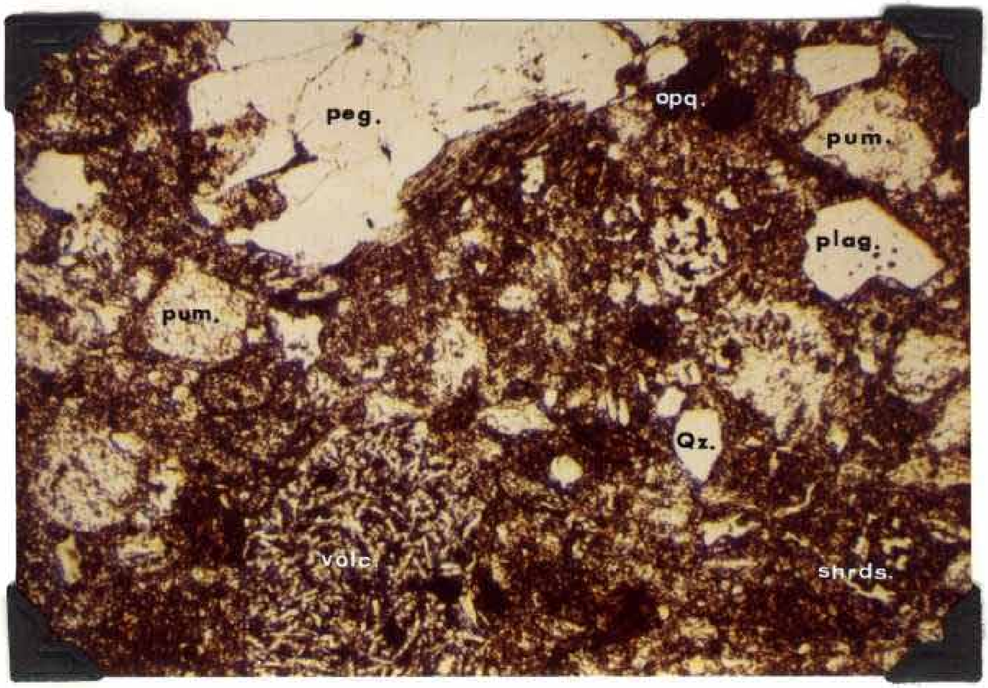

Figure 12. Photomicrograph of matrix constituents in a tuffaceous mudflow breccia within the Tms unit. Matrix consists of devitrified glass shards (shrds.), pegmatite fragments (peg.), volcanic extrusive fragments (volc.), quartz (Qz.), opaques (opq.), broken plagioclase laths (plag.) and pumice fragments (pum.). Field of view 2.0 x 1.45 mm without crossed nicols, (sample A.D. 46d; Appendix A).

1,200 feet of sediments are present near the southern border of the mapped area. Lucchitta (1966) reports over 2,000 feet of sediments further north along the Grand Wash Trough. The best exposures of individual lithologies are in the western flank of Lone Jack ridge due to headward erosion of the western drainages (Figure 6, page 23).

These fanglomerates are moderate- to well-consolidated alluvial fan deposits consisting of fine to very coarse clasts of crystalline rocks. A massive conglomerate-breccia contains a heterogeneous assemblage of Precambrian metamorphic clasts that represents the bulk of the formation. Angular to subrounded clasts range in size from pebbles to large boulders and the clast/matrix ratio is highly variable both laterally and vertically. Internal structures are mainly disordered with an occasional weak "chaotic" stratification (imbrication ?) of clastic sandstone layers. The whole sequence is pervaded by caliche cement. Quaternary erosion and reworking of these deposits are associated with local concentrations of detrital gold in the younger gravels. This is evident along the eastern flank of Grapevine Mesa where old placer mining operations are located.

Minor lithologies include tuffaceous sediments and muddy lithic sandstones. Volcanic tuffs are 2-8 feet thick, lenticular, massive and discontinuous. These layers are light blue-grey to light grey-white and consist of impure tuffs intermixed with approximately 15% large detrital lithic clasts. In thin section, the tuffs are very immature texturally and mineralogically. The matrix is poorly sorted and consists of a heterogeneous size fraction of volcanic materials (pumice and glass shards) that are slightly to moderately devitrified. Lithic and crystal fragments make up 10% of the matrix composed of quartz, feldspars, biotite, and hornblende with a mixture of metamorphic rock types. Volcanic composition of these tuffs is indeterminate because of the contamination of the tuffs by detrital constituents (samples A.D. 36, 37, 43; Appendix A). However, these lenticular tuffs are distinguishable in hand specimen and by petrographic analysis from the tuffaceous sandstones within the mudflows-rhyolitic sediments unit (Tms).

The muddy lithic sandstone is grain supported and composed of a diverse assemblage of detrital fragments. It is very immature texturally and mineralogically. Petrographic analysis shows a wide dispersion of grain sizes, with angular to subangular grains supporting a muddy matrix filling the interstices. Strong oxidation was pervasive, with minor caliche cement but most pronounced is the absence of any volcanic material (sample A.D. 92; Appendix A). Note that this sample is in the immediate vicinity of the contact between the granitic migmatite ($P\mathcal{C}_4$), the mudflow-rhyolitic sediments (Tms) and the Muddy Creek fm. (Tmc).

The age of the Muddy Creek fm. has been determined by radiometric age dates from a sill at Frenchman Mountain at 11.8 $\pm$ 0.7 million years B.P. and the Fortification Basalt member of the Muddy Creek fm. near Hoover Dam at 10.6 $\pm$ 1.1 million years B.P. (Damon, 1965). This indicates a late Miocene (?) to early Pliocene age for the Muddy Creek fm. and corresponds with the mapping by Blacet (1975) and confirms the field relationships in the Grand Wash Trough discussed by Lucchitta (1966, 1967).

Lucchitta's study (1966) of the Cenozoic geology in the vicinity of the Grand Wash Cliffs provides an in depth description and correlation of the Muddy Creek fm. on a regional scale. Classification of the Muddy Creek fm., in the mapped area of this study, using his scheme would be as follows:

Complex - Muddy Creek Complex

Assemblage - Grand Wash Assemblage

Association - Grapevine Wash Association

Facies - Conglomerate-breccia facies

Subfacies - Crystalline-clast conglomerate - subfacies present in mapped area of this study,

- Gold Butte - bearing conglomerate - subfacies present to the north in vicinity of Meadview containing huge boulders of the Gold Butte granite (Volborth, 1962),
- Sedimentary - clast conglomerate - subfacies east of the Grapevine Wash containing sedimentary clasts shed from the Grand Wash Cliffs.

Quaternary Gravels (Qg) - The Quaternary gravels represent unconsolidated arroyo gravels and alluvium deposited along active washes fed by ephemeral streams. The Holocene sediments consist of loose sands and gravels ranging in size from very fine grains to small boulders. The major source for the clastic debris comes from the erosion of the Muddy Creek fm. (Tmc). Talus or colluvium eroding directly from the fanglomerate and older lithified gravels, younger than Pliocene but cropping out above active drainages, are included in the Quaternary gravels (Qg). These gravels contain coarse to fine detrital gold in the recent drainages but the gold content is highly variable. The gold is considered to be largely derived from the underlying Miocene-Pliocene fanglomerates (Blacet, 1969).

An interesting geomorphic feature about this unit is the rate of headward erosion of the eastward drainages. In the northern portion of the mapped area erosion has breached through the fanglomerate and incorporates part of the Precambrian surface. Whereas south of Wall Street, the degree of headward erosion has not reached Lone Jack ridge.

Igneous Rocks

Intrusives -

Dikes - Two types of dikes are present: an unmetamorphosed younger set and an older metamorphosed group. Both types of structures were too small to map on the scale used in this study. Two outcrops represent the younger intrusives. One is located in the Altered Valley, S.W. $\frac{1}{4}$ of the N.W. $\frac{1}{4}$ of section 9 and the other is in the southern portion of Wall Street, N.E. $\frac{1}{4}$ of the S.W. $\frac{1}{4}$ of section 16 T.29N., R.17W. The dike in the Altered Valley is non-resistant and poorly exposed due to alluvial cover. The intrusion is approximately 350 feet in length, less than 10 feet wide and has a northern trend but the dip was indeterminate. In hand specimen, it is dark brown, fine grain, massive, strongly oxidized and altered beyond recognition. Only in thin section is this unit recognized as being of igneous origin (samples A.D. 9, 68; Appendix A).

The second dike trends northwest with a vertical attitude and shows a weak conformity to the regional trend in foliation of the host rock. The unit is 5 feet thick, 200 feet in length, and displays some minor fault displacement. In hand specimen, it is light-medium brown, massive, with strong limonitic oxidation and has a faint aphanitic igneous texture. The rock is intensely altered and abundant quartz-calcite-oxidized pyrite (?) veinlets, (a few mm wide), penetrate this unit at random (samples A.D. 56a, 96a, 96b; Appendix A).

In thin section, both dikes show a strong igneous diabasic intersertal texture (Figures 13, 14). The plagioclase laths are completely altered to kaolinite or replaced by very fine grained sericite. The igneous texture has been moderately masked by an interlocking mosaic texture from the alteration matrix containing Fe_2O_3 and calcite. Enough calcite was present in the Wall Street dike that secondary unaltered

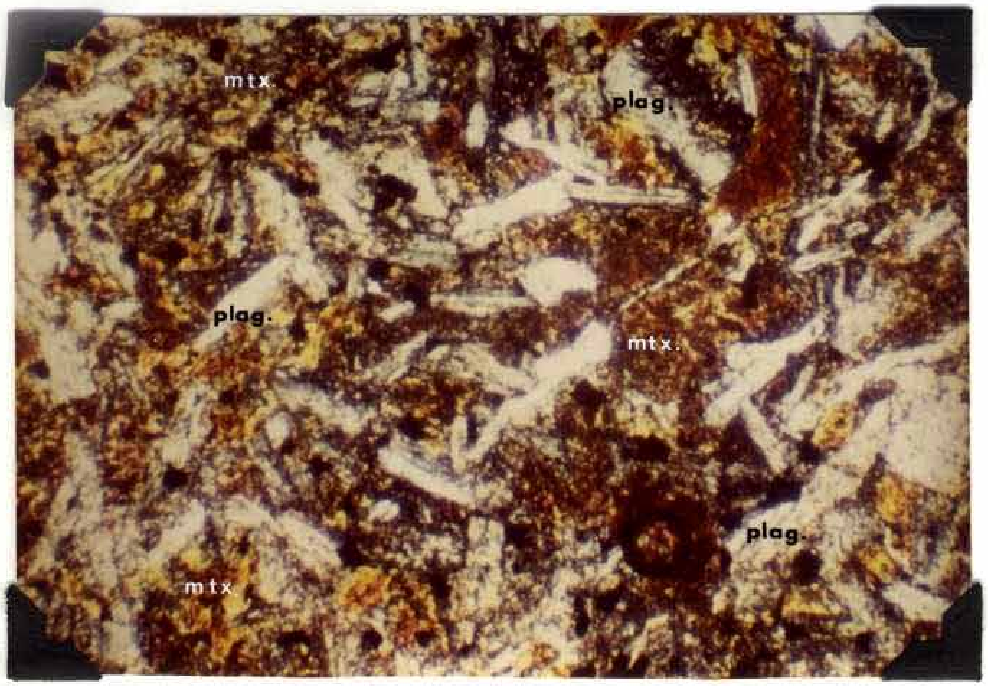

Figure 13. Photomicrograph of relict igneous diabasic-intersertal texture characteristic of andesite-diabase dike within $P\epsilon_2$ unit in the Altered Valley. Note the remnant plagioclase laths (plag.) randomly oriented in an alteration matrix (mtx.) of kaolinite, calcite and Fe_2O_3. Field of view 2.0 x 1.45 mm with crossed nicols, (sample A.D. 9; Appendix A).

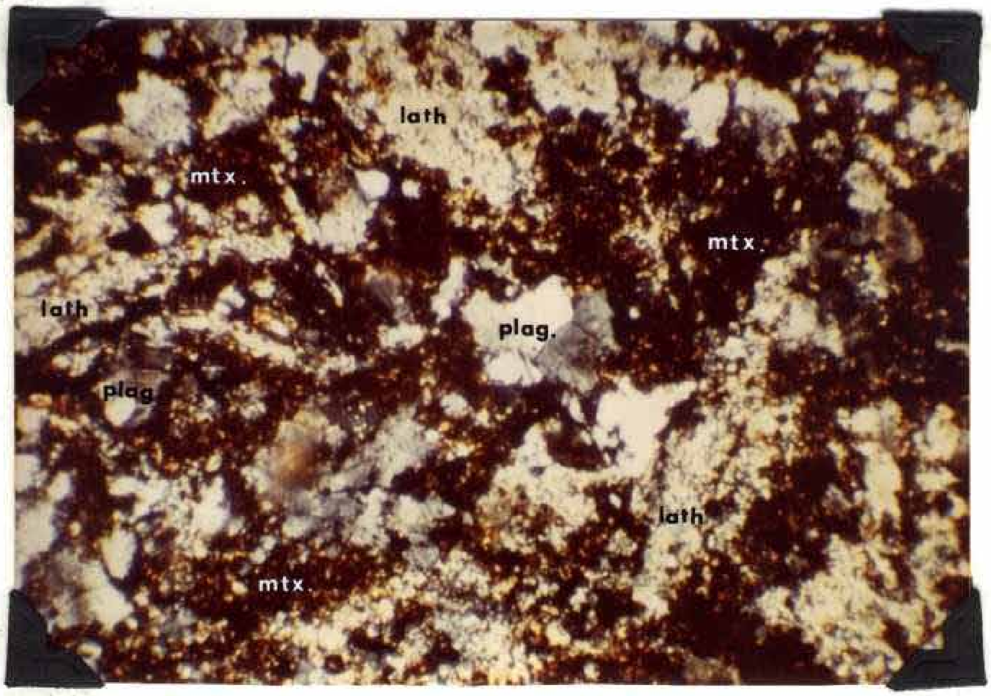

Figure 14. Photomicrograph of relict igneous diabasic-intersertal texture characteristic of andesite-diabase dike within P€$_2$ unit in Wall Street. Skeletal outlines of plagioclase laths (lath) completely replaced by kaolinite and sericite. Matrix (mtx.) is Fe_2O_3 and calcite due to hydrothermal alteration. Note the generation of secondary unaltered calcium-rich plagioclase (plag.) filling interstices. Field of view 2.0 x 1.45 mm with crossed nicols, (sample A.D. 56a; Appendix A).

andesine plagioclase was generated within the interstices (Figure 14). This secondary generation could be due to percolation of weak hydrothermal fluids and/or a weak metamorphic event. No noticeable metamorphic textures or fabrics were observed in either of these dikes which probably indicates a post-Precambrian age for these younger intrusive units.

Outcrops of the older group of dike-like structures are found within the migmatitic gneiss ($P\epsilon_1$). Several amphibolites, 4-8 feet thick, with limited lateral exposure have an acute discordance to the foliation of the adjacent rocks and exhibit a definite metamorphic fabric in hand specimen. In thin section, these rocks show a vague relict igneous texture but metamorphism has superimposed a decussate-nematoblastic texture over the original structure of the rocks (samples A.D. 81, 89, 90b, 101; Appendix A). Three samples were taken in the vicinity of the andesite dike mapped by Krish (1974) and these may correspond with his unit. Unfortunately none of these rocks displayed the degree of igneous texture characteristic of the younger dikes. The author does consider these older dike-like structures to correspond with the late-Precambrian diabasic intrusives mentioned by Blacet (1975).

Plutons - Many of the granitic rocks in northwest Arizona and southern Nevada are plutonic assemblages representing different ages of intrusive activity. Of these three particular groups are of interest. Thomas (1949) proposed the term "Cerbat complex" for "a basement assemblage of metamorphic and igneous rocks of Archean age," and mapped two intrusive facies of the "Ithaca Peak porphyry". One was the Chloride granite which was dated by Damon and Giletti (1961) as 1.21 b.y. old. Based on descriptions of the Chloride intrusion by Dings (1951, p. 129-130), the granitic migmatite ($P\epsilon_4$) mapped in the Lost Basin Range could be correlated with the Chloride granite intrusive.

A younger and larger pluton composed of coarse porphyritic perthite-biotite granite was described by Volborth (1962) as the Gold Butte granite in the South Virgin Mountains of Nevada. Large boulders of this intrusive are present in the Gold Butte-bearing conglomerate subfacies of the Muddy Creek fm., just north of this study area (Lucchitta, 1966). A marked dissimilarity between the Gold Butte granite and the granitic migmatite ($P\epsilon_4$) was observed by this author. Volborth (1962) gave a Rb-Sr age date for potash-feldspars from this granite as 1.06 b.y. old and 1.09 b.y. old. He suggested a correlation of the porphyritic granites in the Cerbat mountains and along the base of the Grand Wash Cliffs with the Gold Butte granite. Mapping by Blacet (1975) inferred that the porphyritic quartz monzonite (eg. porphyritic granite ?) exposed along the Grand Wash Cliffs and in the Garnet Mountain pluton to the south, are younger than the migmatite (granitic migmatite, $P\epsilon_4$) mapped within the Lost Basin Range.

The other intrusive mapped by Thomas (1949) is describes as Laramide quartz diorite, quartz monzonite porphyry and quartz porphyry by Eidel, Frost and Clippinger (1968) at Mineral Park in the Cerbat Mountains. An age of 72 m.y. B.P. for this intrusive sequence was given by Mauger and Damon (1965). The only intrusive of this age bracket in the vicinity of the Lost Basin Range was mapped by Blacet (1975) in the Gold Basin district to the southwest. This intrusive is a quartz monzonite pluton associated with peripheral gold-quartz veins.

Pegmatites - Tabular to lenticular pegmatite dikes and sills are present throughout the Precambrian complex. In the field, age relationships of the pegmatites are difficult to establish due to the dominant conformity in trends with the foliation of the host rocks. Several of the intrusives locally demonstrate a variation from concordant to discordant attitudes to the layering and metamorphic fabric of the adjacent rocks

(Figure 15). Such field relations suggest the pegmatites are younger than the metamorphism of the complex. Radiometric age dating by Wasserburg and Lanphere (in Volborth, 1962) of pegmatites cutting gneisses in the South Virgin Mountains, showed Rb-Sr ages of 1.63 b.y. old and 1.70 b.y. old, suggesting an age of the pegmatites younger than the regional metamorphism.

In hand specimen, the pegmatites are light grey-white to light grey-pink, coarse phaneritic to pegmatitic, highly variable in thickness and exhibiting a range in composition from granite to granodiorite with quartz monzonite representing the majority. The mineralogy consists primarily of perthitic microcline, micrographic orthoclase, plagioclase and quartz with accessory biotite and muscovite. Contact zones with the host rocks are sharp and distinguishable without any apparent contact aureoles. One exception is present in the vicinity of a recumbent fold in amphibolite adjacent to a discordant pegmatite intrusion (Figure 15). This exposure represents a 15 foot diameter zone of intense propylitic alteration and replacement of the amphibolite associated with the fold (Figure 16). The fold apparently acted as a dilation zone in which hot fluids driven off by the pegmatite were accumulated, resulting in local metasomatism of the host rock.

Blacet (1969) mentioned that "mineralized veins appear transitional into carbonate and sulfide bearing pegmatites" and suspected the veins to be of a late Precambrian age. Observations by Post (1970) indicated quartz-carbonate veins accompanied the pegmatite dikes; Trites (1974) agreed with a possible contemporaneous introduction of pegmatites and quartz veins. Veins from a few mm to 2 feet thick were observed containing bull quartz, minor amounts of iron carbonate (siderite and/or ankerite ?) and fine disseminated oxidized pyrite. These veins were commonly

Figure 15. A large pegmatite discordant to the regional trend in foliation within the paragneiss complex ($P\epsilon_2$). View from the western limb of mountain crest. (Location--northern portion of N.W. $\frac{1}{4}$ of S.E. $\frac{1}{4}$ of section 8, T.29N., R.17W.).

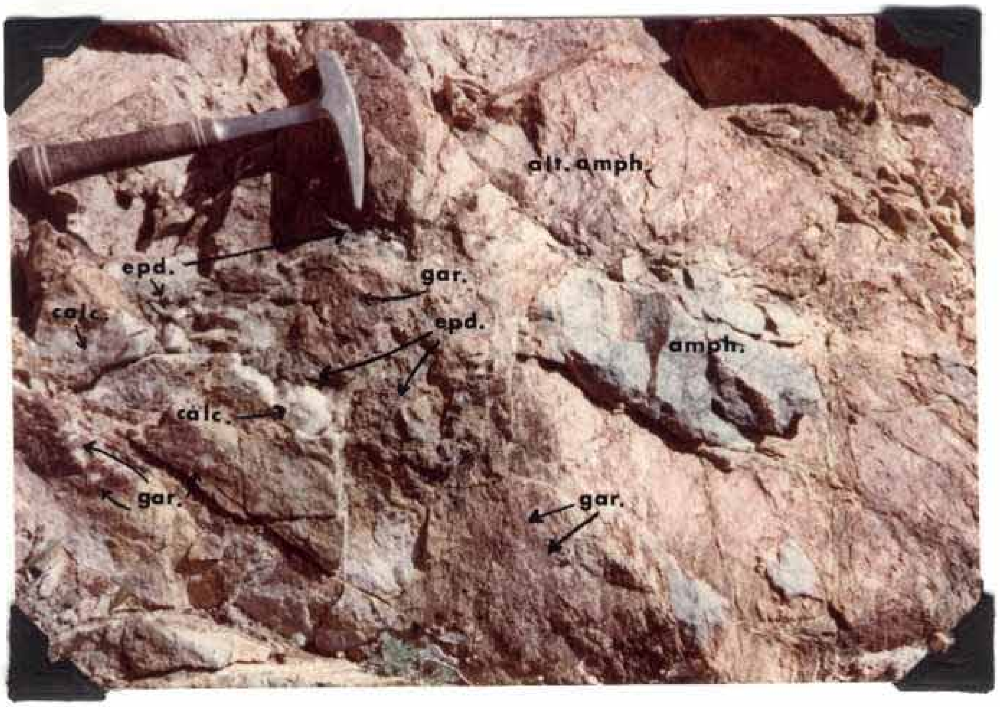

Figure 16. Propylitic alteration of amphibolite adjacent to contact with pegmatite and a large recumbent fold of amphibolite. Remnant amphibolite (amph.) engulfed in altered and bleached amphibolite (alt. amph.). Note massive replacement by epidote (epd.), calcite (calc.) and garnet (gar.). (Location--vicinity of Figure 15).

associated with quartz cores within pegmatites and appeared to transgress the pegmatites and host rock. Such structures were considered the result of outward migration and permeation of residual fluids from the pegmatites and not a hydrothermal mineralizing event. Economic mineralization associated with this type of vein structure was not observed in the field.

A special texture characterizes the pegmatites locally in this study area--the results of dynamic metamorphism (Spry, 1976). The effects are limited to a narrow zone that corresponds with the strike of major faulting in the area and are most pronounced along the Altered Valley southward into Wall Street. In hand specimen, the texture resembles "flow banding" around augen of quartz and microcline. Such a macroscopic texture may represent the metamorphosed rhyolitic beds described by Krish (1974, p. 51). Petrographic analyses reveal four stages of deformational development within these pegmatites. The deformation is characterized by the following petrographic features:

1) development of porphyroclasts,
2) bent crystals,
3) strong undulose extinction,
4) deformation (bending) of twinning,
5) structural inversion (orthoclase-microcline),
6) compositional segregation into layers,
7) exsolution of feldspars,
8) hydration of matrix (eg. chloritization or sericitization).

The descriptions of the four stages of deformation are modified from the classification by Spry (1976) and are defined as follows:

1) Cataclastic (crush) Breccia - consisting of large angular fragments produced by tectonic fragmentation of a pre-existing rock. Has an angular fragmental to powdered matrix, unfoliated with secondary

cements common. Appears to have been crushed instead of granulated. Common in immediate vicinity of faulting (Figure 17),

2) Protomylonite - 10-50% of matrix is granulated, may show weak foliation of matrix, deformed crystals and twinning. Abundant porphyroclasts, strong undulose extinctions. No cements (Figure 18). This is a transition from a breccia to mylonite,

3) Mylonite - 50-90% of matrix is granulated and moderately foliated. Strained porphyroclasts are embedded in matrix and tend to become lenticular with increased deformation. Development of compositional layering and no secondary cements (Figure 19),

4) Ultramylonite - 90-100% of matrix is granulated and strongly foliated ("flow banded") in which less than 10% of remaining porphyroclasts survived granulation. Porphyroclasts are lenticular and may undergo exsolution or inversion. Compositional layering is well developed and remnant quartz is elongated and strained. Possible hydration and recrystallization of matrix but no secondary cements (Figure 20).

The development of cataclastic breccias indicates faulting in the immediate area which is confirmed by breccias and fault gouge with slickensides along the fault zone. The cataclastic breccias are present in various rock types with angular fragments contained in a crushed or pulverized matrix cemented by secondary calcite or hematite.

The three developmental stages of mylonitization are easily distinguished from the breccias in hand specimen and thin section. The mylonites are pronounced only within the pegmatites and appear to be related to the more brittle minerals of the rock assemblage. Shearing is the dominant mechanism resulting in rounding and granulation of the mineral constituents and a development of "flow banding" around augen without the introduction

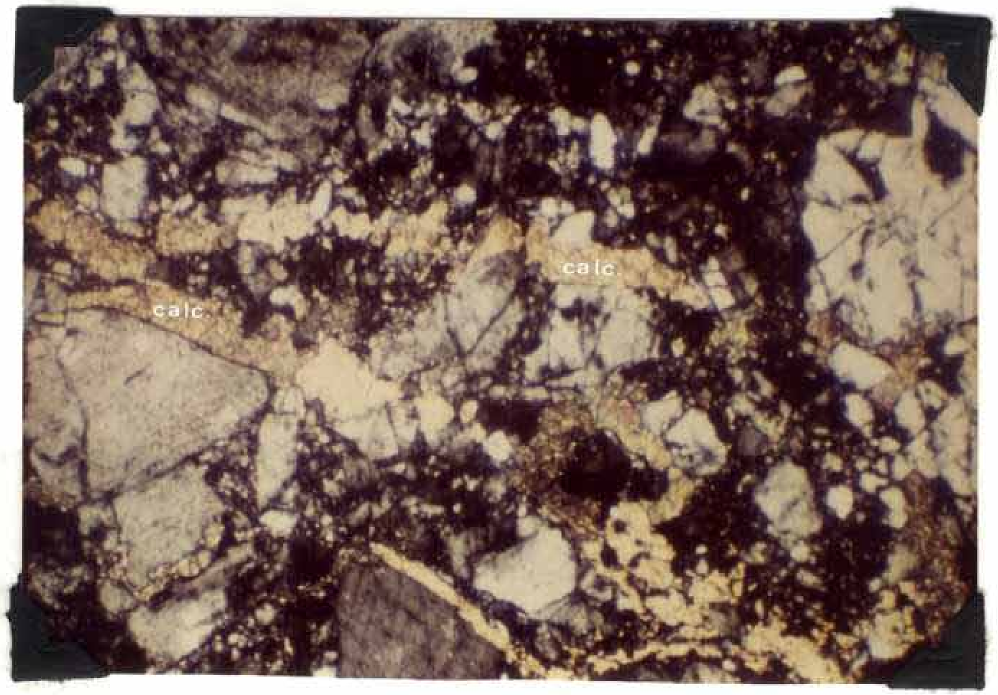

Figure 17. Photomicrograph of cataclastic breccia texture. Note angular fragments are fractured and crushed with the cryptocrystalline matrix unfoliated. Interstices filled with secondary calcite (calc.). Field of view 2.0 x 1.45 mm with crossed nicols, (sample A.D. 91; Appendix A).

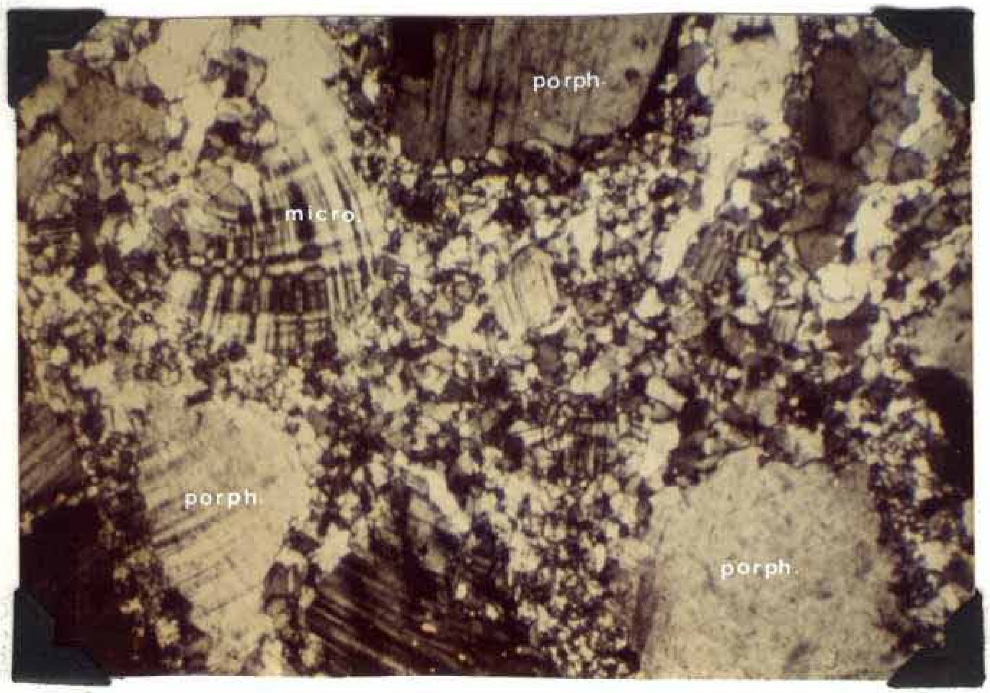

Figure 18. Photomicrograph of protomylonite texture. Strained, granulated porphyroclasts (porph.) are rounded and embedded in non-foliated cryptocrystalline matrix (mortar structure). Note deformed-bent gridiron twinning in microcline (micro.). Field of view 2.0 x 1.45 mm with crossed nicols, (sample A.D. 60; Appendix A).

Figure 19. Photomicrograph of porphyroclastic mylonite texture. Lenticular porphyroclast contained in moderate foliated cryptocrystalline matrix with compositional layering developed. Note bent-deformed gridiron twinning in microcline (micro.). Field of view 2.0 x 1.45 mm with crossed nicols, (sample A.D. 61a; Appendix A).

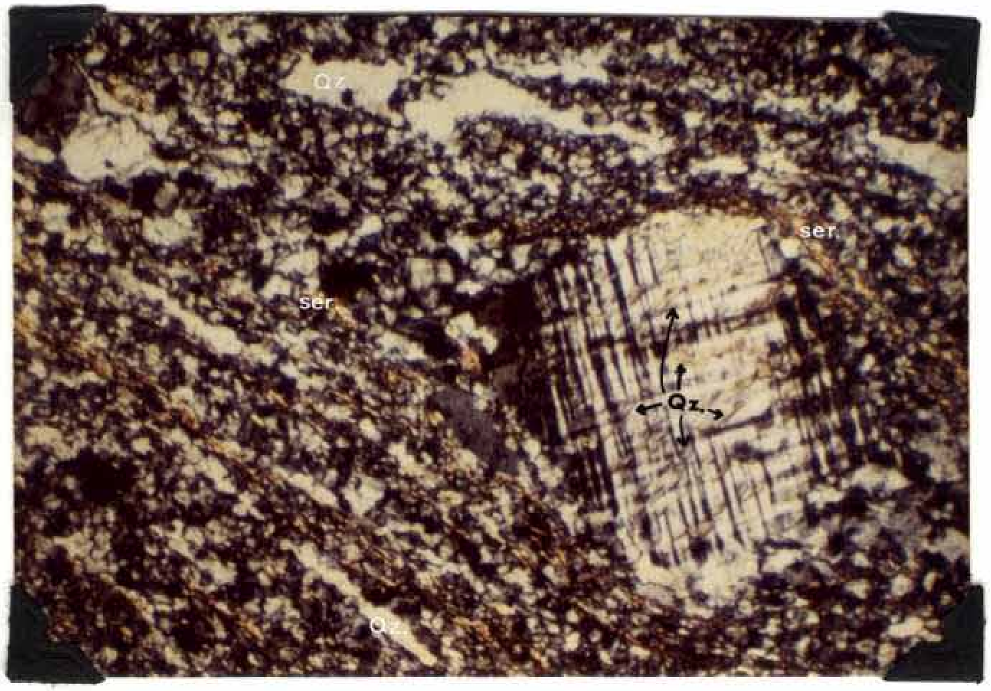

Figure 20. Photomicrograph of ultramylonite texture with remnant porphyroclast. A small lenticular porphyroclast of microcline with micrographic intergrowth of quartz blebs (Qz.) engulfed in a well foliated matrix exhibiting parallel compositional banding enhanced by strained, elongated quartz (Qz.; recrystallized ?) and hydration of matrix with very fine grained sericite (ser.). Field of view 2.0 x 1.45 mm with crossed nicols, (sample A.D. 97; Appendix A).

of secondary cements.

Extrusives - The Tertiary mudflows and rhyolitic sediments (Tms) are composed of volcanic extrusive materials deposited in a standing water environment. Deposition of such a unit represents a secondary (indirect) reworked deposit of volcanic materials whereas primary (direct) extrusive volcanic activity was not observed in the Lost Basin Range. However, the entire region is recognized as having a considerable amount of Cenozoic volcanism. Immediately to the south, Blacet (1975) mapped Miocene basalt flows capping Iron Mountain and noted basalt plugs near the Iron Springs Basin.

North of Lake Mead, Lucchitta (1967) discussed the significance of the youngest lavas in the area that overlie alluvial gravels deposited by the Colorado River. These lavas flowed from the north down into Iceberg Canyon and out to Sandy Point (west of the Lost Basin Range). He considered the flows equivalent to the Grand Wash Bay lavas. Damon (1965) provided radiometric age dates of 2.0 $\pm$ 1.4 m.y. B.P. for the Grand Wash Bay basalts and 2.6 $\pm$ 0.9 m.y. B.P. for the basalts at Sandy Point. Further north in the Virgin Mountains near St. Thomas Gap, Longwell (1921) described the Horse Spring fm., which is older than the Muddy Creek fm., but the beds are tilted steeply and are overlain unconformably by younger deposits. Lucchitta (1967) mentioned that the Horse Springs fm. was deposited on a surface of high relief that was tectonically unstable. Volcanic tuffs within this formation have been age dated using potassium-argon methods. Armstrong (1963) showed an age of 23 m.y. B.P. and Damon (1965) reported 19.6 $\pm$ 0.8 m.y. B.P.; an early to middle Miocene age is agreed upon.

Young (1966) studied the Cenozoic deposits on the Hualapai Plateau to the southeast and decribed the Hualapai volcanics which contain the

Peach Springs tuff. A potassium-argon age date of 18.3 ± 0.6 m.y. B.P. was reported by Damon (1964) for the Peach Springs ignimbrite.

Early descriptions by Schrader (1909) of the Kingman volcanic series to the southwest were elaborated on by Thomas (1953). Thomas distinguished four separate volcanic events. The Bull Mountain series, the oldest, is 1,000 feet thick containing flows, tuffs and breccias of andesitic to basaltic composition overlying an erosional surface cut into the Precambrian basement. The next unit, the Kingman rhyolite series, overlies the Bull Mountain series along an erosional and faulted contact consisting of pyroclastic material, rhyolitic to andesitic in composition. Then, capping a faulted and bevelled surface on the Kingman series is an andesite flow. The last episode is represented by an olivine basalt flow interbedded with alluvial gravels. Lucchitta (1966) suggested the gravels are equivalent to the Muddy Creek fm. and inferred a Miocene-Pliocene age for the latest event.

A similar sequence of extrusives occurs in the vicinity of Hoover and Davis Dams to the west (Longwell, 1963) where volcanics unconformably overlie the Precambrian complex. The Patsy Mine andesites and basalts (Oligocene or older) are overlain by the Golden Door pyroclastic volcanics which are rhyolitic to andesitic in composition. These rhyolitic rocks were dated by Armstrong (1963) as 17 ± 1.0 m.y. old and are overlain by the late Miocene Mount Davis andesites and basalts (Lucchitta, 1966). The Tertiary mudflows and rhyolitic sediments (Tms) were suggested by Blacet (1975) to be "equivalent to the middle Miocene Mount Davis volcanics (12-15 m.y. old)."

Discussion and Correlation

Tentative correlation of the Precambrian rocks of the Cerbat Mountains with those from the Virgin Mountains and the Vishnu schist of the Grand Canyon was considered by Thomas (1953). Both Longwell (1936) and Volborth (1962) suggested the Precambrian rocks of the upper Lake Mead area corresponded in age to the Vishnu series. Krish (1974) directly correlated the Precambrian complex in the Lost Basin Range as being equivalent to the Cerbat complex. This author considers the Lost Basin Range equivalent in age to the Cerbat and Virgin Mountains; many of the lithologies are similar but the post-Precambrian plutonic intrusives characterizing the Cerbat complex are absent within the Lost Basin Range.

The absence of Paleozoic and Mesozoic rocks in western and southern Mohave County could be interpreted as: 1) the result of non-deposition during that period of time for the area; 2) deposition and removal of a thin veneer of sediments; or 3) deposition of a thickness of sediments comparable to the surrounding areas with later removal by an extended period of erosion. Based on isopach maps and regional correlations of thicknesses, the third hypothesis is most acceptable (Lucchitta, 1966).

A regional correlation of Tertiary volcanic rocks deposited in pre-Muddy Creek time was developed by Lucchitta (1966). During deposition of the Horse Springs fm., pyroclastic volcanic activity occurred and the percentage of volcanic material increased to the west, suggesting possible volcanic sources in that direction. He considered the older Bull Mountain volcanic series near Kingman (Figure 1) similar to the Patsy Mine volcanics to the west, near Davis Dam. Lucchitta (1966) did point out that the volcanic sequence on Hualapai Plateau thinned to the northeast and suspected the volcanic sediments were derived from a source to the southwest beyond the Grand Wash Cliffs. He correlated the Peach Springs tuff on the plateau (Young, 1966) with the Golden Door volcanics near Davis Dam (Longwell, 1963) and the lower tuff unit of the Horse Springs fm., in the Virgin Mountains (Figure 1). He further suggested the Kingman rhyolite series is possibly equivalent in age to these regionally distributed volcanic horizons.

Such a correlation of pre-Muddy Creek volcanics suggests a similar age association for the Tms volcanic sequence in the mapped area (Figure 2, Plate I) based on stratigraphic position and volcanic composition. However, the relations between thickness and distance to known eruptive centers make these correlations speculative regardless of the age dates and lithologic correlations (Lucchitta, 1966).

Lucchitta (1966) did consider the Horse Springs fm. to have extended to the south and east for short distances from the type locality in the Virgin Mountains (Figure 1). This formation represents the youngest stratigraphic unit deposited prior to the main episode of Basin and Range faulting that dominates the upper Lake Mead area. This area is contained in the Grand Wash Trough which developed after deposition of the Horse Springs fm. to the north and the Tms unit in the map area, but prior to deposition of a majority of the Muddy Creek fm. (between 10 and 20 m.y. old).

The contact between the Horse Springs fm. and the Muddy Creek fm., to the north (Figure 1), and the tuffaceous mudflow and rhyolitic sediments (Tms) and the Muddy Creek fm., in the mapped area (Figure 2), represents a period of intense deformation followed by erosional planation during deposition of the fanglomerates (Tmc). The deformation consists chiefly of high-angle, normal faulting with a dominant dip-slip movement, producing structural basins which acted as catchment basins for the various facies of the Muddy Creek fm. It resulted in the unconformable contact between the Muddy Creek fm. and older rocks (eg. Horse Springs fm. and Tms unit).

The Muddy Creek fm. in the study area has been slightly deformed and tilted with original depositional attitudes preserved locally along Grapevine Mesa. An interesting feature is the elevation of Lone Jack ridge which nearly exceeds Pai Peak. Lucchitta (1966) considered the crystalline-clast subfacies of the Muddy Creek fanglomerate to have been partially derived locally from the Precambrian complex in the Lost Basin Range (Infernal Mountains). However, he did point out that the elevation of Grapevine Mesa indicated the Infernal Mountains were an inadequate source area for such a thick accumulation of sediments. Instead he inferred a higher, more western source for this portion of the fanglomerate.

An important correlation is the age of the mudflows and rhyolitic sediments unit (Tms). Lucchitta (1966) considered these sediments part of the Muddy Creek complex. The author considers these sediments to be approximately eqivalent in age to the Golden Door rhyolitic volcanics near Davis Dam and the Kingman rhyolitic series in view of Lucchitta's regional correlation of the Tertiary pre-Muddy Creek volcanics. The Tms unit is considered a separate lithologic unit from the Muddy Creek fm. based on:

1) a marked angular unconformity between the units;
2) the degree of deformation of the Tms unit exceeds any deformation observed within the Tmc and the stratigraphic position tends to infer more of a correlation to the Horse Springs fm.;
3) overall compositional diversity between the two units;
4) considerable contrast in hand specimen and thin section of the tuff layers between Tms and Tmc;
5) major dissimilarities in composition between the mudflows of the Tms unit and the crystalline-clast conglomerates of the Tmc unit;
6) thick, cyclic sequence of volcanic derived sediments within the

Tms unit; whereas the Tmc unit exhibits no internal structure or structured layering resembling the Tms unit and volcanic content is considerably less;

7) the volcanic and clastic material in the Tms unit suggests a more distant source (eg. Kingman and/or Mount Davis volcanics and Cerbat porphyritic granites) vs. a nearby source (White Hills and Lost Basin Range Precambrian complexes) for the Tmc unit;
8) the deposition of the Tmc unit onto a surface cut across the Tms unit and the Precambrian granitic migmatite ($P\mathcal{E}_4$);
9) depositional environments for the Tms and the Tmc units are contrary (Tms--quiet water, horizontal finely stratified deposition; Tmc--semiarid, inclined alluvial deposition).

These lithologic distinctions establish a pre-Muddy Creek depositional unit which is being exhumed from beneath a thick basin fill and is separated from the Muddy Creek fm. by deformation and an erosional surface. Lucchitta (1966, p. 68) mentions that, prior to the main deformation of the area and deposition of the Muddy Creek fm., "the sedimentary and the volcanic rocks of the area were subhorizontal and relatively undeformed, and showed a regional dip of a few degrees to the northeast." Vigorous erosion during pre-Muddy Creek volcanism is indicated by coarse clastic deposits, beveled flows and pronounced erosional surfaces in the volcanic rock terrains near Hoover and Davis Dams and in the vicinity of Kingman (Figure 1). This implies a south to southwest volcanic source area for the mudflows and rhyolitic sediments unit (Tms) that was transported to the north and deposited in the Lost Basin Range.

STRUCTURE

Regional Setting

The Lost Basin Range is included within the Basin and Range structural province but lies along the eastern margin. The Grand Wash Cliffs define the western margin of the Colorado Plateau as well as the eastern fault boundary of the Basin and Range Province. The western portion of the Virgin Mountains, to the northwest, marks the eastern limit of a Laramide thrust belt that was later modified by high-angle faulting. The Lost Basin Range is contained in the Grand Wash Trough (Lucchitta, 1966) which represents a large tilted-block basin within the Basin and Range Province. The main structural features in the "Trough" are late Miocene, north to northeast trending, high-angle normal faults with the west side downthrown and tilting to the east. In this area, faulting dominates over folding.

Unconformities

Nonconformity - The depositional surface cut on the Precambrian complex beneath the Tertiary sediments represents a prolonged period of regional uplift and extensive erosion of the sedimentary cover. The boundary is generally inferred from topographic relief because a thin colluvium weathers from the fanglomerate concealing the actual contact. A sharp contact exposing considerable depositional relief was observed in the Migmatite Valley, between the granitic migmatite ($P€_4$) and the mudflows and rhyolitic sediments (Tms) and the Muddy Creek fanglomerates (Tmc).

Angular Unconformity - The contact relationship between the Tms and Tmc map units is marked by a distinct angular discontinuity in strikes and dips between the two units. A period of severe deformation folded the Tms unit into a steeply dipping isoclinal syncline. Following the deformation, erosion cut a nearly plane surface upon which the Tmc unit was deposited.

Folds

Antiforms and Synforms - Folding of the Precambrian rocks in the study area is minimal; infrequent minor asymmetric folds within amphibolites are present. The general strike of foliation of this area is dominant to the northwest. In the northern portion of the mapped area, the strikes vary from a north to northeast direction. The change is attributed to small folds, along the northwestern flank of the range, plunging north to northwest and causing foliation to curve to the northeast (Krish, 1974). Other major variations in foliation are present in the vicinity of Copper Blowout basin and the northern portion of Wall Street. A broad antiform structure, plunging to the north, is included in the quarry area with the eastern limb of the fold obscured by alluvium. An antiform and synform with a common limb is exposed in the upper portion of Wall Street; the folds strike northwest across the southern portion of the Altered Valley and terminate abruptly against a major fault zone (see Plate I).

Domal Structure - In the S.W. $\frac{1}{4}$ of section 4 and the N.W. $\frac{1}{4}$ of section 9 of T.29N., R.17W., along Copper Blowout ridge, alwell-developed domal structure of low relief is outlined by foliation and compositional layering within the migmatitic gneiss unit ($P\!\!\!\!C_1$). This structure appears related to metamorphism of the Precambrian complex rather than the result of deformation during a later structural event.

Synclinal Fold - The mudflows and rhyolitic sediments (Tms) in the Migmatite Valley are folded into an isoclinal syncline with near vertical dips. The beds are upright except in one exposure towards the eastern outcrop margin, where the rocks are overturned. The overturning is attributed to a slump block of Muddy Creek sediments and appears to be a local feature. The Tms is bounded to the north by a low angle fault. Adjacent to the fault, the strike of the bedding bends sharply around from N.30°W. to N.50°E., but without local brecciation or disruption of the bedding structures.

Joints

Minor development of joint sets in the study area is generally associated with zones of faulting. A northeast striking set is dominant with a secondary set of northwest joints poorly developed. The northeast joints are sporadic with moderate to steep dips and are indeterminate away from the fault zones. In a few locations, mineral lineations in the rocks had a northwest strike and a low to moderate plunge to the northwest.

Faults

General - The majority of faults within the Precambrian complex of the Lost Basin Range are high-angle normal faults with the west side downthrown and accompanied by tilting or rotation of the fault-blocks to the east. The age relationship of these structures is difficult to establish, but most faults that can be traced to the Muddy Creek contact disappear under the fanglomerate. The area immediately north of this map area was mapped by Krish (1974) and is dominated by a series of northeast trending faults with secondary northeast and northwest trending sets of mineralized fractures. The faults generally dip steeply to the northwest with the downthrown block on the west. The area mapped in this study contains three basic types of fault structures: 1) a major, north-trending, normal fault with a subordinate northeast striking set of faults; 2) a high-angle reverse fault; and 3) a low-angle transverse fault.

Normal Faults - A prominent north-trending fault extends the length of the mapped area in the Lost Basin Range. Fault gouge and breccia are prevalent along the trace of the fault. Strong mylonitization of pegmatites, adjacent to faulting, suggests shearing as an important component of the displacement. In the southern portion of the mapped area (see Plate I), a roughly parallel series of faults branch from the main structure, extending into the Wall Street area and outlining a tilted fault-block of paragneiss ($P\mathcal{E}_3$) to the west. These fractures continue south along the western flank of the Migmatite Valley after being offset to the west by later faulting. The fissures dip steeply to the west with the western blocks downdropped. Trends of fault striae and slickensides range from directions parallel to dip-slip to directions parallel to strike-slip of the steep fault surfaces. Vertical dip-slip movement represents the major component of displacement; however, the amount of displacement is indeterminate. Additional evidence suggesting normal movement is found in the western portion of the Copper Blowout basin and further north in the western $\frac{1}{4}$ of section 4, T.29N., R.17W. This evidence consisted of well-developed drag folding of several amphibolites and unmineralized quartz veins adjacent to the fault trace. Right-lateral strike-slip movement may also have occurred at some point along this main fracture. A lack of continuity of individual lithologic layers across the structure suggests such an offset. Displacements of larger magnitude have been reported in the Lake Mead region and therefore cannot be dismissed from this area entirely (Longwell, 1974; Bohannon and Anderson, 1978).

The axis of the Altered Valley is occupied by this major fracture. The Altered Valley is the expression of a zone of extensive fracturing and confined alteration-mineralization of the Precambrian host rock, about 1,200 feet wide. Deposition of mineralized veins occur within this fault zone and brecciation of vein material is common (Figure 21, page 74). Major displacement occurred after regional metamorphism had established the principal foliation trends in the Precambrian rocks and was prior to vein intrusion and mineralization (late Cretaceous ?). Dings (1951) considered the major activity along fissures in the Cerbat Mountains to have occurred early in the Nevadian orogeny (late Jurassic-early Cretaceous). The association of veins with the fault suggests it existed as a preferred zone of weakness for the hydrothermal fluids. Brecciation of the veins indicates considerable movement during and/or after their injection. Such activity could represent later fault adjustments or renewed displacement along these previous structures. Similar features were described by Dings (1950) in the Cerbat complex.

The subordinate set of northeast trending faults has generally less than 100 feet of displacement on individual fractures and are of limited extent. Normal dip-slip movement, on steeply dipping fault traces, can be determined by offsets of small drag folds or occasional marker beds (eg. magnetite-bearing quartzite). Only one fault in section 5 could be directly correlated to the major fault fissure. The other two sets of faults in section 5 are of indeterminate age or association.

Reverse Fault - A high-angle reverse fault is shown in the northwest corner of the map area. This fault had previously been mapped by Krish (1974) as a low-angle normal fault. Outcrops west of the fault zone represent the thick sequence of amphibolites and pegmatites which characterize the lower stratigraphic horizon of the paragneiss complex ($p\mathrm{C}_2$). Similar outcrops are exposed to the southeast along the mountain crest. Mapping to the north along the strike of the fault zone indicates a fault trace dipping steeply west and supports an interpretation that reverse faulting has repeated part of the lower section of the $p\mathrm{C}_2$ unit. The strike of the fault gradually curves to the northeast where dips on the fault surface become lower and indications of movement are much less discernible.

Transverse Fault - A low-angle, northeast striking, normal fault, of limited exposure (Figure 6), intersects some of the major fault structures in the map area and disappears under alluvial gravels in the Migmatite Valley. The transverse fault displaces north-trending fractures towards the western side of the valley and the Muddy Creek fm. is juxtaposed against the paragneiss complex ($P\epsilon_2$) in Wall Street. The trace of the fault is characterized by abundant breccia and sharply contrasting lithologies. A low-angle south-dipping attitude is inferred from exposures of the fault in a few drainages and it's relations with topography. A minimum of 300 feet of displacement with the southern block downthrown is estimated from an average dip of 20°E. for the Muddy Creek fanglomerate. The fault is post-Muddy Creek in age and one of the youngest structural features in the area. Similar structures of greater magnitude are reported by Longwell (1945) in Iceburg Canyon between the Lost Basin Range and the South Virgin Mountains. The bending of the beds in the Tms map unit may be attributed to activity along this structure but this could not be confirmed.

Discussion - The strike length of the Migmatite Valley is characterized by a large depression that extends north along the axis of the Altered Valley. This physiographic feature may be the result of a paleo-drainage or scour zone which was later filled with Tertiary gravels or preferably an expression of a major downdropped, rotated fault-block that developed during late Miocene Basin and Range deformation.

The north-trending fault fissures on the western flank of the Migmatite Valley contributed local variations of fault-block rotation along the southern portions of this structure. Field evidence south of the mapped area consists of displaced Tertiary sediments (Tmc) juxtaposed against sheared and brecciated Precambrian rocks along the eastern portion of the valley (Lucchitta, 1966). Such outcrops suggest a fault structure along the eastern side of the Migmatite Valley representing a large downthrown western block with major rotation of the fault-block. Blacet (1975) projected a north-trending fault paralleling the contact between the Muddy Creek fm. and the mudflows-rhyolitic sediments along the western limb of Grapevine Mesa. The older Tms unit could be preserved in a downdropped rotated fault block by the following sequence of events:

1) horizontal deposition of Tms volcanic sequence on an erosional surface cut in the Precambrian rocks;
2) late Miocene folding of the Tms unit prior to fault displacement;
3) normal, high-angle, dip-slip faulting to the west with a strong rotational component downdropping and preserving a portion of the deformed Tms unit against the Precambrian complex along the fault zone;
4) Erosional planation and deposition of the Muddy Creek fm. over the Tms unit, the Precambrian complex and the fault structure;
5) later displacement by reactivation along the previous fault structure could displace the fanglomerates (Tmc) locally;
6) recent erosion of the fanglomerates along the retreating western flank of Grapevine Mesa, exposing the geology concealed beneath the Tmc unit.

The author considers a northern extension of an eastern-most structure possible, however in the mapped area, no faulting between the Tms and Tmc units was found (as mapped by Blacet, 1975). A continuation of the poorly defined fault structure, along the eastern flank of the Altered Valley, into the Migmatite Valley is feasible. The only feature in the mapped area that could infer faulting along the eastern boundary of the Migmatite Valley is the exposure of overturned (Tms) sediments associated with a slump block of fanglomerate (in N.W. $\frac{1}{4}$ of section 21). The overturning of the near vertical sediments might be the result of movement (?) along an unexposed fault.

Later displacement along the transverse fault possibly enhances the physiographic expression of the Migmatite Valley by severing the north-trending structures from their northern extensions and preserving a thick sequence of Muddy Creek sediments along Lone Jack ridge (Figure 6).

METAMORPHISM

Regional

The Precambrian rocks of the Lost Basin Range represent a high-grade, regionally metamorphosed terrain that has been strongly deformed during several periods of folding, faulting and granitic (migmatite) intrusion (Blacet, 1975). An age date of 1.7 b.y. for the regional metamorphism was reported by Krish (1974, p. 54), from Rb-Sr methods on hornblende from Garnet Mountain, nine miles south of the Lost Basin prospect.

The paragneiss ($P\epsilon_2$) and granodiorite gneiss ($P\epsilon_3$) complexes represent the principal rock types in the Precambrian complex of the Lost Basin Range. The foliation trends in the complex parallel layering; the compositional layering appears to be primarily the result of metamorphic differentiation. A gneissic-granoblastic to schistose-nematoblastic texture dominates the Precambrian complex and represents a strong regional metamorphism resulting in extensive metamorphic recrystallization of the original mineral assemblages. These rocks were formed by a moderate-grade (amphibolite facies) regional metamorphism of older sedimentary rocks with complete obliteration of original sedimentary structures.

Petrographic evidence in amphibolites from the mapped area supports criteria suggested by Spry (1976) indicating a moderate to high grade of metamorphism. This evidence includes: 1) a general increase in grain sizes, particularly felsic minerals, 2) a tendency towards equivalence in grain sizes, 3) a change from ragged to smooth, straight grain boundaries, and 4) a decrease in the number of mineral inclusions and poikiloblastic textures. A few amphibolites, discussed earlier (p. 14, 42), exhibit relict igneous textures; however, plagioclase has recrystallized to granoblastic aggregates and hornblende is only slightly poikiloblastic with quartz inclusions. Variations of layered to "striped" amphibolites are common, representing a strong development of leucocratic and melanocratic layers as a result of metamorphic differentiation. These features support a moderate to high degree of metamorphism characteristic of the amphibolite facies.

The occurrence of granitic migmatite ($P\epsilon_4$) in the Precambrian complex indicates a late injected phase of assimilated rock originating in a higher temperature-pressure regime than associated with the $P\epsilon_2$ and $P\epsilon_3$ rocks. This rock unit exhibits two differentiated (zonal) facies (p. 25) with deformed and contorted boundaries suggesting an intrusive nature. Petrographic evidence from the outer schistose zone of the granitic migmatite suggests an upper amphibolite to sillimanite facies of metamorphism, based on sillimanite, garnet and magnetite replacing abundant biotite (Figure 7).

Retrograde

An approximate 1,200 foot wide zone containing an intense pervasive mineral alteration suite characterizes the length of the Altered Valley down into Wall Street and along the western flank of the Migmatite Valley. In hand specimen, the original rock lithologies are difficult to identify and the mineralogy is indeterminate due to the amount of oxidation and mineral breakdown. Only by petrographic examination was the author able to confirm relict grains from pre-existing mineral assemblages common in the moderate-grade (amphibolite facies) regional metamorphism. The alteration assemblage represents a more hydrous "lower grade" metamorphic suite replacing and altering the higher grade mineral group. The dominant breakdown of biotite into chlorite liberated enough iron to produce magnetite dust that forms halos around the relict crystal outlines. Later, supergene weathering processes further oxidized the iron to limonite. Hornblende is also strongly chloritized and partially replaced by epidote and calcite. The potash-feldspars are argillically altered with slight to moderate sericitization of the cores. The plagioclases are intensely altered to kaolinite and contain abundant sericite. Only a minor amount of albite with epidote, zoisite-clinozoisite or calcite replaces the plagioclase.

Petrographic evidence suggests this zone represents a moderately strong retrograde metamorphism. The extent of this zone coincides with the boundaries of the rotated fault-block previously described (p. 64-66). This fault-block of Precambrian rock contains the only significant folding observed in the Precambrian complex and was subjected to strong post-Precambrian faulting and mineralization. Therefore, it is possible to attribute a retrograde metamorphism, that is imposed on the regional assemblage, to a combination of the following:

1) influences of structural deformation (eg. folding) as described by Carpenter (1968);

2) the effects of dynamic metamorphism (mylonitization; Spry, 1976, p. 301) observed within the pegmatites and in the immediate vicinity of faulting; and

3) the introduction of fluids during restricted hydrothermal activity.

The individual effects from each of the events are petrographically irresolvable. Whether the events are simultaneous or separate is indeterminate; however, the events do complement each other in terms of the results.

MINERALIZATION AND ALTERATION

INTRODUCTION

Mineralization within the Apache Oro mining claims is represented by three feasible types of deposits: 1) hydrothermal vein mineralization containing principally gold, silver and copper; 2) placer gold deposits adjacent to the mountain range; and 3) a possible porphyry copper deposit at depth. Major interest in the Lost Basin Range since 1886, has been in the gold mineralization. Schrader (1909, 1917) mentioned the development of small mining prospects along gold and silver-bearing veins, mostly occurring in the southern half of the range. A later discovery of placer gold deposits was made in 1931-1932, flanking the range on the east and west (Wilson, 1933). Since that time renewed investigations by Mallory (1971a, 1971b, 1974b), Post (1970), and Krish (1974) have suggested a possible porphyry copper prospect within the Lost Basin Range and considered it to be associated with the other types of deposits.

VEIN MINERALIZATION

Occurrence

Quartz veins observed in the study area represent three basic types of vein structures. The first type, mentioned earlier (page 44) consists of "bull" quartz to quartz-iron carbonate veins with minor pyrite; these appear to be transitional into the pegmatites. Type 1 veins are limited in extent and show no signs of mineralization. The remaining two types of veins are related to hydrothermal mineralization in the area. A second type consists of quartz-iron carbonate-sulfide veins with a general northwesterly trend and "appeared related" to the pegmatites (Trites, 1974). However, sporadic gold, silver and copper mineralization is found in these veins and they are considered subordinate to the major vein structures which constitute the third type of vein. Type 2 veins show marked dissimilarities in field relationships, textures and mineralogy from type 1. The second type of veins are contained within subordinate fractures that developed adjacent to pegmatites during pre-hydrothermal tectonic deformation (p. 63). The pegmatites acted as rigid buttresses during faulting within the Precambrian complex and produced secondary fractures in the vicinity of the pegmatites. This ground preparation provides avenues for later hydrothermal vein deposition along the open space fractures. Type 2 veins seldom exceeded 4 feet in width and are less than 100 feet in length; they are too small and mineralization is too sparse to be of economic value.

The third type of vein consists of major vein structures associated with the north trending fault zones in the area. The veins fill breccia zones along the faults and commonly dip steeply to the west; several show reversals in dip along the strike. Pronounced pinching and swelling along strike and dip is common. Type 3 veins have significant gold, silver and copper values and range from 4 to 8 feet wide. They can be traced as discontinuous lenses and en echelon bodies for about $1\frac{1}{2}$ miles along the southern portion of the fault system in sections 9, 16 and 17 of T.29N., R.17W. Type 3 veins have higher grades of mineralization localized in small ore shoots as shown by the distribution of previous mine workings plotted along the fissure zones (see Plate I). Veins similar to types 2 and 3 have been described further north of this study area in the vicinity of the Ford mine (Trites, 1974).

The Copper Blowout knoll and quarry, and the Golden Copper area (Plate II) exhibit strong gossans that are derived in part from the oxidation of sulfides and gangue minerals and in part are inherent with the hydrothermal suite. Krish (1974) described "indigenous goethitic and hematitic limonites after pyrite and chalcopyrite" and noted that these minerals were commonly masked by secondary limonitic coatings formed by the oxidation of the sulfides and the iron carbonate gangue.

The most pronounced copper mineralization is in the Copper Blowout area, in the S.W. $\frac{1}{4}$ of S.W. $\frac{1}{4}$ of section 4 and the N.W. $\frac{1}{4}$ of N.W. $\frac{1}{4}$ of section 9, T.29N., R.17W. Remnants of hypogene mineralization consist primarily of pyrite and chalcopyrite in numerous subordinate veinlets permeating the host rock. These appear to be controlled by fault zones that parallel the axial planes of the antiform structure in the quarry and the domal structure on the knoll. Weak pervasive propylitic alteration affects the peripheral host rock with moderate phyllic and argillic alteration adjacent to the veinlets (samples A.D. 77, 83, 102, 103; Appendix A). Later remobilization of copper, iron and other metals by groundwater solutions may account for the localized oxidation, and the pervasive staining and precipitation along hairline fractures by secondary minerals (eg. malachite, azurite, minor chrysocolla, wulfenite (?), goethite and limonite). Type 3 veins are absent in the Copper Blowout area.

Mineralization in the Golden Copper area, in the middle of section 5 (Plate II), resembles that of the Copper Blowout area and was described by Krish (1974). The major distinction in the Golden Copper area is a single quartz-carbonate-sulfide vein (one foot wide) associated with two sub-parallel faults.

Characteristics

Several characteristics are common to the hydrothermal quartz-carbonate-sulfide veins observed within the study area. The basic descriptions apply to all types of mineralized veins with emphasis on the larger type 3 vein structures.

External Features - The most significant ore deposits fill north-trending fault fissures and occur as discontinuous lenses that commonly pinch and swell along strike and dip (Figure 21). The higher grades of mineralization are localized along small irregular ore shoots but wall rock control of the ore shoots is not apparent. Wider veins are commonly associated with steeper dips along the fault fissures; changes in strike and dip of the faults generate open spaces as do intersections of conjugate veins or faults. Open space filling seems to have been the mechanism of deposition for vein minerals. Trites (1974) reported ore shoots in the Ford mine, were "as much as 20 feet long, 5 feet wide and 45 feet in vertical height." He noted the gold values dropped off abruptly along the borders of these brecciated veins and that the gouge and less fractured vein material "usually contained less than 0.05 oz/ton of gold." The altered wall rock seldom exceeded 0.006 oz/ton of gold indicating a lack of any sigificant mineralization in the vein walls.

Ore mineralization of wall rock is absent although fine-grained disseminated pyrite commonly impregnates wall rock for distances ranging from less than one inch to several feet from the veins. Alteration of wall rock is moderate to slight, with a restricted phyllic (sericitization) zone adjacent to the veins. The outer fringes show a weak argillic alteration commonly masked by minor propylitic assemblages. Local silicification is found along zones of intense brecciation and shearing but silicification is never extensive.

A majority of the larger veins are intensely brecciated and shattered from post-mineralization movement along the faults. These fractured veins are recemented by later generations of quartz, calcite and iron oxides. Outcrops are usually resistant, milky white in color, and have occasional

Figure 21. Lenticular quartz-carbonate-sulfide-gold vein within the granodiorite gneiss complex (P€$_3$). Note the irregular concentric zoning of the brecciated white bull-quartz (Qz.) enclosing massive Fe carbonate (carb.), (sample A.D. 45a-c; Appendix A; location: S.E. $\frac{1}{4}$ of S.E. $\frac{1}{4}$ of section 17, T.29N., R.17W.).

splotches of limonitic brown to hematitic red oxides staining the quartz. Internal structures of the quartz veins range from irregular and massive to a poorly defined comb structure with a few vugs. A crude banding of massive quartz and iron carbonate gangue is common (Figure 21), while sulfides generally occur in narrow stringers and irregular masses.

Mineralogy - Milky white massive quartz accompanied by iron carbonate (siderite and/or ankerite ?) with varing amounts of subhedral to euhedral fine-grained pyrite are the most abundant gangue minerals. Minor amounts of specular hematite are associated with the carbonate and secondary quartz; calicte and iron oxides (limonite and hematite) fill fractures. Sulfides, in order of decreasing abundance, consist of fine- to coarse-grained, euhedral to massive blebs of oxidized pyrite, fine-grained, anhedral chalcopyrite and fine- to medium-grained, subhedral galena.

Gold occurs as native metal ranging in size from microscopic flecks to very fine megascopic blebs. The majority of visible gold is associated with limonite pseudomorphs after pyrite cubes. A considerable amount of gold is embedded in vuggy, brecciated quartz coated with either hematite or limonite and associated with secondary copper minerals. Trites (1974) suggested these oxidized deposits in the Lost Basin area are the result of secondary enrichment from oxidation of the primary sulfides, and he considered them equivalent to "bonanza gold ores." Similar enrichment of gold in the Cerbat complex has been reported by Hernon (1938). The major source of the silver in these veins is from the gold and argentiferous galenas. Unlike the Cerbat complex, no silver minerals in either the primary or secondary mineral suites of the Lost Basin District are reported.

Secondary minerals present in the veins are malachite, azurite, limonite, hematite, wulfenite, vanadinite and lesser amounts of chrysocolla and anglesite (?). The relative abundance of these minerals increases northwards towards the Copper Blowout area from the Van-Wulf portal and the High Voltage shaft (see Plate II).

Zoning - Internal zoning or partitioning of sulfides within individual veins is absent; however, field observations and geochemical results completed in this study suggest a subtle zoning of metal abundances with respect to their spatial distribution in the field (see Table 3 and Plate I). The majority of samples taken between the Van-Wulf portal, High Voltage shaft and the Copper Blowout area, have above average contents of Ag, Cu, and Pb with detectable amounts of Zn, Mo and V. Samples south of the Van-Wulf portal show higher ratios of Au-Ag and a marked decrease in other metals.

Schrader (1909, 1917) noted two sets of mineralized veins in the Lost Basin Range. One set is dominant north-trending Au-Ag bearing quartz veins that are abundant on the western slopes of the range. The second set is northwest-trending quartz veins, chiefly copper-bearing, in the central and eastern portions of the mountains. Mallory (1972, 1974a) has accumulated geochemical and geophysical data on the Lost Basin District and has plotted the dominant mineralogies observed in veins throughout the range. His information suggests a peripheral outer series of veins that are essentially barren of copper. Moving inward towards the Copper Blowout area and a "magnetic low" (see Figure 24), copper increases and higher gold values are found. In the Copper Blowout area gold values decrease considerably as lead, silver, molybdenum and copper increase in anomalous amounts (Mallory, 1971a).

Additional geochemical sampling by Post (1970) from the Wall Street area into the Copper Basin area, due north of this study, showed anomalous amounts of Au, Ag, Cu, Pb, Zn, Mo, Ni, Cr, Ba, As, V and Hg. His results appear to support Mallory's (1971a) regional zoning pattern for the metals. Post (1970) reports several high mercury anomalies in both the gold and copper-bearing veins. He noted that "although richer in the gold deposits, mercury appears to be associated both with the gold and copper mineralization, suggesting that they are contemporaneous and not Precambrian, for such high mercury values are seldom found in Precambrian ores."

Krish (1974) correlates his study area to the northern 2/3 of a Cu-Pb-Ag inner zone of mineralization and he defined three trace element zones within the Lost Basin property that coincided with the visible mineralization and the unaltered country rock.

Paragenetic Sequence

Based on petrographic analyses of samples from several mineralized veins and field observations, a basic paragenesis for vein mineralization in the Apache Oro mining claims has been developed (samples A.D. 29b-f, 44ab, 45a-c, 51, 52e, 53, 54b, 55, 56a, 77; Appendix A). The generalized paragenetic sequence is depicted in Figure 22. This figure demonstrates only a relative succession of hydrothermal deposition and two periods of post-depositional variation of vein mineralogy. The post-depositional periods represent 1) a MAJOR EVENT - characterizing a period of extensive brecciation followed by pronounced oxidation and fracture fill, and 2) a MINOR EVENT - representing a much later period of minor fracturing, oxidation and fracture fill. An example of the criteria used in determining the paragenetic scheme is shown in Figure 23. The example shows both grain contacts and cross-cutting relationships of individual minerals within a vein and the adjacent wall rock.

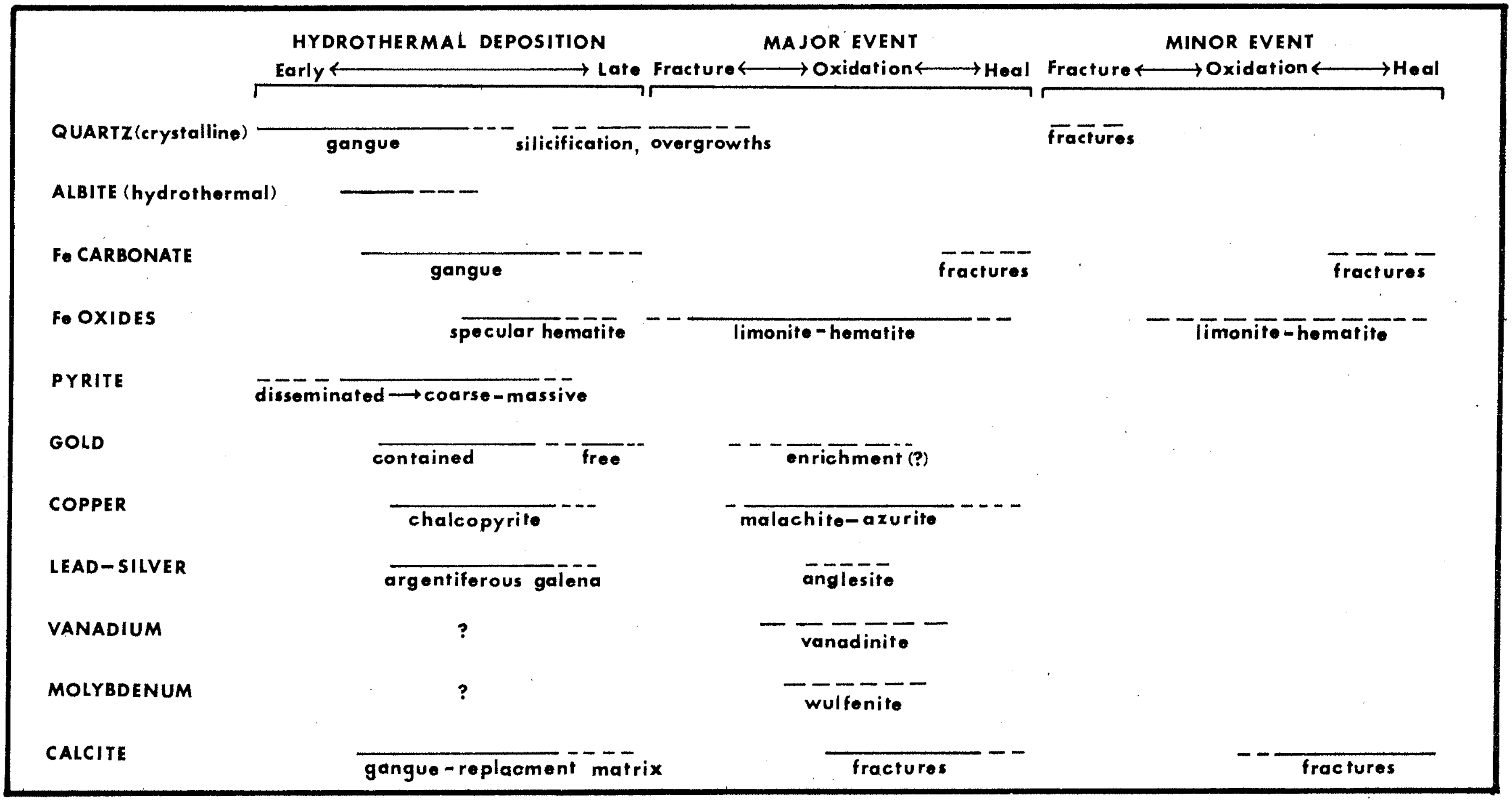

Figure 22. Paragenetic sequence of the hypogene and secondary minerals associated with vein mineralization observed on the Apache Oro mining claims.

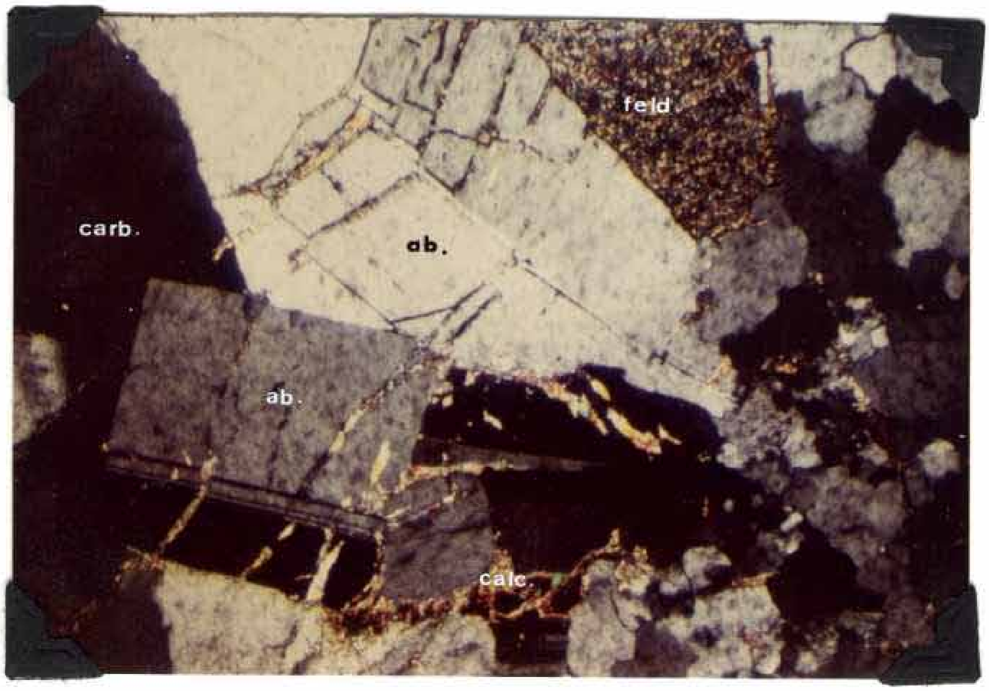

Figure 23. Photomicrograph of hydrothermal (?) plagioclase. Euhedral secondary unaltered albite (ab.) phenocrysts contained in Fe carbonate (carb.) vein. Note late fracturing filled with calcite (calc.) and altered feldspar (feld.) in host rock. Field of view 2.0 x 1.45 mm with crossed nicols, (sample A.D. 103; Appendix A).

Source

Earlier work by the U.S.G.S. indicated the mineralization in the Lost Basin and Gold Basin areas comprised two types of deposits: 1) gold-bearing quartz-carbonate-sulfide veins that "locally appear transitional into carbonate and sulfide-bearing pegmatites", and 2) gold-bearing porphyritic leucosyenite pipes (Blacet, 1969). A late Precambrian age was suspected for both types of deposits. The field relationships of the various types of veining in the study area noted earlier (p. 70) does not support a Precambrian age for the gold-copper mineralization nor is it directly associated with Precambrian pegmatites. Younger post-Precambrian pegmatites are possible but field data provides no evidence for such an occurrence. The leucosyenite pipes are not present in this map area and previous investigations in the Lost Basin Range by others do not report such structures. These deposits may exist only within the Gold Basin area and not in the Lost Basin District.

Krish (1974, p. 58) reported an age of 67 m.y. using muscovites from two widely scattered mineralized veins. Fluid inclusion work on quartz crystals from the veins indicates a temperature range of 190° to 220°C with the presence of CO_2 and a chloride brine. This information and the previous discussion of the vein mineralization suggest the vein deposits in the Lost Basin Range bridge the temperature boundary between the mesothermal and epithermal-type deposits discussed by Park and MacDiarmid (1975).

Geochemical analyses on native golds from the veins in the Lost Basin Range by Antweiler and Campbell (1979) yield gold signatures resembling signatures reported by Antweiler and Campbell (1977) from known porphyry copper deposits. These analyses are from samples less than six km apart at three localities along the crest of the Lost Basin Range. Antweiler and Campbell (1979) consider the results suggestive of the possible presence of an undiscovered porphyry copper deposit. Antweiler and Sutton (1970) reported one sample of Lost Basin lode gold, taken from section 8, T.29N., R.17W., containing a gold signature similar to the porphyry copper signatures.

Analyses of other gold-bearing veins, located elsewhere in the Lost Basin Range, are different than the clustered samples and when compared to the signatures from the placer golds, there is a noticeable dissimilarity (Antweiler and Campbell, 1979). A summary of analyses from both types of gold signatures determined from the Lost Basin vein gold is contained in Table 1 with a comparison of gold signatures from known porphyry copper deposits by Antweiler and Campbell (1977).

Additional spectrochemical analyses of native golds from approximately 77 lode gold samples from the Lost Basin Range are summarized in Table 2 (J.C. Antweiler, unpub. data, 1975), and substantiate the published analyses on the vein gold, from Lost Basin, reported by Antweiler and Campbell (1979). The magnetic intensity values associated with the data were provided by Mallory and apparently represent magnetic susceptibilities, however, the magnetic correlations are inconclusive (J.C. Antweiler, pers. comm., 1980).

The results of the gold signature analyses indicate the gold-bearing veins in the Lost Basin Range are not the source for a majority of the placer gold, adjacent to the range, when compared to the gold signatures of the placer golds reported by Antweiler and Sutton (1970) and Antweiler and Campbell (1979). The similarities of several lode gold signatures with those from porphyry copper deposits is striking and warrants continued investigation of such a possible association.

Table 1. GOLD SIGNATURES FROM PORPHYRY COPPER DEPOSITS AND THE LOST BASIN RANGE, ARIZONA

Location	Au %	Ag %	Cu %	Au/Ag	Au/Cu	Characteristic Trace Elements (In order of abundance)
Butte, Montana*	74.0	25.9	0.05	2.9	1500	Pb, Bi, Sb, Zn, Sn, Cr, Ni
Mineral Park,* Arizona	70.3	29.6	0.04	2.4	1800	Pb, Bi, Sb, Zn, As, Te
Cala Abajo,* Puerto Rico	74.8	25.1	0.15	3.0	500	Pb, Bi, Sb, Zn, Sr, Cr
Lost Basin Prospect,** Arizona	76.0	24.0	0.07	3.2	1085	Pb(20,000 ppm), Mo(1,000 ppm), Bi(100 ppm), Sn(70 ppm)
Lost Basin vein Au,*** Arizona (avg. 155 analyses)	80.5	19.4	0.08	4.1	1006	Pb, Bi, Mo, Sb, Zn, Pd, Ni, Cr, V, Te, Sn, As
Lost Basin Placer Au,*** Arizona (avg. 70 analyses)	88.7	11.2	0.029	7.9	3058	Pb, Bi, Mo, Sb, Zn

* Taken from Antweiler and Campbell (1977)

** Adapted from Antweiler and Sutton (1970)

*** Adapted from Antweiler and Campbell (1979)

Table 2. A SUMMARY OF GOLD SIGNATURES FROM LODE GOLD SAMPLES IN THE LOST BASIN RANGE, ARIZONA

(J. C. Antweiler, unpub. data, 1975)

No. of Au Samples # Analyses / # Samples	Magnetic Intensity (gammas)	Gold Average Fineness / Avg. %	Gold Range %	Silver (%) Avg. / Range	Copper (ppm) Avg. / Range	Au/Ag	Au/Cu	Hg (ppm)	Pb (ppm)	Bi (ppm)	Mo (ppm)	Other
4/6	1000-1050	741/73.7	70.6-76.7	26.0/23.0-29.0	390/220-560	2.85	1890	3,000	62,000	27	800	Sb, Zn
22/11	1050-1100	837/81.9	76.5-90.2	17.1/9.6-20.7	650/185-1500	4.78	1260	8,500	30,900	12	494	As, Zn, Sb, Te, W, Cd
37/15	1100-1150	750/74.0	61.4-86.6	24.6/12.8-34.9	716/300-3700	3.01	1033	12,700	7,500	385	325	Te, Pb, Sb, Zn, As, Sn, W
66/14	1150-1200	816/81.2	68.3-89.0	18.0/9.7-21.5	864/70-1300	4.51	940	6,900	6,000	56	153	Sb, As, Zn, Te
18/19	1200-1250	844/84.1	82.6-87.3	15.5/12.5-17.5	670/225-2250	5.43	1255	2,700	3,600	67	100	Pd, Te
24/12	1250-1300	855/85.0	71.5-91.4	14.7/8.5-29.2	378/75-700	5.78	2250	2,200	9,800	26	20	Te, Zn, Cd, Pd, Nb

Alteration

Hydrothermal alteration of the wall rock is generally irregular and confined to the immediate vicinity of the mineralized veins. A major exception is in the Altered Valley where the alteration is combined with a pervasive retrograde metamorphism that affects the Precambrian host rock the entire length of the valley.

Three basic zones of alteration were observed in thin-sections and hand specimens. These alteration zones represent a temperature difference between the host rock and the invading solutions, promoting reactions that permeate the host rock. The principle alteration assemblages include variable amounts of chlorite, sericite, clay (kaolinite ?), epidote and lesser amounts of silica and zoisite-clinozoisite. Accompanying the alteration is the apparent introduction of fine grained pyrite, calcite and iron carbonate into the alteration halos immediately adjacent to the vein.

The phyllic zone is a narrow, relatively high-temperature alteration zone immediately adjacent to the veins. The vein walls are sharply defined and characterized by restricted chloritization and sericitization of the adjoining wall rock. Chlorite commonly replaces biotite, hornblende and garnet while abundant sericite invades feldspar, showing preferential alteration of the plagioclase. Introduction of calcite, pyrite and quartz from the vein is pronounced.

Argillic alteration represents an irregular, discontinuous zone bordering the phyllic alteration with gradational boundaries. Strong alteration of potash-feldspar and plagioclase to clay characterizes this vague halo, with subordinate sericite replacing feldspar along the inner margins. Commonly, propylitic minerals replace both plagioclase and hornblende. The argillic zone is not always present and often difficult to distinguish when a considerable overlap of the other zones occurs.

A strong pervasive zone of propylitic alteration occurs within the Altered Valley and is attributed in part to the hydrothermal activity and in part to the retrograde metamorphism. This alteration suite represents the outer halo. The alterations are less complete and vestiges of the original mineralogy are common. Chlorite alters the fringes of biotite and hornblende while minor replacement of feldspar by epidote, quartz, and zoisite-clinozoisite is present. Minor amounts of pyrite, albite and carbonate were introduced. This alteration suite is more pronounced within more intermediate compositional rocks such as amphibolite.

Geochemistry

General - Geochemical samples of mineralized quartz veins and adjacent host rock were collected to assist the author in evaluation of the degree of mineralization of the Apache Oro claims. Twenty-six samples were analyzed for 7 major elements of economic importance by atomic absorption techniques. The elements of interest were Au, Ag, Cu, Pb, Zn, Mo and V. These metals were chosen due to the types of mineralization observed in the field and a suspected zoning of those metals based on observations.

Sampling and Analytical Methods - Sampling was conducted by first removing the top few inches of exposed rock to minimize surface contamination prior to sampling. Those samples taken from vein outcrops, or from within mines, were sampled continuously across the width of the cut. Those samples taken from the mine tailings represent larger composite samples taken in a radial pattern while descending the dump, in an attempt to minimize high-grading of the samples. Descriptions of each sample are given in Appendix E. Samples 45a and 45b were duplicated to evaluate the relative degree of reproductibility during analysis. A blank sample of Glorietta sandstone taken east of Socorro, N.M. was also submitted to evaluate the lower limits of detectability for each element and possible contamination as a result of sample preparation.

The method of sample preparation is described in Appendix E and is a modification of the basic procedures established by Allman and Lawrence (1972) and Hutchinson (1974). Analyses were run on a Perkin-Elmer model 403 atomic absorption spectrophotometer by a technican employed by Resources International Corp., on the Apache Oro mining property.

Results and Interpretations - Results of the analyses are summarized in Table 3 and the locations of the samples are shown on Plate II, with the exception of A.D. 57a and 57b which were taken on Evert Putnam's property adjacent to the Climax mine in section 33, T.30N., R.17W. During digestion of the samples, there appeared to be minor difficulties with a silver residue causing some of the values to be reported as a minimum due to incomplete solution (Bruce Maxwell, pers. comm., 1979). There is a discrepancy in the duplication of sample 45b*.

As discussed earlier, the most striking aspect of these results is a subtle zoning of metals. Samples A.D. 23, 78, 102, 103 and 104 suggest an inner zone towards the Copper Blowout area with higher values in Ag, Cu, Pb, Zn, and Mo. Samples A.D. 28, 45a-c, 52a-c and 105 tend to represent higher Au-Ag contents, with lower values in the other metals. These latter samples are located further away from the Copper Blowout area

---

*This sample had been analyzed for Au earlier by the author at the New Mexico Bureau of Mines laboratory using similar atomic absorption techniques on a Perkin-Elmer model 303 spectrophotometer. The assay results (duplicated) showed a Au value of 0.442 oz/ton, so the author considers the duplicated assay on 45b, reporting Au = 0.486 oz/ton, Ag = 0.055 oz/ton, etc., as being more representative than the first results.

Table 3

GEOCHEMICAL ANALYSIS OF MINERALIZED SAMPLES
Determined By Atomic Absorption Spectrographic
Techniques, Resources International, Meadview Arizona

Sample No.	Au (oz/ton)	Ag (oz/ton)	Cu (ppm)	Pb (ppm)	Zn (ppm)	Mo (ppm)	V (ppm)
AD-21 -77	0.069	0.004†	25	160	12	12	7
" 23 "	0.465	1.172	10600	7700	285	178	401
" 28 "	0.117	0.010	34	163	26	9	20
" 29a "	0.124	0.133	12	65	11	4	4
" 29b "	0.026	—	15	130	46	8	89
" 29e "	0.107	0.003	14	40	11	2	3
" 29f "	0.049	0.008†	10	140	27	19	35
" 44 "	0.006	0.006†	15	150	19	3	8
" 45a* "	0.002	—	34	82	7	1	36
	—	—	21	53	9	1	40
" 45b* "	0.159	0.002†	6	110	3	3	7
	0.486	0.055†	137	94	18	8	19
" 45c "	0.004	0.016†	7	25	9	1	1
" 52a "	—	0.012†	16	47	12	6	6
" 52b "	0.006	0.001†	16	83	7	3	62
" 52c "	2.091	0.903	490	56	52	18	70
" 54 "	—	0.004†	14	41	15	10	21
" 55 "	—	—	21	259	9	1	22
" 56a "	0.006	—	74	19	100	18	40
" 56b "	—	—	12	1	520	2	117
" 57a "	0.161	0.013	18	184	24	1	2
" 57b "	—	0.004†	41	1734	76	5	41
" 78 -78	—	0.072†	336	4332	2125	193	27
" 79 "	0.008	0.014†	21	14	124	3	32
" 102 "	0.067	0.684	10384	1528	109	4	6
" 103 "	0.172	0.007	31	410	60	14	23
" 104 "	0.154	0.311	2092	6856	342	1498	655
" 105 "	0.416	0.147	850	160	11	2	27
Glory-1	—	0.005	10	40	10	3	19

* sample repeated
— no values reported
† assay value reported as minimum due to incomplete analysis

(Plate II). The ratios of Au/Ag, Au/Cu and Au/Pb are another indicator of zoning:

Zone	Sample	Au/Ag	Au/Cu**	Au/Pb**
Au-Cu-Pb	23	0.397	0.001	0.002
	102	0.098	0.0002	0.002
	104	0.495	0.002	0.001
Au-Ag	28	11.7	0.118	0.025
	45b	8.84	0.121	0.177
	52c	2.32	0.146	1.279
	57a	12.40	0.306	0.030
	105	2.83	0.017	0.089

** The conversion of copper and lead values in ppm to oz/ton was by using ppm x 0.0292 = oz/ton as a conversion factor.

Such information is not conclusive or definitive of the zonal relationships suggested above. It does provide credence for the field observations and suggests the need of a more detailed and accurate geochemical sampling program if an accurate interpretation is to be made.

Drill Hole Analyses

A statistical study of Au and Ag assays from 54 shallow drill holes, in the study area, was evaluated using the computer facilities at New Mexico Institute of Mining and Technology. The computer program used was designed to calculate the means, standard deviations and a simple correlation coefficient matrix as described by Till (1974, p. 83-103). A list of the drill hole assays reported by Resources International Corp.

are in Appendix C and the drill hole locations are plotted on Plate II.

The drill hole assay intervals were converted into elevations based on approximated collar elevations ($\pm$ 5 feet) for each drill hole. This allowed each drill hole to represent a given observation with 20 variables (assay elevations) into which the gold or silver assay values could be programed. These 20 variables covered the ranges in sample elevations from 4075 feet to 3885 feet inclusively, for all 54 drill holes.

The purpose of this approach was to examine the possibilities of any limiting controls on the mineralization either vertically or horizontally. It was hoped that the presence of any secondary enrichment or a given horizon of higher gold-silver values would become evident in such an investigation. In addition, a majority of the drill holes were located within the Altered Valley and the author felt that the data examined might determine the potential of a broad, extensive, low-grade "gold fault zone" as described by Mallory (1974b).

Unfortunately, the results are inconclusive due to insufficient data. Approximately half the drill holes reported only 3 or fewer assays per drill hole. This limited number of observations resulted in randomly generated, repeated values by the computer within the lower portion of the matrix. However, such an approach still seems warranted providing a more consistent drilling pattern with uniform sampling intervals is designed to penetrate a specific target and establish a lower elevation boundary for sampling, (eg. 100 foot centered drill holes cross-cutting the fault zone diagonally down the strike length of the Altered Valley; core drilling, a minimum of 300 feet per hole, and continuous sampling in 5 foot composite intervals).

PLACER DEPOSITS

Occurrence

Placer gold deposits, flanking the Lost Basin Range on the east and west, have been sporadically mined since their discovery in 1931-1932 (Wilson, 1933). The detrital gold is derived from the crystalline-clast conglomerate subfacies of the Muddy Creek fm., which has subsequently been correlated as late Miocene-early Pliocene in age (Lucchitta, 1966, 1967). Wilson (1933) noted that the richer gold-bearing gravels were "confined mainly to the arroyo-bottoms." These deposits are generally less than 2 feet thick and rest upon untested, gold-bearing, caliche-cemented gravels. A majority of the placer mining of unconsolidated gravels derived from the Muddy Creek sediments, was done in an area of 8 to 10 square miles east of the Lost Basin Range, in the vicinity of the King Tut mine (Blacet, 1969). Knowledge about the average content or distribution of gold in the parent fanglomerate is minimal. The U.S.G.S. (1968) reported that the "potential gold resources in the King Tut area" could exceed 500 million cubic yards of gold-bearing fanglomerate "averaging 0.01-0.02 oz gold per cubic yard." These U.S.G.S. figures are based on an average depth of 100 feet for the gravels (Mallory, 1971b). Blacet (1969) mentioned gold values in the Quaternary arroyo gravels "to be highly variable" but that an average ore-grade in the vicinity of the King Tut mine "has probably been about 0.04-0.05 oz gold per cubic yard." This suggests reworking of the gold from the Tertiary fanglomerate and concentrating it in recent arroyo gravels. Presently, the Apache Oro placer mining claims represent approximately 17 square miles of unexplored fanglomerate on the eastern and western borders of the Lost Basin Range (Mallory, 1974b).

Characteristics

The detrital gold occurs in part as flour gold, from microscopic to visible flecks, and in part as coarse, ragged nuggets ranging up to 1/6 oz in weight. Both the gold and alluvial gravels become progressively finer grained towards the northeast (Wilson, 1933). An abundance of black sand is associated with the gold, consisting mostly of oxidized pyrite, magnetite, garnet, ilmenite, hematite and limonite. Gold recovered from the recent mine operations by Resources International Corp. is coarse and rough indicating a limited amount of transport from a source area. There is a noticeable abundance of dark grey chalcedonic matrix and inclusions within the coarser gold nuggets. This type of matrix is markedly dissimilar from the quartz gangue characterizing the vein mineralization in the Lost Basin Range.

Blacet (1969) noted that more than 50% of the placer gold represented ragged grains, one millimeter or more across, and the erratic distribution and coarseness made accurate sampling difficult. He reported that "rhombohedral and cubic molds, as well as pyrite pseudomorphs" were commonly preserved in the gold and that measurements of interfacial angles "established that much of the gold was originally deposited on euhedral clusters of ferruginous carbonate." Based on such observations, he concluded that the gold was of a detrital rather than accretionary origin.

Heavy Mineral Analyses

General - Heavy minerals were extracted from alluvial gravels, representing two separate drainage systems, to describe and evaluate a provenance for black sands commonly associated with the placer gold deposits. Analysis of the mineral concentrates from 5 samples was done by emission spectrograph and volume percentage estimations of mineral content were measured by grain population counts. Four samples were taken in the S.W. $\frac{1}{4}$ of section 16, and N.W. $\frac{1}{4}$ of section 20, T.29N., R.17W. These samples contain heavy mineral assemblages from a westward drainage representing the southern portion of Wall Street and the northern portion of the Migmatite Valley. The fifth sample consists of mineral concentrates recovered from the recent placer mining operation by Resources International Corp.; this sample contains heavy mineral assemblages representing a northeastward drainage. The King Tut placer mine and the Copper Blowout area are included in the headwaters of this drainage.

Sampling and Analytical Methods - Descriptions of the gravel samples are included in Appendix D and the locations of samples G-1 through G-4 are indicated on Plate II. Sample G-5 does not have a specific location, it represents a composite sample mined from a major drainage in the S.W. $\frac{1}{4}$ of section 3, T.29N., R.17W. The techniques used in this study for sampling, preparation and concentration of the heavy minerals are given in Appendix D. These basic procedures are a modification of the separation methods described by Carver (1971, p. 427-452).

Representative samples for emission spectrographic analysis were coned and quartered, then halved. One half of each sample was submitted to a commerical lab for analysis. The other half of the samples were sieved into two size fractions (<60 to ≥ 65 mesh and <100 to ≥ 115 mesh, using the Tyler sieve series (Wentworth, 1922)). Extraction of a majority of magnetite from each size fraction was done prior to population counts. The approximate weight percentages of magnetite for each sieve size, per sample, is given in a table of weight distributions in Appendix D. It includes the weights of the heavy mineral fractions during sample preparation and handling.

Population counts for each sieve size were done on the non-magnetic portion of each sample using a Zeiss petrographic microscope equipped with a mechanical stage. The mineral grains were mounted on a slide coated with a thin film of silicone gel, (to minimize distortion of refracted light). Identification of opaque minerals was accomplished in reflected light, using the criteria for determining microscopic opaques established by Krumbein and Pettijohn (1938). The reliability of the point counting results was determined from a chart by Van Der Plas and Tobi (1965).

Results and Interpretation - Both the geochemical analyses and the heavy mineral percentage estimation represent a qualitative evaluation. The most obvious correlation substantiated by this investigation is that a major fraction of heavy minerals indicates a metamorphic terrain for both drainages. Results from the emission spectrographic analyses (Appendix D), show little variation between samples. From these results, the lack of any significant amount of sulfides, except pyrite, is indicated; this is also evident from the population counts (Table 4). It is interesting that no gold values are reported, suggesting a lack of gold contained in pyrite. Based on observations, the pyrite in samples G-1 through G-4 is fine grained, subhedral to euhedral, and resembles the disseminated pyrite contained in the local metamorphic rocks. This pyrite shows a marked contrast from the gold-bearing pyrite in the mineralized veins. Gold is absent from the pyrite in sample G-5, yet the pyrite is coarser grained and resembles the gold-bearing pyrite found in the veins. The drainage represented by samples G-1 through G-4 characterizes a large area with mixed lithologies, predominantly unmineralized, so gold-bearing pyrite was not anticipated. However, sample G-5 contains abundant coarse pyrite possibly derived from the Altered Valley, so gold-bearing pyrite

Table 4
HEAVY MINERALS PERCENTAGE ESTIMATION†
Based on Microscopic Point Count Procedure

Sample No.- Sieve Size	Total Grains	Garnet	Pyrite	Amphibole	Quartz	Feldspar	Zircon	Apatite	Spinel	Iron Carbonate	Oxides*	Epodite Zoisite	Mica** Group	Lithic Aggregates
G-1-65††	481	5.8/2	4.8	11.2/3	8.1/2.5	2.1	0.4	0.20	——	——	31.9/4	7.3/2	23.7/4	4.4
G-1-115††	550	11.2/3	1.8	19.1/3.5	1.8	1.5	——	0.18	——	0.2	16.2/3	11.5/2.5	34.5/4	2.0
Average		8.7/2	3.2	15.4/2	4.8	1.8	0.2	0.19	——	Trace	23.5/3	9.5/2	29.5/3	3.1
G-2-65	538	10.6/3	4.8	9.1/2.5	8.2/2.5	2.9	0.6	——	0.2	——	28.4/4	9.1/2.5	19.7/3.5	6.3/2
G-2-115	457	12.0/3	4.6	9.8/2.5	5.5/2	4.8	1.5	0.22	——	1.3	24.7/4	13.1/3	17.1/3.5	5.3/2
Average		11.3/2	4.7	9.5/2	6.9/1.5	3.8	1.0	Trace	Trace	0.6	26.7/3	10.9/2	18.5/3.5	5.8/1.5
G-3-65	480	22.5/4	11.6/3	8.3/2.5	3.1	0.8	0.8	——	0.2	——	27.7/4	11.0/3	8.9/2.5	4.8
G-3-115	498	23.5/4	9.8/2.5	7.6/2	2.6	2.0	0.6	0.40	0.4	——	27.3/4	13.1/3	9.2/2.5	3.4
Average		23.0/3	10.7/2	7.9/1.5	2.8	1.4	0.7	0.20	0.3	——	27.5/3	12.1/2	9.1/2	4.1
G-4-65	481	12.5/3	9.6/2.5	3.7	3.5	3.7	0.2	0.4	——	——	39.5/4.5	5.0/2	14.9/3	6.4/2
G-4-115	651	21.6/3	9.9/2	5.2/2	2.5	2.0	——	0.9	——	——	30.1/3.5	7.5/2	16.4/3	2.2
Average		17.7/2.5	9.8/2	4.6	2.9	2.7	Trace	0.7	——	——	34.1/3	6.5/1.5	15.8/2	3.9
G-5-65	570	30.3/4	10.2/2.5	1.2	3.7	2.5	0.7	0.4	1.2	——	33.7/4	11.9/2.5	2.8	1.2
G-5-115	496	23.2/4	10.5/2.5	0.20	5.0/2	3.2	0.6	1.4	1.0	——	33.1/4	15.9/3	4.0	1.6
Average		27.0/3	10.3/2	0.7	4.3	2.8	0.6	0.8	1.1	——	33.4/3	13.8/2	3.4	1.4

† Reported as volume %/reliability %; reliability % determined for volume percentages $\geq$ 5%, from a reliability point count chart in Van Der Plas and Tobi (1965).

†† Sample sizes range from <60 to $\geq$65 and <100 to $\geq$115; using Tyler sieve series.

* Oxides-includes the following minerals decreasing in abundance with respective order (hematite, ilmenite, magnetite, limonite).

** Mica group-includes the following minerals decreasing in abundance with respective order (Biotite, Chlorite, Muscovite).

Trace $\leq$ 0.10%

was expected. The lack of gold suggests the coarse pyrite in sample G-5 is not derived from the mineralized veins observed in the Altered Valley.

Samples G-1 through G-4 contain between 24% and 35% magnetite for each sieve size. Sample G-5 contains 60% to 67% magnetite. Thus G-5 has twice the amount of magnetite as compared to the other samples. This difference suggests a different source with a higher magnetite content than is represented for samples G-1 through G-4.

The most important results from the heavy mineral percentage estimation (Table 4), is the contrast in abundance of amphibole and micas between sample G-5 and the remaining samples. Sample G-5 has an unusually low percentage of both minerals. This suggests two possibilities. One, the Copper Blowout area is characterized by hydrothermal alteration, and would reflect the breakdown and alteration of the amphibole and micas resulting in low percentages present; or two, the fanglomerate gravels are not derived from the Precambrian rocks in the Lost Basin Range. The first concept is unlikely since the Precambrian rocks in this area are characterized by a thick sequence of amphibolites within the $P\text{Є}_2$ unit; also, there is an abundance of mica schists in the $P\text{Є}_1$ and $P\text{Є}_2$ rock units. Furthermore, based on petrographic analyses, the pervasive alteration has not eliminated a majority of amphibole or micas in the altered areas.

The second interpretation for the lack of these minerals suggests that these older fanglomerates are derived from a source area further to the west and southwest (eg. White Hills). A more distant source would contain a metamorphic terrain similar to the Precambrian complex in the Lost Basin Range; however, there would be a marked decrease in abundance of amphibolites and mica schists. Such a source area would also contain nearly twice the amount of magnetite than observed in the Lost Basin Range. The gold would occur as free gold in a hydrothermal vein system rather than be dominantly associated with the limonitic pseudomorphs of pyrite observed in the Lost Basin Range. This conclusion, drawn from the heavy mineral analyses, coincides with several external physiographic features (p. 98) of the Muddy Creek fm., which suggest a more distant, western source area for the fanglomerates.

Gold Geochemistry

Spectrochemical analyses of placer golds from the Lost Basin property were done by Antweiler and Sutton (1970), and Antweiler and Campbell (1979). Their results are shown in Tables 1 and 5. Based on analyses of 21 native gold samples, the average percentage of silver contained in the placer gold was 7.0% and the average copper content was 210 ppm (Antweiler and Sutton, 1970, p. 12). When these results are compared with the gold signature values for the lode gold from the Lost Basin Range (Table 1 and 2), a strong dissimilarity in elements is observed. The placer gold contains lower values in silver, copper, and lead. Antweiler and Sutton (1970, p. 9 and 11) mentioned there was a slight increase in gold purity in the Lost Basin placer samples, with a decrease in grain size. They suggested the higher purity be attributed to surface refining of the gold in either the oxidizing environment of the lode source or in the detrital environment.

Source

Post (1970) and Mallory (1971a) considered the eastern placer deposits, in the vicinity of the King Tut mine, to have originated from the erosion of a peripheral halo of gold-bearing veins above a copper, lead and silver rich core in the Copper Blowout area. Recent work by Antweiler and Campbell (1979) and observations by this author, suggest a more distant source

Table 5. SPECTROCHEMICAL ANALYSES OF PLACER GOLD SAMPLES FROM THE APACHE ORO MINING CLAIMS (KING TUT AREA, SEC. 9, T.29N., R.17W.) LOST BASIN DISTRICT, MOHAVE COUNTY, ARIZONA

(adapted from Antweiler and Sutton, 1970)

Sample No.	Ag	Fe	Ti	Mn	Cu	Bi	Cr	Pb	Pd	Pt	Ni	V	Zr	Other Elements
	percent			parts per million										
1	9.0	0.15	---	15	500	N20	N10	500	N1.5	N70	N3	N5	N10	
2	9.0	.15	---	15	700	N20	10	100	N1.5	N70	N3	N5	10	
3	11.0	.01	---	N5	200	L20	N10	30	1.5	N70	N5	N5	10	
4	8.6	.013	---	N5	150	20	N10	30	1	N70	N5	N5	N10	
5	12.0	.2	---	N5	300	30	N10	30	3	N50	N5	N3	N7	Co 3; Mo 3.
6	13.0	.07	---	N5	200	50	N10	30	3	N50	N5	N3	20	
7	2.8	.03	.005	15	50	N70	N7	N50	N2	N20	N3	N10	100	
8	7.2	.007	.005	N2	200	N100	N10	N100	N5	N50	N5	N15	N30	La 1,000; Y 50.
9	2.1	.05	.01	N2	300	N70	N7	100	N3	N30	N3	N10	N20	La 1,500; Sc 50; Y 50.
10	5.8	.07	.02	5	100	N70	N7	N100	N5	N50	N3	N10	150	La 1,500; Sc 70; Y 100.
11	5.1	.05	.007	N2	100	N70	N7	L100	N5	N50	N3	N10	150	La 2,000; Y 300.
12	6.4	N.005	.007	N2	50	N100	N10	N100	N5	N50	N5	N5	N30	
13	6.3	.02	.005	N2	200	N100	N10	N100	N5	N50	N5	N15	N30	
14	9.5	N.01	N.01	N10	500	N500	N50	N500	N20	N200	N20	N70	N150	
15	4.9	.05	.007	N2	200	N100	N10	N100	N5	N50	N5	N15	N30	
16	5.4	.02	.01	N1.5	100	N100	N10	N100	N5	N50	N5	N15	N20	
17	6.0	.015	.007	N1.5	150	N70	N70	N70	N5	N50	N3	N10	N20	
18	6.8	.15	.02	L2	150	N50	N50	100	N2	N20	N2	N7	100	
19	5.2	.015	.007	N1.5	150	N70	N70	N70	N3	N30	N3	N10	N20	
20	6.2	.005	.007	N1	100	N50	N50	N50	N2	N20	N2	N7	N10	
21	3.8	.007	.015	N1.5	200	N70	N70	N70	N3	N30	N3	N10	N20	

N - not detected at limit of detection, the value shown
L - detected, but below limit of value shown
--- - not looked for

for a majority of the placer gold.

A combination of the following characteristics for the placer deposits implies an undiscovered source for the placer gold contained in the fanglomerate. The geochemical analyses by Antweiler and Sutton (1970) and Antweiler and Campbell (1979) report gold signatures on the vein and placer golds in the Lost Basin area. These signatures exhibit a sharp contrast between the two types of golds. The low percentage of amphibole and micas, along with a high weight percentage of magnetite, infer a different provenance for the placer deposits other than the central area of the Lost Basin Range. The dark grey chalcedonic matrix commonly associated with the coarse placer gold is not typical of the quartz gangue in the mineralized veins of the Lost Basin Range. A discrepancy in grain sizes occurs when comparing the dominant size of visible free gold in the veins to the size range of the placer gold (Blacet, 1969). There is a pronounced lack of coarse gold in the veins, so it appears unlikely the coarse placer gold came from the nearby lode deposits. Gold is absent in the abundant, coarse-grained, oxidized pyrite from the placer deposits; however, the coarse, oxidized pryite in the mineralized veins, in the Lost Basin Range, contains a majority of the gold. The ragged and coarse nature of the placer gold implies a limited amount of transport, but structures observed in the gold substantiate a detrital rather than accretionary origin (Blacet, 1969). This eliminates the complications of an elaborate remobilization mechanism to transport the gold in solution.

Factors suggesting a source area for the gold-bearing fanglomerate further to the west or southwest reflect the general physiographic nature of the Muddy Creek fm. adjacent to the Lost Basin Range. There is a direct correlation between the various facies of Tmc and the source areas with regard to the extensive, regional distribution of the sediments.

Confinement of the placer gold mining to an area of 8 to 10 square miles around the King Tut mine, suggests only the crystalline-clast subfacies of the Muddy Creek fm. contains any appreciable amounts of gold. The Gold Butte subfacies, further to the north around Meadview Arizona, appears barren of gold. The source for the Gold Butte conglomerate is to the northwest in the South Virgin Mountains (Lucchitta, 1966); whereas the crystalline-clast conglomerate in the vicinity of the Lost Basin Range was derived from a western to southwestern source.

The low-dipping attitudes of the Tmc, in the mapped area, are in part the result of inclined deposition and in part due to minor post-depositional deformation; however, the low topographic expression of the fanglomerates infer a more distant source beyond the Lost Basin Range. The crystalline-clast subfacies of the Muddy Creek fm. and the placer gold deposits become progressively finer-grained to the east and northeast with considerable distance (Lucchitta, 1966; Wilson, 1933).

No abrupt changes in the degree of sorting, decrease in clast size with distance, or a marked variation in the volume of sediments were observed that could be attributed to a local, adjacent source area (eg. Lost Basin Range). Instead, these factors indicate a more distant source area with a more gradational distribution of sediments. In the southern portion of Grapevine Mesa, along Lone Jack ridge, the volume and elevations of the fanglomerate imply a more westerly derivation other than the Lost Basin Range (Lucchitta, 1966, p. 138).

Taking into consideration the volume and distribution of the Tmc sediments, a projection of the Lost Basin Range (only 4 miles wide and less than 20 miles long) as a source for the fanglomerates would require the size of a mountain range that is inconceivable in view of it's present extent. Therefore, the Lost Basin Range does not appear to be an adequate source for the Muddy Creek fm. and could not be the source for the paleo-placer deposits.

Recent work by Antweiler and Campbell (1979) comparing gold signatures between the vein and placer gold, suggests "only a small percentage of placer gold was derived from the veins" and that the major source of the placer gold was not from the vein mineralization in the Lost Basin Range. Instead, an undiscovered lode source 12-22 miles further to the west or southwest is considered to have been the source area for the placer gold in the Muddy Creek fm. (J.C. Antweiler, pers. comm., 1980).

It is conceivable that post-depositional erosion of the gold-bearing Muddy Creek fanglomerate and the gold-bearing veins in the Precambrian complex of the Lost Basin Range has resulted in a mixing and concentration of both golds within the Quaternary arroyo gravels. However, the contribution of lode gold from the Lost Basin Range appears to be minor in view of the results reported by Antweiler and Campbell (1979).

Assuming the placer gold in the fanglomerate is derived from an undiscovered source and the crystalline-clast subfacies of the Muddy Creek fm. is derived from a source area further to the west-southwest, then a likely source area for both would be in the White Hills. The most feasible source would be the peripheral gold veins associated with a late Cretaceous intrusion of porphyritic quartz monzonite mapped by Blacet (1975) in sections 18 and 19, T.28N., R.18W.

PORPHYRY COPPER PROSPECT

General

Earlier work on the Apache Oro mining claims suggested the presence of an undiscovered porphyry copper deposit in the Precambrian complex of the Lost Basin Range. Obvious indicators of a porphyry deposit are absent and only indirect lines of evidence are available for consideration. This study investigated the geology in the vicinity of a proposed target area and evaluated the relationships of the observable mineralization. No major association between the placer gold and the adjacent mineralized veins was established. This would exclude the placer deposits as being derived from a porphyry copper source in the immediate area. The degree of vein mineralization was restricted, minimizing the economic importance of the vein deposits; however, certain aspects of the veining should be considered in the evaluation of a porphyry copper prospect.

The following summary of positive and negative factors for a porphyry copper prospect, in the Lost Basin Range, is based on field observations by the author and on criteria discussed by Post (1970), Mallory (1971a, 1971b, 1974b), Krish (1974) and Antweiler and Campbell (1979).

Positive and Negative Factors

Positive factors tending to substantiate porphyry copper type mineralization of the Apache Oro claims in the Lost Basin Range include the following:

1) subtle zoning of metal abundances; a peripheral halo of anomalous gold-silver values which decreases inwards towards anomalous values of silver, copper, and lead, in the vicinity of the Copper Blowout area;
2) gold signatures from native gold in selected veins along the crest of the range show a close similarity to gold signatures from gold associated with known porphyry copper deposits;
3) a tentative age date on the mineralized veins of 67 m.y. (potassium-argon date using muscovites in veins) and anomalous amounts

of Hg reported in both the gold and copper-bearing veins inferring both types of veins are contemporaneous and younger than Precambrian;

4) an aeromagnetic survey with a magnetic low, in part coinciding with the Copper Blowout area and extending northeast into the eastern fanglomerate in sections 3, 4, 34, 35, T.29N., R.17W. and sections 22 and 27, T.30N., R.17W. (see Figures 24 and 25); and

5) three specific zones of trace elements in the Lost Basin Range are related to trace element distributions in some porphyry copper deposits and prospects (Krish, 1974, p. 124-125).

Negative factors militating against porphyry copper type mineralization on the Apache Oro claims include:

1) lack of a felsic igneous intrusion of post-Precambrian age in outcrop; only two small restricted andesite dikes have been observed in the Altered Valley;

2) lack of pervasive hydrothermal alteration of the country rock typical of a porphyry type deposit; instead retrograde metamorphism combined with limited hydrothermal alteration associated with vein mineralization, along major fault structures, is present and locally intensified in the Altered Valley;

3) lack of a gossan cap rock; the alteration in the Copper Basin area is in a paleo-drainage later subjected to supergene weathering processes (Krish, 1974, p. 59; Lucchitta, pers. comm., 1977);

4) observed mineralization produces restricted amounts of high-grade gold and silver along ore shoots but the extent of mineralization over the map area is discontinuous and highly variable;

5) vein mineralization is not genetically related to pegmatites in the Precambrian complex, (Note: Krish (1974, Figure 20) reported

a distinct absence of any trace elements in a pegmatite contained in his geochemical Traverse B; whereas, anomalous values of trace elements corresponded directly to mineralized veins);

6) absence of pervasive, finely disseminated sulfides in the country rock with the exception of pyrite found in the immediate vicinity of mineralized vein fissures;
7) absence of radial and concentric fracture patterns;
8) absence of any hypogene mineralized stockwork pattern; and
9) the temperature contrast between fluid inclusion studies on veins in the Lost Basin Range and the fluid inclusion temperatures in a pre-intrusive cover over a buried pluton reported by Bodner and Beane (1977).

Geophysics

An aeromagnetic intensity and scintillation survey was conducted by Heinrichs Geoexploration Co. (1967) on the Apache Oro mining claims in the Lost Basin Range. The results are shown in Figure 24 and a series of schematic sections corresponding to magnetic profiles are depicted in Figure 25. The noticeable feature is a broad magnetic depression that extends northeastward from the Copper Blowout area, into Tertiary sediments for $3\frac{1}{2}$ miles. The majority of this magnetic low is covered by the Tertiary Muddy Creek fanglomerate, and surface exposures of the Precambrian complex could not be examined.

The pronounced embayment in the depression pattern was reported by Post (1970) as the result of black sand tailings accumulated from the King Tut placer mine in the N.E. $\frac{1}{4}$ of section 9 of T.29N., R.17W. The magnetic highs adjacent to the depression represent higher magnetic susceptibilities of individual blocks of the $p\epsilon_3$ rock unit (Figure 25). It

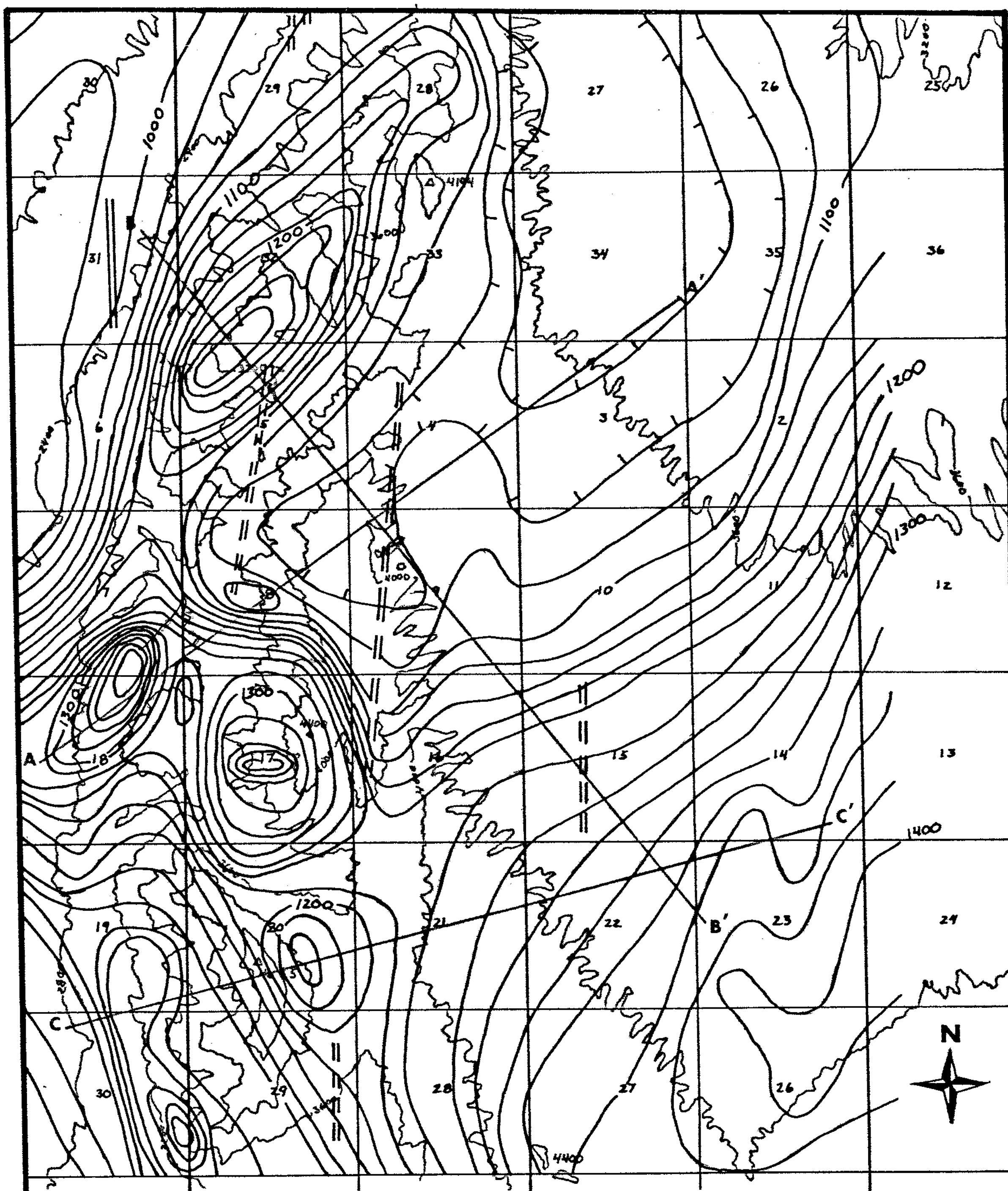

AIRBORNE PROTON TOTAL MAGNETIC INTENSITY AND SCINTILLATION SURVEY

Legend

Magnetic contour interval = 25 gammas

Scintillation anomalies

- :::: 1 1/2 - 2 times background
- ═══ 2 - 3 1/2 times background

Flight elevation = 500′ above terrain

Elevation contour interval = 400′

A—A′ Schematic section, Magn. profile

Scale
1 ½ 0 1 mile

adapted from Heinrichs(1967)

Figure 24.

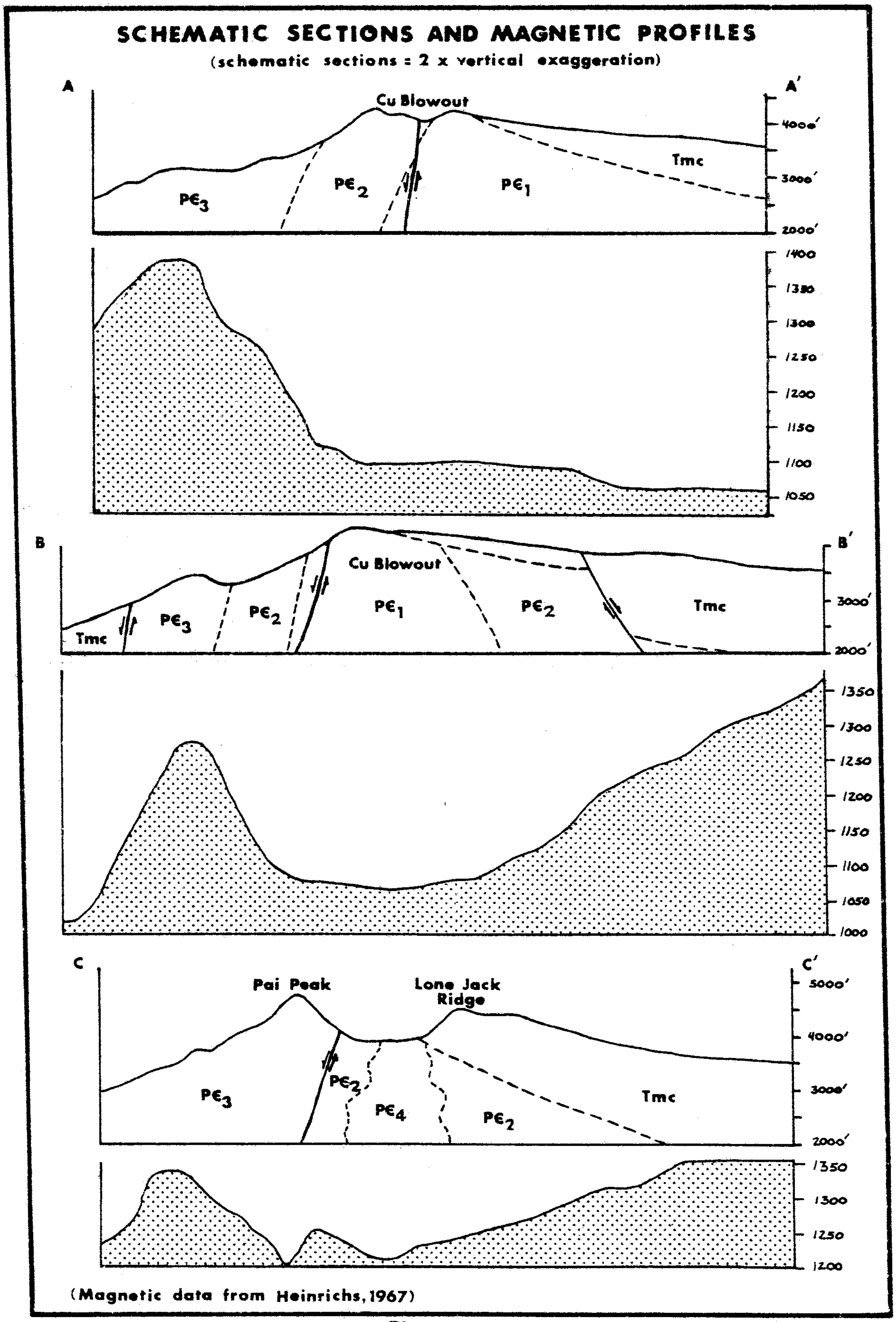
SCHEMATIC SECTIONS AND MAGNETIC PROFILES
(schematic sections = 2 x vertical exaggeration)
A
A'
Cu Blowout
PЄ3
PЄ2
PЄ1
Tmc
4000'
3000'
2000'
1400
1350
1300
1250
1200
1150
1100
1050
B
B'
Cu Blowout
Tmc
PЄ3
PЄ2
PЄ1
PЄ2
Tmc
3000'
2000'
1350
1300
1250
1200
1150
1100
1050
1000
C
C'
Pai Peak
Lone Jack Ridge
PЄ3
PЄ2
PЄ4
PЄ2
Tmc
5000'
4000'
3000'
2000'
1350
1300
1250
1200
(Magnetic data from Heinrichs, 1967)

Figure 25.

should be noted that the magnetic contours south of the Copper Blowout area exhibit a sharp deflection and trend south along the strike length of the Altered Valley. This could be the result of hydrothermal alteration associated with vein mineralization along a major fault fissure, and the effects of retrograde metamorphism localized in the valley.

Three possible explanations for the magnetic depression should be considered. First, the alteration in the Copper Basin, in the northern $\frac{1}{2}$ of section 4 T.29N., R.17W., represents a paleo-drainage during deposition of the fanglomerate. The magnetic low could reflect weathering processes that altered the bedrock beneath the conglomerate. This seems unlikely since the major direction of drainage and deposition for the Muddy Creek fm. is to the east, while the anomaly trends 90° to the paleo-drainage. Another explanation could be a northeastward extension of the alteration exposed in the Altered Valley. If correct, this would imply limited hydrothermal activity along structural zones further to the east than has previously been observed. The third explanation is that it could represent a buried intrusive with a lower magnetic susceptibility than the adjacent Precambrian complex (Post, 1970).

An interesting feature of the geophysical survey is the way the magnetic pattern contours the southern portion of Grapevine Mesa, in the vicinity of Lone Jack ridge. This area has apparently the thickest accumulation of Muddy Creek fanglomerate in the mapped area and it is unlikely that the fanglomerate would influence the magnetic intensities. A more likely interpretation is a concealed block of Precambrian rock beneath Grapevine Mesa, representing the eastern, upthrown fault-block of a major north-trending fault structure (?), previously discussed (p. 64), in the Migmatite Valley.

The results of this geophysical survey should be compared to the results reported by Sumner and Aiken (1974) on regional geophysical patterns associated with porphyry copper deposits in Arizona. The influences of the Muddy Creek stratigraphy should also be considered in view of the results Anderson and Laney (1974) reported on impoundment-related seismicity in the Lake Mead area and the effects of a thick, late Cenozoic cover.

Discussion

In view of available information, the presence of a porphyry copper deposit on the Apache Oro claims is indeterminate. Several investigators (Krish, 1974; Mallory, 1971a, 1974b; Post, 1970) have considered the metal zoning, trace element distributions and alteration in the Lost Basin Range representative of an unaltered peripheral halo in the Precambrian rocks overlying a porphyry copper deposit at depth. The absence of the characteristic alteration halos found around producing porphyries is attributed to insufficient erosion of the mountains to expose these features. If a mineralized intrusion is present, it would be at a considerable depth because the Precambrian complex lacks the proper mineralization, alteration, and ground preparation for a near surface deposit. The economic feasibility of mining a deep porphyry structure is unfavorable under present conditions.

Field observations in the study area cannot substantiate the presence of a porphyry copper deposit. Geochemical investigations by Antweiler and Campbell (1979) are encouraging; however, additional geophysical and geochemical exploration is necessary to delineate any mineralized intrusion. The presence of Duval's porphyry copper deposit at Mineral Park, 40 miles south, and the general similarity in rock types and vein structures between the Lost Basin Range and the Wallapai mining district (Thomas, 1949) may not be fortuitous.

GEOLOGIC HISTORY

The Precambrian structural history of the Lost Basin Range must be supplemented by information from the Virgin Mountains, to the north, and the Cerbat Mountains, to the south, because of the meager information available in this particular range. The Precambrian complex in the study area suggests a sequence of sedimentary rocks interbedded with igneous rocks but clear cut distinctions have been obliterated by regional metamorphism. Moore (1972, p. 55) considered this period of metamorphism in the Virgin Mountain region to be the product of the older Precambrian "Mazatzal Revolution" which was summarized by Wilson (1962, p. 12). Therefore, structural trends in the metamorphic complex of the Lost Basin Range are attributed to the "Mazatzal Revolution" on the basis of local evidence and regional correlation. Recognition of Precambrian structures is often difficult since they are obscured by more recent episodes of tectonism.

Wilson (1949) discussed characteristics of the older Precambrian (Mazatzal), younger Precambrian (Grand Canyon), Nevadian, Laramide and late Cenozoic periods of deformation. He noted the Mazatzal, Nevadian and Laramide orogenies were featured by folding, reverse faulting and batholithic invasions that predominated over normal faulting. The younger Precambrian and late Cenozoic deformations represented regional uplift, volcanic activity, and normal faulting dominating over broad flexing, folding and thrust faulting.

The Nevadian disturbance was strong in western Arizona and Dings (1950, 1951) attributed the major tectonic activity along fault fissures in the Cerbat complex to this period. More intense effects of the Laramide Revolution occurred northwest of this study area, in the vicinities of the Muddy, Beaverdam and Virgin Mountains (Moore, 1972; Longwell, 1928). Present topography in the Lost Basin area is derived from Basin and Range type faulting during late Cenozoic tectonism (Lucchitta, 1966). Locally, much of the late Cenozoic displacement was superimposed on earlier developed structures.

A large gap occurs in the geologic record between Precambrian and late Cenozoic time, in the vicinity of the Lost Basin Range. Several thousand feet of Paleozoic sediments comprise the Grand Wash Cliffs, 7 miles to the east, however the Paleozoic-Mesozoic sediments are markedly absent in the study area and in the Cerbat Mountains. Thomas (1953) and Lucchitta (1966) considered a former extension of these rocks over those areas feasible but they were probably much thinner. The lack of this portion of the stratigraphic record represents a considerable interval of time marked by regional uplift and extensive erosion of the sedimentary cover preceeding late Cenozoic events.

Based on field evidence and regional relationships, the geologic structure for the mapped area appears to have developed over a considerable span of time. Establishment of the north-trending structural pattern in the Precambrian complex occurred after regional metamorphism; the north-trending faults disrupt the metamorphic fabric. This faulting preceeded mineralization since the principal mineralized veins are associated with the faults. By correlating structures and rock types in the Lost Basin Range with those in the Cerbat complex, it is possible to infer that the major diastrophism that affected the Cerbat complex could also involve the Lost Basin Range. This would suggest a late Jurassic to early Cretaceous age for the major structures prior to the hydrothermal event. Krish (1974) reports an unpublished age date by Blacet on the hydrothermal vein mineralization in the Lost Basin Range as being late Cretaceous.

Tectonic adjustments or renewed displacement during and/or following ore deposition is indicated by strong brecciation of vein structures associated with these major faults (Trites, 1974). This is interpreted as a result of the late Miocene deformation of the Grand Wash Trough described by Lucchitta (1966) for the entire region. He also mentions that strong folding occurred before major faulting and this would be preserved in the deformation that affected the mudflows and rhyolitic sediments (Tms). The author considers the initial development of a depression or rotated fault-block that extends from the Migmatite Valley north into the Altered Valley to have occurred during this period of deformation. It is inferred that the minor northeast-trending fault structures were developed at this time. These northeast-trending faults correspond to the younger transverse structures mentioned by Dings (1951).

The depositional environment in the area south of Lake Mead (Figure 1), during middle to late Miocene time, prior to the main episode of normal faulting, was higher to the south and southwest with drainages flowing to the north and northeast. The area to the south and southwest represented a regional upwarp subjected to extensive erosion and frequent intervals of explosive and effusive volcanism (eg. the Kingman and Mt. Davis volcanic series). The Grand Wash Cliffs were not a prominent barrier and the area north of Lake Mead was a topographic low, accumulating sediments through much of the late Tertiary period. During Miocene time, the area was occupied by one or more lakes receiving abundant clastic sediments from the southwest and tuffaceous material from volcanic activity (Lucchitta, 1966). The Tms unit was deposited during this period of sedimentation.

These conditions were disrupted markedly by intense normal faulting towards middle to late Miocene time. The Grand Wash Cliffs became a prominent barrier during deposition of the Muddy Creek fm., while ranges were elevated much higher than present elevations. The formation of rotated, fault-block basins resulted in the development of interior drainages (Lucchitta, 1966). Widespread erosion and deposition of the various facies of the Tmc unit into structurally defined basins occurred during the waning stages of Basin and Range faulting. Minor deformation and displacement occurred along previous structures during and following deposition of the Muddy Creek fanglomerates. Renewed fault displacement (?) along the eastern front of the Lost Basin Range occurred during the late stages of deposition of the Muddy Creek fm. in the southern portion of the Migmatite Valley (Lucchitta, 1966). This displacement could correspond with the poorly delineated fault structure along the easternmost extent of the Altered Valley.

Finally, the latest displacement is defined by the low-angle transverse fault in the southern portion of the mapped area. This fault was active after deposition of the Muddy Creek fm. and is younger than the normal faulting based on displaced fault traces. Presumably, this low-angle displacement terminated before or during the extensive erosion that incised the Muddy Creek fm. during development of more recent drainage patterns into the Colorado River (Lucchitta, 1966, 1967). This structure may have been a factor in preserving the thick sedimentary sequence of Muddy Creek fanglomerate representing Lone Jack ridge. The rates of Quaternary headward erosion of the eastern drainages on Grapevine Mesa between the southern and northern portions of the mapped area suggest a structural influence.

CONCLUSIONS

The geologic investigation of the Apache Oro mining claims in the Lost Basin Range recognizes four mappable rock units in the Precambrian metamorphic complex and two Tertiary sedimentary units. Spacial relationships of these rock units and the mineralization are outlined. Surface mineralization on the Apache Oro claims consists of limited quartz-carbonate-sulfide veins in metamorphic rocks and gold-bearing Tertiary fanglomerate deposits adjacent to the range. The examination of lithologies and alterations in this area of the Precambrian complex does not support the presence of a porphyry copper deposit at depth. The most favorable indicator of such a deposit in the vicinity of the Lost Basin Range could be the geochemical results reported by Antweiler and Campbell (1979).

No direct association between vein mineralization in the mapped area and a porphyry copper deposit could be substantiated. The sulfide mineralization is low-grade and sporadic except in structurally controlled ore shoots which show higher sulfide content. Major north-trending fault fissures developed during the Nevadian orogeny and provided the structural control for the late Cretaceous (?) vein mineralization. Because of it's limited extent, hypogene mineralization may prove to be of only minor economic significance unless possible supergene enrichment of the vein gold along the brecciated veins can be established.

The placer gold in the Muddy Creek fanglomerate indicates a derivation from an undiscovered source area further to the west and southwest. The only possible association the placer gold has with the lode gold from the Lost Basin Range would be the reworking and concentration of the paleoplacer deposits in Quaternary arroyos during erosion of the adjacent range. Then a minor contribution of lode gold mixing with placer gold from the recent erosion could be expected. These arroyo gravels offer the best potential for mining in view of the current market price for precious metals. However, the stratigraphic distribution of gold in both the Tertiary fanglomerate and Quaternary channel gravels has not been delineated.

SUGGESTIONS FOR FURTHER WORK

In order to evaluate the mining potential of the known deposits, additional exploration is warranted. The emphasis of further exploration should focus on the specific distribution of the placer gold and the amount of mineralization in vein ore shoots. Prospecting for a porphyry copper deposit should be postponed until a detailed investigation of the accessable deposits has determined the actual extent of economic mineralization in the area and available ore reserves.

The existence of a porphyry copper ore body on the Apache Oro claims would have to be proven by drilling since the surface expression of such a structure is absent. Present information does not sufficiently outline a specific drill target, or justify the expense of drilling. Therefore, supplemental ground geophysical surveys oriented east-west across the mountain range and into the adjacent valleys are recommended in an attempt to define an intrusive body at depth or other structures which may have influenced the previous magnetic survey (Heinrichs, 1967). Detailed geochemical studies and additional mapping in the area could provide information vital in the geophysical interpretations. If the results of these investigations suggest an intrusive target then the feasibility of deep drilling should be considered.

Exploration for placer gold should investigate the White Hills area for an undiscovered lode source, using gold compositional analyses as an exploration tool. Locating a source in the White Hills could indicate peripheral boundaries for the placer gold distribution. These boundaries would help centralize exploration in both the Hualapai Wash and Grapevine Wash by recognizing the limited distribution of higher concentrations of placer gold in the older gravels.

Development of the eastern placer could be enhanced by use of a grid pattern ground magnetic survey along the strike length of the crystalline-clast conglomerate subfacies of the Muddy Creek fanglomerate contained in Grapevine Mesa. This would assist in centralizing paleo-channels with significant concentrations of magnetic black sands. It is recommended that detailed measured stratigraphic sections be taken of the Muddy Creek fm. cropping out in the vicinity of Lone Jack ridge. Identification of stratigraphic positioning of favorable layers would assist in delineating potential horizons of gold-bearing paleo-channels.

The search for hypogene mineralization along vein ore shoots should be supplemented by additional fluid inclusion studies and age dating of mineralization to better understand the hydrothermal plumbing system that existed during ore deposition. A shallow core drilling program should be designed using portable scout (Winkie) drills for locating potential ore shoots, and determining ore grades and structural extent. The drilling could be angled towards the dip slopes of the veins, perpendicular to strike, with expected intercepts generally less than 300 feet deep. Such a program could provide AX or EX core which could be systematically assayed and examined for any indicators of secondary enrichment of gold via supergene processes.

REFERENCES CITED

Allman, M., and Lawrence, D.F., 1972, Geological laboratory techniques: Arco Publishing Co. Inc., New York, 335 p.

Anderson, R.E., and Laney, R.L., 1974, Influence of late Cenozoic stratigraphy on distribution of impoundment-related seismicity at Lake Mead, Nevada-Arizona (Abstract): from 70th Geol. Soc. Amer. Cordilleran Sect. Ann. Meetings, Las Vegas, Nev., P. 138-139.

Antweiler, J.C., and Sutton, A.L., 1970, Spectrochemical analyses of native gold samples: U.S. Geol. Survey Rept. USGS-GD-70-003, 28 p., available from U.S. Dept. Commerce Nat'l. Tech. Info. Service, Springfield, Va. as Rept. PBI-94809.

Antweiler, J.C., and Campbell, W.L., 1977, Application of gold compositional analyses to mineral exploration in the United States: U.S. Geol. Survey, Paper in press, to be published in an Australian Symposium proceedings at a later date.

Antweiler, J.C., and Campbell, W.L., 1979, Application of gold compositional analyses to mineral exploration in a part of Mohave County, Arizona (Abstract): Exploration Geochemistry in the Basin and Range Province, Meeting of the Assoc. of Exploration Geochemists, April 9-10, 1979, Tucson, Arizona, p. 10.

Armstrong, R.L., 1963, Geochronology and geology of the eastern Great Basin in Nevada and Utah: Ph.D. Dissertation, Yale University, New Haven, Conn.

Blacet, P.M., 1969, Geological survey research 1969: U.S. Geol. Survey Prof. Paper 650A, Chapter A, p. A1-A2.

Blacet, P.M., 1975, Preliminary geologic map of the Garnet Mountain quadrangle, Mohave County, Arizona: U.S. Geol. Survey Open File Map 75-93, 1 sheet.

Bodnar, R.J., and Beane, R.E., 1977, Temperature variations in pre-intrusive cover over a buried pluton (Abstract): from 73rd Geol. Soc. Amer. Cordilleran Sect. Ann. Meetings, Seattle, Wash., p. 903.

Bohannon, R.G., and Anderson, R.E., 1978, Tertiary tectonic history of the eastern Basin and Range province in the vicinity of Lake Mead in southern Nevada and western Arizona (Abstract): from 74th Geol. Soc. Amer. Cordilleran Sect. Ann. Meetings, Tempe, Ariz., p. 96-97.

Carpenter, J.R., 1968, Apparent retrograde metamorphism--another example of the influence of structural deformation on metamorphic differentiation: Contributions to Mineralogy and Petrology, v. 17, n. 3, p. 173-186.

Carver, R.E., 1971, Heavy-mineral separation, p. 427-452 <u>in</u> Procedures in sedimentary petrology: Wiley Interscience, New York.

Damon, P.E., 1964, Correlation and chronology of ore deposits and volcanic rocks: Ann. Prog. Report COO-689-42, Contract AT(11-1)-689, Research Div. U.S. Atomic Energy Comm., Arizona University Geochronology Labs, 117 p.

Damon, P.E., 1965, Correlation and chronology of ore deposits and volcanic rocks: Ann. Prog. Report COO-689-50, Contract AT(11-1)-689, Research Div., U.S. Atomic Energy Comm., Arizona University Geochronology Labs, 157 p.

Damon, P.E., and Giletti, B.J., 1961, The age of the basement rocks of the Colorado Plateau and adjacent areas: New York Acad. Sci. Annals, v. 91, article 2, p. 443-453.

Dings, M.G., 1950, Wallapai mining district, Mohave County, Arizona, <u>in</u> Arizona zinc and lead deposits, Part I: Ariz. Bureau of Mines Bull. 156, p. 138-142.

Dings, M.G., 1951, The Wallapai mining district, Cerbat Mountains, Mohave County, Arizona: U.S. Geol. Survey Bull. 978-E, p. 123-163.

Duffield, W.A., and Bacon, C.R., 1978, Origin of reverse-graded bedding in pumiceous air-fall deposits (Abstract): from 74th Geol. Soc. Amer. Cordilleran Sect. Ann. Meetings, Tempe, Ariz., p. 103.

Eidel, J.J., Frost, J.E., and Clippinger, D.M., 1968, Copper-molybdenum mineralization at Mineral Park, Mohave County, Arizona, <u>in</u> Ridge, J.D., ed., Ore deposits of the U.S. 1933-1967: A.I.M.E., Graton-Sales, v. 2, p. 1258-1281.

Heinrichs Geoexploration Company, 1967, Airborn proton total magnetic intensity and scintillation survey: Lost Basin Project, Private Apache Oro Co. Map, 1 sheet.

Hernon, R.M., 1938, Cerbat mountains, <u>in</u> Some Arizona ore deposits: Univ. of Arizona, Ariz. Bureau of Mines Bull. 145, p. 110-117.

Hutchison, C.S., 1974, Laboratory handbook of petrographic techniques: John Wiley & Sons, New York, 527 p.

Krish, E.J., 1974, Relationship of trace element distribution to level of erosion in some porphyry copper deposits and prospects, southwestern U.S. and northwestern Mexico: Colorado School of Mines, M.S. Thesis, unpub., 156 p.

Krumbein, W.C., and Pettijohn, F.J., 1938, Manual of sedimentary petrography: D. Appleton Century Company Pub., p. 412-458.

Longwell, C.R., 1921, Geology of the Muddy Mountains, Nevada, with a section to the Grand Wash Cliffs in western Arizona: Am. Jour. Sci., 5th series, v. 1, n. 1, p. 39-62.

Longwell, C.R., 1928, Geology of the Muddy Mountains, Nevada: U.S. Geol. Survey Bull. 798.

Longwell, C.R., 1936, Geology of the Boulder Reservoir floor, Arizona and Nevada: Geol. Soc. Amer. Bull., v. 47, p. 1393-1476.

Longwell, C.R., 1945, Low-angle normal faults in Basin and Range province: Am. Geophys. Union Trans., v. 26, pt. 1, p. 107-118.

Longwell, C.R., 1963, Reconnaissance geology between Lake Mead and Davis Dam, Arizona-Nevada: U.S. Geol. Survey Prof. Paper 374-E, 51p.

Longwell, C.R., 1974, Large scale lateral faulting in southern Nevada (Abstract): from 70th Geol. Soc. Amer. Cordilleran Sect. Ann. Meetings, Las Vegas, Nevada, p. 209.

Lowell, J.D., and Guilbert, J.M., 1970, Lateral and vertical alteration-mineralization zoning in porphyry ore deposits: Econ. Geol., v. 65, n. 4, p. 373-408.

Lucchitta, I., 1966, Cenozoic geology of the upper Lake Mead area adjacent to the Grand Wash Cliff, Arizona: Penn. State Univ., Unpub. Ph.D. Dissertation, 218 p.

Lucchitta, I., 1967, Pierce Ferry area, in Evaluation of the Colorado River in Arizona: from the Symposium on Cenozoic Geology of the Colorado Plateau in Arizona, Museum of Northern Arizona Bull. 44, Flagstaff, Arizona, 67 p.

Mallory, W.M., 1971a, Factors indicating the possibility of a large copper porphyry (?) in the Lost Basin mining district of Mohave County, Arizona: Private Apache Oro Company Report, 5 p.

Mallory, W.M., 1971b, Proposed exploration program, gold placer and copper-molybdenum bedrock properties, Lost Basin and Gold Basin mining districts, Mohave County, Arizona (revised Aug. 1972): Private Apache Oro Company Report, 11 p.

Mallory, W.M., 1972, Mineralization plot: Private Apache Oro Company Map.

Mallory, W.M., 1974a, Geophysical and geochemical data compiled on the Lost Basin mining district: Private Apache Oro Company Report.

Mallory, W.M., 1974b, Summary of gold, silver, copper-molybdenum deposits of Lost Basin, Mohave County, Arizona: Private Apache Oro Company Report, 7 p.

Mauger, R.L., and Damon, P.E., 1965, K-Ar ages of Laramide magmatism and copper mineralization in the southwest: Atomic Energy Comm. Ann. Progress Report, n. COO-689-50, p. AII-1-A-II-8.

McKee, E.D., and Weir, G.W., 1953, Terminology for stratification and cross-stratification in sedimentary rocks: Geol. Soc. Amer. Bull., v. 64, p. 381-390.

Moore, R.T., 1972, Geology of the Virgin and Beaverdam Mountains, Arizona: Arizona Bureau Mines Bull. 186.

National Park Service, 1972, Lake Mead National Recreation Area, Arizona-Nevada: park brochure published by the National Park Service, U.S. Dept. of the Interior.

Park, C.F., and MacDiarmid, R.A., 1975, Ore deposits: W.H. Freeman and Company, 529 p.

Post, E.V., 1970, Porphyry copper potential, Apache Oro properties, Lost Basin Range, Mohave County, Arizona: Private Apache Oro Company Report, 14 p.

Schrader, F.C., 1908, The mineral deposits of the Cerbat Range, Black Mountains and Grand Wash Cliffs, Mohave County, Arizona: U.S. Geol. Survey Bull. 340, p. 53-83.

Schrader, F.C., 1909, Mineral deposits of the Cerbat Range, Black Mountains and Grand Wash Cliffs, Mohave County, Arizona: U.S. Geol. Survey Bull. 397.

Schrader, F.C., 1917, Geology and ore deposits of Mohave County, Arizona: Amer. Inst. Mining Eng. Trans., v. 56, p. 195-236, maps.

Spry, A., 1976, Metamorphic textures: Pergamon Press Inc., New York, p. 227-231.

Sumner, J.S., and Aiken, C.L., 1974, Regional geophysical patterns and porphyry copper deposits in Arizona (Abstract): from 70th Geol. Soc. Amer. Cordilleran Sect. Ann. Meetings, Las Vegas, Nevada, p. 263-264.

Thomas, B.E., 1949, Ore deposits of the Wallapai district, Arizona: Econ. Geol., v. 44, p. 663-705.

Thomas, B.E., 1953, Geology of the Chloride Quadrangle, Arizona: Geol. Soc. Amer. Bull., v. 64, p. 391-420.

Till, R., 1974, Statistical methods for the earth scientist: Halsted Press, New York, 154 p.

Trites, A.F., 1974, Evaluation of the gold deposits of the Ford Mine and surrounding area of the Lost Basin mining district, Mohave County, Arizona: Private Apache Oro Company Report, 9 p.

U. S. Geological Survey, 1968, Heavy metals program, progress report 1966 and 1967: U.S. Geol. Survey Circular 560, p. 6.

Van Der Plas, L., and Tobi, A.C., 1965, A chart for judging the reliability of point counting results: Amer. Jour. of Sci., v. 263, p. 87-90.

Volborth, A., 1962, Rapakivi-type granites in the Precambrian complex of Gold Butte, Clark County, Nevada: Geol. Soc. Amer. Bull., v. 73, p. 813-832.

Wentworth, C.K., 1922, Grade and class for clastic sediments: Jour. of Geology, v. 30, p. 377-392.

Wilson, E.D., 1933, Arizona gold placers, <u>in</u> Arizona gold placers and placering: Univ. of Arizona, Arizona Bureau of Mines, Mineral Technology Series 35, v. IV#6, Bull. 135, p. 83-85.

Wilson, E.D., 1939, Precambrian Mazatzal Revolution in central Arizona: Geol. Soc. Amer. Bull., v. 50, p. 1113-1164.

Wilson, E.D., 1949, Structure of Arizona (Abstract): Geol. Soc. Amer. Bull., v. 60, p. 1929.

Wilson, E.D., 1962, A resume of the geology of Arizona: Univ. of Arizona, pub., Ariz. Bureau of Mines Bull. 171, 140 p.

Young, R.A., 1966, Cenozoic geology along the edge of the Colorado Plateau in north-western Arizona: Ph.D. Dissertation, Washington University, Dept. Earth Sciences, St. Louis, Missouri, 167 p.

Appendix A

DETAILED PETROLOGIC DESCRIPTIONS OF THIN SECTIONS

Specimen Number AD-1-77

I. Hand Specimen Description

Color (F - fresh, W - weathered): green-grey to pink-white (F), green-grey with MnO_2 staining (W)

Mineralogy: quartz, orthoclase-albite, chlorite, minor biotite, opaques

Texture and Grain Size-Shape: medium-fine grain, subhedral-anhedral, gneissic-weak lepidoblastic texture

Structures:

Layering: 2 cm felsic band

Banding: weak gneissic bands

Foliation: moderate schistose foliation

Other:

Alteration: biotite to chlorite

Mineralization:

Deformation Features:

II. Microscopic Thin Section Description

A. Mineralogy - estimated modes (%)

		%	Alteration of:	%
Essential				
	orthoclase-microcline	15	sericite & kaolinite	29
	plagioclase (remnant)	15	opaque (magnetite)	10
	quartz	10	epidote	8
	cordierite	7		
Varietal			chlorite	5
Accessory	biotite-relic	1		

Plagioclase Composition: oligoclase-andesine with
(Michel-Lévy Method) pericline & albite twinning

B. Texture and Grain Size-Shape

Essential orthoclase: medium-fine grain, subhedral, granoblastic. plagioclase: medium grain, subhedral-anhedral, porphyroblastic. quartz: fine grain, an-

Varietal hedral-subhedral.cordierite: subhedral, medium to fine grain, granoblastic.

Accessory biotite: fine grain, anhedral, remnant grains

Alteration of:

Essential sericite & kaolinite matrix: very fine grain, fibrous. epidote: fine grain, anhedral.

Varietal chlorite: very fine grain, anhedral

Accessory

Special Textures: Magnetite, biotite & chlorite are confined in thin phacoidal layers, commonly associated with the sericitization of the plagioclase. Granoblastic-gneissic texture, weak foliation

Alteration: biotite to chlorite-magnetite, argillic-sericitic alteration of plagioclase (40-60%), very weak epidotization of feldspar

Mineralization:

Structures:

Mineral Paragenesis:

Rock Type-Name: cordierite granodiorite gneiss

Geologic Occurrence: within P€$_2$ unit along ridge section

Specimen Number AD-2-77

I. Hand Specimen Description

Color (F - fresh, W - weathered): grey-green (F), green-black (W)

Mineralogy: amphibole, minor quartz and feldspar

Texture and Grain Size-Shape: fine grain, subhedral, strong nematoblastic-schistose texture

Structures:
Layering: moderately thin compositional layers

Banding: strong gneissic banding, very thin, continuous

Foliation: strong parallel grain alignment, schistose foliation

Other: good parting along foliation

Alteration: moderate chloritic alteration

Mineralization:

Deformation Features:

II. Microscopic Thin Section Description

A. Mineralogy - estimated modes (%)

		%	Alteration of:	%
Essential				
	amphibole (hornblende)	50	chlorite	30
	plagioclase-remnant	8		
Varietal	quartz	5	sericite	3
	magnetite	<1	epidote	2
Accessory	orthoclase	1		

Plagioclase Composition: indeterminate
(Michel-Lévy Method)

B. Texture and Grain Size-Shape

Essential amphibole: fine grain, subhedral, granulose plagioclase: fine grain, anhedral, decussate texture

Varietal quartz: fine grain, anhedral, decussate texture. magnetite: fine grain, anhedral, decussate texture

Accessory orthoclase: fine grain, anhedral, decussate texture

Alteration of:

Essential chlorite: fine matrix

Varietal sericite: very fine grain, anhedral epidote: fine grain, anhedral

Accessory

Special Textures: granulose to very strong nematoblastic texture, strongly foliated, well defined compositional layers

Alteration: very strong chloritization of amphibole, complete chloritization of feldspars, weak replacement of amphibole with epidote

Mineralization:

Structures:

Mineral Paragenesis:

Rock Type-Name; chlorite-amphibolite schist

Geologic Occurrence: within P€$_2$ unit along ridge section

Specimen Number AD-3-77

I. Hand Specimen Description

Color (F - fresh, W - weathered): grey-white to dark green-grey (F), light pink with MnO_2 staining (W)

Mineralogy: quartz, chlorite, feldspar, trace opaques

Texture and Grain Size-Shape: medium-fine grain, anhedral-subhedral granoblastic-gneissic texture

Structures:

Layering: compositional zones

Banding: gneissic discontinuous bands

Foliation: moderate-strong elongated grains

Other: well developed asymmetric folding

Alteration: chloritic

Mineralization: none

Deformation Features:

II. Microscopic Thin Section Description

A. Mineralogy - estimated modes (%)

	%	Alteration of:	%
Essential			
quartz	30	kaolinite	23
orthoclase	20	chlorite	10
plagioclase-remnant	15		
Varietal		epidote	2
Accessory			
opaque (magnetite)	<1		
biotite (remnant grains)	1		

Plagioclase Composition: albite- based on relict twinning
(Michel-Lévy Method)

B. Texture and Grain Size-Shape

Essential quartz: medium-fine grain, anhedral, granoblastic, orthoclase: medium to fine grain, anhedral, granoblastic, plagioclase: fine grain, anhedral,

Varietal granoblastic

Accessory

Alteration of:

Essential kaolinite: fine grain, subhedral, chlorite: subhedral matrix

Varietal epidote: very fine grain, anhedral

Accessory

Special Textures: strained quartz grains, elongated, show undulatory extinction, weak mortar texture, weak granoblastic to gneissic texture

Alteration: argillic alteration of feldspar(50-70%), chlorite completely replacing biotite, weak replacement of plagioclase with epidote

Mineralization:

Structures:

Mineral Paragenesis:

Rock Type-Name: quartz monzonite gneiss

Geologic Occurrence: within P€$_2$ unit along ridge section

Specimen Number AD-4-79

I. Hand Specimen Description

Color (F - fresh, W - weathered): grey-white (F)
light pink-grey (W)

Mineralogy: quartz, feldspar, chlorite, opaques

Texture and Grain Size-Shape: fine grain, subhedral-anhedral, granoblastic, weak gneissic texture

Structures:

Layering: massive, weak gneissic layers

Banding: very weak gneissic bands

Foliation: very weak grain alignment

Other:

Alteration: chloritic

Mineralization:

Deformation Features:

II. Microscopic Thin Section Description

A. Mineralogy - estimated modes (%)

		%	Alteration of:	%
Essential	quartz	40	kaolinite-sericite	20
	orthoclase	20	mixture	
	(microcline)		epidote	8
Varietal	plagioclase	5	chlorite	5
	(remnant)			
Accessory				
	magnetite	1		
	biotite (remnant)	1		

Plagioclase Composition: oligoclase-andesine(?) with
(Michel-Lévy Method) albite & pericline twinning

B. Texture and Grain Size-Shape

Essential quartz, orthoclase: medium-fine grain, anhedral, granoblastic.

Varietal plagioclase: medium grain, anhedral, relict twinning

Accessory magnetite: fine grain, relict euhedral grains

Alteration of:

Essential kaolinite-sericite matrix: very fine grain, anhedral, fibrous. epidote: fine grain, anhedral

Varietal chlorite: very fine grain, anhedral

Accessory

Special Textures: overall texture - decussate-granoblastic very weak gneissic foliation

Alteration: biotite altered to chlorite, plagioclase argillic-sericitic alteration, with minor epidote replacement (70-90%)

Mineralization:

Structures: strained quartz grains, elongated along foliation

Mineral Paragenesis:

Rock Type-Name: quartz monzonite gneiss

Geologic Occurrence: within P€$_2$ unit, near upper contact with P€$_3$ within 100 yards of the Van-Wulf portal

Specimen Number AD-5-77

I. Hand Specimen Description

Color (F - fresh, W - weathered): green-grey-white (F) grey-white (W)

Mineralogy: quartz, feldspar (plagioclase, orthoclase)

Texture and Grain Size-Shape: subhedral, coarse-medium grain, phaneritic-porphyritic texture

Structures:

Layering:

Banding:

Foliation: massive pegmatitic structure

Other:

Alteration: weak argillic alteration of feldspar

Mineralization:

Deformation Features:

II. Microscopic Thin Section Description

A. Mineralogy - estimated modes (%)

	%	Alteration of:	%
Essential			
quartz	30	sericite-kaolinite	15
plagioclase	30		
orthoclase-microcline	20		
Varietal		clinozoisite	3
		calcite	2
Accessory			

Plagioclase Composition: albite with albite twinning
(Michel-Lévy Method)

B. Texture and Grain Size-Shape

Essential quartz: medium grain, porphyroblastic, strained, feldspar: medium grain, anhedral, porphyroblastic

Varietal

Accessory

Alteration of:

Essential sericite-kaolinite: very fine grain, anhedral fibrous aggregate aligned with cleavage of feldspar

Varietal clinozoisite: fine grain, anhedral aggregates calcite: very fine grain matrix

Accessory

Special Textures: quartz: strong, undulatory extinction and interlocking grains, weak mortar texture, phaneritic-pegmatitic texture

Alteration: argillic-sericitic altered feldspar (20-60%) relict twinning in plagioclase, weak hydrothermal replacement of plagioclase by clinozoisite

Mineralization:

Structures: no foliation or orientation, the weak cataclastic texture of quartz with interlocking boundaries demonstrates some mild mylonitic event

Mineral Paragenesis: injection of pegmatite within P€$_2$ complex, later structural event generating mylonitization, synchronous and/or later hydrothermal alteration

Rock Type-Name: granodiorite pegmatite (weakly hydrothermally altered)

Geologic Occurrence: within P€$_2$ unit along mountain ridge in vicinity of lithologic contact with P€$_3$ unit

Specimen Number AD-6-77

I. Hand Specimen Description

Color (F - fresh, W - weathered): light green-white (F), grey-white (W)

Mineralogy: quartz, feldspar, biotite, chlorite

Texture and Grain Size-Shape: medium to fine grain, subhedral to anhedral, granoblastic-weak gneissic texture

Structures:

Layering: weak compositional layers

Banding: vague gneissic zoning

Foliation: weak foliation, weak alignment of micas

Other:

Alteration: weak chloritic alteration

Mineralization:

Deformation Features:

II. Microscopic Thin Section Description

A. Mineralogy - estimated modes (%)

	%	Alteration of:	%
Essential			
quartz	25	kaolinite, sericite	23
microcline	25	chlorite	5
orthoclase	15		
plagioclase	5		
Varietal		epidote	2
Accessory			
magnetite (trace)			

Plagioclase Composition: oligoclase with pericline and minor albite twinning
(Michel-Lévy Method)

B. Texture and Grain Size-Shape

Essential quartz: fine grain, anhedral. microcline: medium to fine grain, anhedral. orthoclase: fine grain, anhedral. plagioclase: medium to fine grain,
Varietal anhedral to subhedral.

Accessory magnetite: fine grain, anhedral.

Alteration of:
Essential kaolinite, sericite: fine grain, subhedral, fibrous. chlorite: fine grain, subhedral (after biotite).
Varietal epidote: fine grain, subhedral.

Accessory

Special Textures: strong brecciation and crushing of grains; broken, fractured grains; weak deformation; mortar matrix filling interstices;relict pegmatitic fabric within breccia fragments

Alteration: moderate argillic alteration with minor sericitic alteration of plagioclase-orthoclase; relict twinning; weak replacement of plagioclase by epidote; complete replacement of biotite by chlorite

Mineralization:

Structures: bent feldspar twinning; myrmekitic texture; fine granular matrix but no layering or banding of mortar matrix

Mineral Paragenesis:

Rock Type-Name: **granite pegmatite cataclastic breccia**
Geologic Occurrence: within P€$_2$ unit in Altered Valley just north of High Voltage Shaft

Specimen Number AD-7-77

I. Hand Specimen Description

Color (F - fresh, W - weathered): medium brown (F)
light brown-limonitic brown (W)

Mineralogy: remnant garnet(?), quartz, altered mica, limonite

Texture and Grain Size-Shape: medium-fine grain, anhedral relict lepidoblastic texture

Structures:

Layering: massive - homogeneous

Banding:

Foliation: schistose with kelyphytic rims

Other:

Alteration: shows limonitic oxidation, chloritic alteration

Mineralization:

Deformation Features: secondary fractures healed with Fe_2O_3

II. Microscopic Thin Section Description

A. Mineralogy - estimated modes (%)

	%	Alteration of:	%
Essential			
quartz	30	kaolinite, sericite,	35
cordierite	13	chlorite matrix	
biotite - remnant	10	Fe_2O_3	10
Varietal			
magnetite	2		
Accessory			

Plagioclase Composition:
(Michel-Lévy Method)

B. Texture and Grain Size-Shape

Essential quartz; fine grain, anhedral, strained. cordierite: fine grain, anhedral. biotote: fine grain, anhedral, fragments

Varietalmagnetite: fine grain, anhedral.

Accessory

Alteration of:

Essential kaolinite-sericite-chlorite matrix: fine grain, fibrous aggregates. Fe_2O_3: translucent

Varietal

Accessory

Special Textures: lepidoblastic - schistose texture with strong developed phacoidal lenses of complete alteration

Alteration: complete alteration of phacoidal lenses by kaolinite, sericite and chlorite,no relict grains or structures, strong fibrous aggregates, strong chloritic alteration of biotite

Mineralization:

Structures: strained, elongated-oriented quartz grains forming bands,relict phacoidal structures (completely altered) contributing to lepidoblastic texture

Mineral Paragenesis:

Rock Type-Name: biotite-cordierite schist

Geologic Occurrence: within $p\epsilon_2$ unit in Altered Valley due east of High Voltage Shaft in vicinity of bulldozer cut

Specimen Number AD-8-77

I. Hand Specimen Description

Color (F - fresh, W - weathered): light grey-black (F), limonitic brown (W)

Mineralogy: quartz, biotite, chlorite, garnet

Texture and Grain Size-Shape: fine grain, anhedral, deformed lepidoblastic texture

Structures:

Layering: weak compositional layering distorted

Banding:

Foliation: strong schistose foliation

Other: contorted folding

Alteration: chloritic alteration

Mineralization: none

Deformation Features:

II. Microscopic Thin Section Description

A. Mineralogy - estimated modes (%)

	%	Alteration of:	%
Essential			
sillimanite	30	sericite	20
quartz	20	chlorite	10
biotite	10	magnetite	5
garnet (almandite)	5		
Varietal			
Accessory			
anatase (trace)			

Plagioclase Composition:
(Michel-Lévy Method)

B. Texture and Grain Size-Shape

Essential sillimanite: medium to very fine grain, fibrous. quartz: medium grain, polycrystalline. biotite: fine grain, anhedral, fragments. garnet:

Varietal poikilitic porphyroblasts.

Accessory anatase: very fine grain, subhedral, red-brown color.

Alteration of:

Essential sericite: fine to very fine grain, fibrous. chlorite: fine grain, anhedral. magnetite: fine grain, anhedral, aligned along relict cleavage.

Varietal

Accessory

Special Textures: strong kelyphytic rims around garnets which are fractured and dissected with chlorite; garnets are weakly poikilitic with quartz inclusions; schistose-lepidoblastic texture with strong disruptive crenulations

Alteration: strong replacement of biotite by sillimanite; sillimanite altered to sericite; garnets moderately altered to chlorite and sericite; weak chloritic alteration of biotite

Mineralization: none present

Structures: deformation and rupture of schistosity; developed kelyphytic rims; lenticular layers of polycrystalline quartz

Mineral Paragenesis: biotite, garnet & quartz progressively metamorphosed to quartz with biotite altered to sillimanite and garnet; then weak retrogressive metamorphism to chlorite and sericite

Rock Type-Name: garnet biotite sillimanite schist

Geologic Occurrence: within $p\epsilon_1$ unit, near lithologic contact with $p\epsilon_2$ in vicinity of a major quartz vein in a saddle on the ridge

AD- 9-77
Specimen Number AD-68-78

I. Hand Specimen Description

Color (F - fresh, W - weathered): dark brown (F), medium brown with Fe_2O_3 staining (W)

Mineralogy: feldspar laths within an altered matrix, irresolvable

Texture and Grain Size-Shape: fine grain, anhedral-subhedral, decussate-mosaic texture with relict aphanitic diabasic texture

Structures:
Layering: massive

Banding:

Foliation:

Other: relict intersertial aphanitic igneous texture

Alteration: very strong oxidation with strong Fe_2O_3 staining

Mineralization:

Deformation Features: fractures healed with calcite and Fe_2O_3

II. Microscopic Thin Section Description

A. Mineralogy - estimated modes (%)

	%	Alteration of:	%
Essential			
plagioclase laths	30	kaolinite	25
magnetite	15	Fe_2O_3-calcite matrix	15
biotite	10		
Varietal		calcite-Fe_2O_3 reaction rims	5
Accessory		calcite (fracture fill)	1

Plagioclase Composition: labradorite(?) based on lath structure & poor relict carlsbad and albite twinning
(Michel-Lévy Method)

B. Texture and Grain Size-Shape

Essential plagioclase: medium-fine grain, subhedral-euhedral (skeletal crystal outlines). magnetite: very fine grain, anhedral-subhedral (interstices).

Varietal biotite: (remnant) fine grain, anhedral. Relict unknown minerals, porphyroblastic

Accessory

Alteration of:

Essential kaolinite: very fine grain, anhedral, fibrous. Fe_2O_3: very fine coating. calcite-Fe_2O_3: medium-fine grain, anhedral.

Varietal

Accessory calcite (fracture): fine grain, anhedral.

Special Textures: relict diabasic-intersertal igneous texture, masked byporphyroblastic kelyphytic rims of calcite core with Fe_2O_3 rims and an overall decussate to mosaic (hydrothermal) texture.

Alteration: very strong argillic alteration of plagioclase (60-80%), complete chloritization and oxidation of biotite, kelyphytic rims of an unknown mineral, strong calcite-Fe_2O_3 alteration matrix.

Mineralization:

Structures: pronounced igneous dike texture with 5% porphyritic structures generating reaction rims completely altering to Fe_2O_3 and calcite, secondary fractures healed with calcite

Mineral Paragenesis:

Rock Type-Name: diabase (hydrothermally altered)

Geologic Occurrence: within P€$_2$ unit along east flank of Altered Valley south of Cu Blowout quarry (see Figure 13)

Specimen Number AD-10-77

I. Hand Specimen Description

Color (F - fresh, W - weathered): dark grey-black (F) mottled black-white (W)

Mineralogy: quartz, amphibole, remnant feldspar

Texture and Grain Size-Shape: fine grain, subhedral-anhedral, granoblastic, nematoblastic texture

Structures:

Layering: thin, weakly developed compositional zones

Banding:

Foliation: moderate schistose foliation of an amphibole

Other:

Alteration: chloritic alteration of amphibole, weak argillic alteration

Mineralization:

Deformation Features:

II. Microscopic Thin Section Description

A. Mineralogy - estimated modes (%)

	%	Alteration of:	%
Essential			
amphibole (hornblende)	7	sericite-chlorite	75
		quartz (recrystallized ?)	10
Varietal			
plagioclase (remnant twinning)	3		
magnetite	3		
Accessory			
garnet (almandite)	<1	calcite (fracture fill)	1
		epidote group (clino-zoisite, inclined extinction)	1

Plagioclase Composition: albite based on very weak relict albite twinning
(Michel-Lévy Method)

B. Texture and Grain Size-Shape

Essential amphibole(hornblende): medium grain, anhedral

Varietal plagioclase remnant: very fine grain, anhedral, original outlines: medium grain, anhedral. magnetite: fine grain, anhedral

Accessory garnet: medium grain, anhedral

Alteration of:

Essential sericite: medium-very fine grain, fibrous-micaceous. chlorite: very fine grain, fibrous quartz: medium-fine grain, anhedral

Varietal

Accessory clinozoisite: very fine grain, anhedral calcite: fine grain, anhedral

Special Textures: pronounced development of kelyphytic rims with sericite-chlorite completely replacing feldspar, poikilitic inclusions of quartz, granoblastic: very weak gneissic texture

Alteration: reaction rims altering feldspar to sericite with outer rim of chlorite, weak replacement of hornblende by clinozoisite and quartz

Mineralization:

Structures: pronounced development of kelyphytic rims around feldspar, replacement quartz appearing as poikilitic inclusions, hairline fractures healed with calcite (post siliceous re-crystallization)

Mineral Paragenesis: amphibolite gneiss subjected to hydrothermal alteration with plagioclase to sericite-chlorite. hornblende going to epidote and quartz, late fracturing with calcite fill

Rock Type-Name: gneissic amphibolite(propylitically altered)

Geologic Occurrence: within P€$_2$ unit along east flank of Altered Valley on knoll just north of the High Voltage Shaft

Specimen Number AD-11-77

I. Hand Specimen Description

Color (F - fresh, W - weathered): grey-white (F)
dark grey-white (W)

Mineralogy: quartz, feldspar, muscovite, kaolinite

Texture and Grain Size-Shape: medium-coarse subhedral-anhedral, phaneritic-porphyritic texture

Structures:

Layering: weak compositional layers

Banding: weak banding of micaceous minerals

Foliation:

Other: moderate pegmatitic appearance

Alteration: moderate argillic alteration of feldspar, weak chloritic alteration

Mineralization:

Deformation Features:

II. Microscopic Thin Section Description

A. Mineralogy - estimated modes (%)

	%	Alteration of:	%
Essential			
orthoclase-plagioclase	30	kaolinite	38
quartz	25		
Varietal			
muscovite	2	sericite	4
Accessory		magnetite (bounded in sericite)	< 1

Plagioclase Composition: oligoclase, remnant albite
(Michel-Lévy Method) carlsbad twins

B. Texture and Grain Size-Shape

Essential feldspar: coarse grain, subhedral, porphyroblast. quartz; medium grain, anhedral, interlocking, polycrystalline

Varietal muscovite: medium grain, anhedral

Accessory

Alteration of:

Essential kaolinite: very fine, fibrous aggregates

Varietal sericite: medium-fine grain, fibrous

Accessory magnetite: very fine grain

Special Textures: relict phaneritic-pegmatitic texture with large porphyroblasts of feldspar, moderately strong mortar texture, strained granulated polycrystalline quartz

Alteration: strong argillic-sericitic alteration of feldspar (60-80%), weak relict twinning

Mineralization:

Structures: strong cataclastic-mortar structures, fractured-deformed grains, granulose mortar matrix show weak banding structures

Mineral Paragenesis: quartz & feldspar retrogressively metamorphosed into quartz, relict feldspar, kaolinite & sericite with minor magnetite, then late tectonic activity generating mylonitization

Rock Type-Name: granodiorite pegmatite mylonite

Geologic Occurrence: within P€$_2$ unit on knoll on eastern flank of Altered Valley, northeast of High Voltage Shaft, in vicinity of quartz vein

Specimen Number AD-12-77

I. Hand Specimen Description

Color (F - fresh, W - weathered): brown (F), dark brown with MnO_2 stain (W)

Mineralogy: sericite, Fe_2O_3 (abundant), remainder undetermined

Texture and Grain Size-Shape: fine grain, anhedral, weak trace schistose texture

Structures:

Layering:

Banding:

Foliation: poor schistose foliation

Other:

Alteration: intense oxidation and sericitization

Mineralization:

Deformation Features:

II. Microscopic Thin Section Description

A. Mineralogy - estimated modes (%)

		%	Alteration of:	%
Essential			Fe_2O_3	30
			kaolinite (fibrous matrix)	30
			sericite	20
			magnetite	15
Varietal	quartz	5		
Accessory				

Plagioclase Composition:
(Michel-Lévy Method)

B. Texture and Grain Size-Shape

Essential

Varietal quartz: medium-fine grain, anhedral

Accessory

Alteration of:

Essential Fe_2O_3: coarse grain translucent aggregates kaolinite: very fine grain, fibrous . sericite: medium-fine grain, anhedral. magnetite: very fine

Varietal grain, confined with sericite

Accessory

Special Textures: relict lepidoblastic-schistose texture masked by strong oxidized mosaic texture - petrographically irresolvable

Alteration: intense oxidation, extensive fibrous argillic-sericitic matrix

Mineralization:

Structures:

Mineral Paragenesis:

Rock Type-Name: indeterminate due to degree of alteration

Geologic Occurrence: within P€$_2$ unit in Altered Valley, due east from High Voltage Shaft

Specimen Number AD-13-77

I. Hand Specimen Description

Color (F - fresh, W - weathered): dark black-grey (F) dull grey-black (W)

Mineralogy: amphibole, trace of opaques, Fe_2O_3

Texture and Grain Size-Shape: medium grain, subhedral, nematoblastic to granoblastic texture

Structures:
Layering: massive

Banding:

Foliation: weak schistose gneissic alignment of amphibole

Other:

Alteration:

Mineralization:

Deformation Features:

II. Microscopic Thin Section Description

A. Mineralogy - estimated modes (%)

		%	Alteration of:	%
Essential	amphibole(hornblende)	60	kaolinite-sericite (matrix)	35
Varietal	magnetite	5		
Accessory				

Plagioclase Composition:
(Michel-Lévy Method)

B. Texture and Grain Size-Shape

Essential amphibole: medium grain, subhedral-euhedral, granoblastic, good cleavage (basal-longitudinal sections)

Varietal magnetite: subhedral, fine grain

Accessory

Alteration of:

Essential kaolinite-sericite: very fine grain, fibrous.

Varietal

Accessory

Special Textures: weak gneissic-nematoblastic texture, homogeneous

Alteration: alteration matrix of kaolinite and sericite completely filling in interstices where presumably feldspars occupied, hornblende unaltered

Mineralization:

Structures:

Mineral Paragenesis:

Rock Type-Name: gneissic amphibolite

Geologic Occurrence: within P€$_2$ unit on eastern flank of Altered Valley, across from the High Voltage Shaft

Specimen Number AD-14-77

I. Hand Specimen Description

Color (F - fresh, W - weathered): green-grey-white (F,W)

Mineralogy: quartz, biotite, chlorite, feldspar (predominantly plagioclase)

Texture and Grain Size-Shape: bimodal: porphyroblasts of plagioclase in medium-fine matrix, subhedral-anhedral, phaneritic-porphyritic texture

Structures:

Layering:

Banding:

Foliation:

Other: moderate pegmatitic appearance

Alteration: chloritic alteration

Mineralization:

Deformation Features:

II. Microscopic Thin Section Description

A. Mineralogy - estimated modes (%)

	%	Alteration of:	%
Essential			
plagioclase	25	kaolinite	30
orthoclase	15	magnetite	10
quartz	10	chlorite	7
Varietal			
		epidote	3
Accessory			
biotite	< 1	sericite (trace)	

Plagioclase Composition: albite with very fine albite twins
(Michel-Lévy Method)

B. Texture and Grain Size-Shape

Essential plagioclase: medium grain, anhedral, porphyroblastic. orthoclase: coarse-medium grain, anhedral. quartz: coarse-medium grain, anhedral,

Varietal strained

Accessory

Alteration of:

Essential kaolinite: very fine grain, anhedral, confined within feldspar structure. magnetite: fine grain, anhedral, restricted to biotite. chlorite: weak,

Varietal indistinguished

epidote: fine grain, anhedral

Accessory

Special Textures: coarse phaneritic-pegmatitic texture, moderate porphyritic plagioclase

Alteration: moderately strong argillic alteration of feldspar (40-60%), very weak chloritic alteration of biotite with strong bleaching, epidote associated with altered biotite, strongly altered feldspar, weakly replaced by epidote

Mineralization:

Structures: quartz grains strained, showing undulatory extinction

Mineral Paragenesis:

Rock Type-Name; granodiorite pegmatite (weakly propylitically altered)

Geologic Occurrence: within P€$_2$ unit along east flank of Altered Valley, across from the High Voltage Shaft

Specimen Number AD-15-77

I. Hand Specimen Description

Color (F - fresh, W - weathered): banded black-grey-white (F), dark red-brown-grey (W)

Mineralogy: garnet, biotite, quartz, plagioclase

Texture and Grain Size-Shape: fine grain, subhedral-anhedral, granoblastic-gneissic texture

Structures:

Layering: strong compositional layers, thin bedded, (2 mm thick)

Banding: strong gneissic bands, continuous

Foliation: strong gneissic

Other:

Alteration: chloritic (very weak)

Mineralization:

Deformation Features:

II. Microscopic Thin Section Description

A. Mineralogy - estimated modes (%)

		%	Alteration of:	%
Essential	quartz	20	kaolinite	10
	feldspar(orthoclase)	15		
	garnet(almandite)	15		
	biotite	20		
	plagioclase	10		
Varietal	magnetite	7	chlorite	2
Accessory	cordierite	1	Fe_2O_3 staining (trace)	

Plagioclase Composition: oligoclase-albite twinning
(Michel-Lévy Method)

B. Texture and Grain Size-Shape

Essential quartz: medium grain, anhedral, feldspar: medium grain, anhedral, plagioclase: medium grain, anhedral, biotite: fine grain, anhedral

Varietal

Accessory cordierite: fine grain, anhedral

Alteration of:

Essential kaolinite: very fine grain, subhedral, fibrous aggregates

Varietal chlorite: very fine grain, anhedral

Accessory

Special Textures: granoblastic with strong developed lepidoblastic layers, strong gneissic foliation

Alteration: very weak chloritic alteration of biotite, weak-moderate argillic alteration of feldspar

Mineralization:

Structures: moderate development of myrmekitic structures in orthoclase

Mineral Paragenesis:

Rock Type-Name: garnet granite gneiss

Geologic Occurrence: within $P\epsilon_2$ unit on eastern flank of Altered Valley, across from the High Voltage Shaft

Specimen Number AD-16a-77

I. Hand Specimen Description

Color (F - fresh, W - weathered): light green-grey to light brown (F), green-grey to yellow brown (W)

Mineralogy: quartz, feldspar, clay, magnetite, sericite

Texture and Grain Size-Shape: medium-fine grain, subhedral-anhedral, phaneritic, decussate texture

Structures:

Layering:

Banding:

Foliation: homogeneous, non-foliated

Other: weak pegmatitic appearance

Alteration: argillic-sericitic alteration

Mineralization:

Deformation Features:

II. Microscopic Thin Section Description

A. Mineralogy - estimated modes (%)

	%	Alteration of:	%
Essential			
feldspar (remnant)	25	kaolinite	35
(predominately plagioclase)		sericite	20
quartz	15		
Varietal			
muscovite	2	magnetite	3
Accessory			

Plagioclase Composition: albite with remnant albite twinning
(Michel-Lévy Method)

B. Texture and Grain Size-Shape

Essential feldspar: medium grain, anhedral with relict twinning, porphyroblastic. quartz: medium-coarse grain, anhedral, weak undulatory extinction

Varietal muscovite: fine grain, anhedral

Accessory

Alteration of:

Essential kaolinite: fine grain. sericite: medium grain, subhedral

Varietal magnetite: euhedral, fine grain

Accessory

Special Textures: coarse phaneritic-pegmatitic texture with feldspar porphyroblasts

Alteration: strong argillic-sericitic alteration of feldspar (60-80%)

Mineralization:

Structures: strained quartz grains

Mineral Paragenesis:

Rock Type-Name: granodiorite pegmatite(argillic-sericitic altered)

Geologic Occurrence: within P€$_2$ unit taken in tractor swipe across from the High Voltage Shaft

Specimen Number AD-16b-77

I. Hand Specimen Description

Color (F - fresh, W - weathered): dark brown (F)
dark grey-brown (W)

Mineralogy: quartz, sericite, matrix irresolvable

Texture and Grain Size-Shape: fine grain, anhedral, relict lepidoblastic-schistose texture

Structures:
Layering: micaceous

Banding:

Foliation: strong relict schistosity

Other:

Alteration: intense oxidation, argillic-chloritic alteration, strong sericitization

Mineralization:

Deformation Features: fracture fill with Fe_2O_3 and calcite

II. Microscopic Thin Section Description

A. Mineralogy - estimated modes (%)

		%	Alteration of:	%
Essential	quartz	10	kaolinite	30
	amphibole (remnant ghost structures)	5	Fe_2O_3 (limonite)	20
			chlorite	15
			sericite	13
			calcite (lenses)	6
Varietal				
Accessory	magnetite	<1	calcite (fracture fill)	1

Plagioclase Composition:
(Michel-Lévy Method)

B. Texture and Grain Size-Shape

Essential quartz: fine-very fine grain, anhedral, strained. amphibole: medium grain, anhedral-subhedral(ghost structures-anhedral)

Varietal

Accessory magnetite: very fine grain, anhedral

Alteration of:

Essential kaolinite-chlorite: fine grain, fibrous . Fe_2O_3: amorphous. sericite: very fine grain, fibrous . calcite: medium-fine grain, anhedral

Varietal

Accessory

Special Textures: strong schistose nematoblastic texture

Alteration: very strong argillization and chloritization of amphibole with complete sericitization-argillization of any feldspar present, strong oxidation of magnetite

Mineralization:

Structures: calcite fracture fills are post-oxidation, moderate development of thin lenses of calcite along foliation

Mineral Paragenesis:

Rock Type-Name: schistose amphibolite(argillically altered)

Geologic Occurrence: within $p\epsilon_2$ unit within thin bedded sequence exposed in tractor swipe across from High Voltage Shaft

Specimen Number AD-16c-77

I. Hand Specimen Description

Color (F - fresh, W - weathered): mottled grey-brown (F) speckled green-grey (W)

Mineralogy: quartz, chlorite, sericite, magnetite, Fe_2O_3, garnet

Texture and Grain Size-Shape: medium-fine grain, anhedral to subhedral, granoblastic, weak schistose texture

Structures:
Layering:

Banding: vague compositional zoning

Foliation: weak schistosity

Other:

Alteration: chloritic-sericitic alteration

Mineralization:

Deformation Features:

II. Microscopic Thin Section Description

A. Mineralogy - estimated modes (%)

	%	Alteration of:	%
Essential			
quartz	20	sericite matrix	40
biotite	15	chlorite	15
garnet(remnant) almandite)	5		
Varietal		magnetite	2
		secondary quartz	2
Accessory			
disseminated pyrite	1		

Plagioclase Composition:
(Michel-Lévy Method)

B. Texture and Grain Size-Shape

Essential quartz: medium grain, anhedral, undulatory extinction. biotite: fine grain, anhedral. garnet: fine grain, anhedral

Varietal

Accessory pyrite: fine grain, euhedral

Alteration of:

Essential sericite: very fine grain, complete replacement

Varietal secondary quartz: fine grain, rounded magnetite: medium grain, euhedral

Accessory

Special Textures: weak schistose foliation, elongation of quartz grains and garnet layers weakly developed

Alteration: garnet (90%) altered to chlorite and sericite, very weak chloritic alteration and bleaching of biotite, no trace of any feldspar

Mineralization:

Structures: kelyphytic rims completely replacing garnet with chlorite and sericite, weak secondary silicification, strained primary quartz

Mineral Paragenesis:

Rock Type-Name: garnet-biotite schist(sericitic altered)

Geologic Occurrence: within P€$_2$ tractor swipe directly across from the High Voltage Shaft

Specimen Number AD-16d-77

I. Hand Specimen Description

Color (F - fresh, W - weathered): mottled grey-black to brown-white (F), dark grey-black with MnO_2 staining (W)

Mineralogy: quartz, biotite, remainder indeterminate

Texture and Grain Size-Shape: fine - very fine grain, anhedral, vague nematoblastic texture

Structures:
Layering: compositional

Banding: moderate discontinuous banding

Foliation: weak schistose habit

Other:

Alteration: intense chloritic oxidation, Fe_2O_3 stains

Mineralization: $CaCO_3$ coating

Deformation Features: secondary fractures healed with $CaCO_3$

II. Microscopic Thin Section Description

A. Mineralogy - estimated modes (%)

	%	Alteration of:	%
Essential			
amphibole	30	chlorite	25
(hornblende)		calcite(fracture,	15
biotite	7	fill & matrix)	
quartz	5	sericite	13
Varietal		magnetite	5
Accessory			

Plagioclase Composition:
(Michel-Lévy Method)

B. Texture and Grain Size-Shape

Essential amphibole: medium grain, subhedral. biotite: medium grain, anhedral. quartz: medium grain, anhedral

Varietal

Accessory -

Alteration of:

Essential chlorite & sericite: very fine grain, anhedral. calcite: medium grain, anhedral. magnetite: fine grain, subhedral

Varietal

Accessory

Special Textures: weak relict schistose texture overprinted with a mosaic alteration texture

Alteration: moderate chloritic-sericitic alteration of biotite and amphibole, strong development of altered matrix basically consisting of calcite, sericite and chlorite, otherwise is petrographically irresolvable

Mineralization:

Structures: fractures healed with calcite with increased alteration in the vicinity of the fractures

Mineral Paragenesis:

Rock Type-Name: schistose amphibolite (propylitically altered)

Geologic Occurrence: within P€$_2$ unit in bulldozer cut due east from the High Voltage Shaft

Specimen Number AD-16e-77

I. Hand Specimen Description

Color (F - fresh, W - weathered): yellow-white to grey (F), grey-white (W)

Mineralogy: fragments of quartz, altered feldspar

Texture and Grain Size-Shape: fine to coarse grain, anhedral, angular, cataclastic texture.

Structures:
Layering:

Banding:

Foliation:

Other: fragments supported in cataclastic matrix

Alteration: argillic alteration (?)

Mineralization:

Deformation Features: intense brecciation-mylonitization

II. Microscopic Thin Section Description

A. Mineralogy - estimated modes (%)

	%	Alteration of:	%
Essential			
plagioclase-orthoclase	25	calcite	20
quartz	20	sericite	15
breccia matrix	15	secondary quartz	5
Varietal			
Accessory			

Plagioclase Composition: andesine with albite-pericline twinning
(Michel-Lévy Method)

B. Texture and Grain Size-Shape

Essential plagioclase: medium grain, anhedral, porphyroblastic. orthoclase: medium-fine grain, anhedral. quartz: medium grain, anhedral, undulatory

Varietal extinction. microcline: anhedral, porphyroblasts.

Accessory

Alteration of:

Essential sericite: very fine grain, subhedral, calcite matrix: very fine grain. secondary quartz: rounded blebs, medium-fine grain.

Varietal

Accessory

Special Textures: relict myrmekitic textures in the orthoclase, minor antiperthitic plagioclase

Alteration: moderate sericitic alteration of plagioclase, strong calcite cemented matrix, weak secondary silicification (?)

Mineralization:

Structures: abundant bent feldspar twinning, fractured-deformed grains, strong cataclastic-mortar texture, abundant healed fractures, crushed breccia matrix with finer calcite-sericite fill.

Mineral Paragenesis: fault generated breccia from a pegmatitic member of $P€_2$ unit.

Rock Type-Name: pegmatite cataclastic breccia

Geologic Occurrence: within $P€_2$ unit in vicinity of High Voltage Shaft near fault zone

Specimen Number AD-17-77

I. Hand Specimen Description

Color (F - fresh, W - weathered): mottled pink-grey-green black (F), same with faint Fe_2O_3 staining (W)

Mineralogy: quartz, feldspar, chlorite, magnetite

Texture and Grain Size-Shape: medium-fine grain, subhedral to anhedral, granoblastic texture

Structures:
Layering: weak compositional layering

Banding: gneissic - discontinuous

Foliation: moderate gneissic foliation

Other:

Alteration: chloritic alteration

Mineralization: weak epidotization confined to fractures

Deformation Features:

II. Microscopic Thin Section Description

A. Mineralogy - estimated modes (%)

	%	Alteration of:	%
Essential			
orthoclase	30	epidote	20
quartz	20	chlorite	10
plagioclase(remnant)	15	sericite	3
Varietal			
		calcite(fracture fill)	2
Accessory			
magnetite	< 1		
sphene (trace)			

Plagioclase Composition: albite-oligoclase, relict very fine albite twinning
(Michel-Lévy Method)

B. Texture and Grain Size-Shape

Essential orthoclase: coarse-medium grain, anhedral, quartz: coarse-fine grain, anhedral. plagioclase: anhedral, porphyroblastic

Varietal

Accessory magnetite: medium grain, anhedral

Alteration of:

Essential epidote: medium-fine grain, subhedral. chlorite: fine grain, subhedral. sericite: very fine grain, anhedral

Varietal calcite: medium grain, anhedral

Accessory

Special Textures: weak gneissic-porphyroblastic texture, relict plagioclase twinning

Alteration: feldspar weakly sericitized and moderately (20-30%) replaced by chlorite and epidote, (pseudo-poikilitic texture within feldspar)

Mineralization: hydrothermal introduction of calcite, epidote, chlorite, magnetite along fracture

Structures: fracture healed with weak hydrothermal calcite and epidote mineralization, strained-elongated quartz grains

Mineral Paragenesis: regional metamorphism generating feldspathic gneiss from arkosic sediments, much later hydrothermal event resulting in strong propylitic alteration

Rock Type-Name: quartz monzonite gneiss (propylitically alt.)

Geologic Occurrence: within P€$_3$ unit on top of the mountain ridge just south, upslope from the Van-Wulf Mine portal

Specimen Number AD-18-77

I. Hand Specimen Description

Color (F - fresh, W - weathered): Dark green-black to red-brown (F), dark green-black with MnO_2 stains (W)

Mineralogy: mineralogically irresolvable except for quartz chlorite, Fe_2O_3 matrix

Texture and Grain Size-Shape: very fine, anhedral, massive aphanitic-granulose texture

Structures:

Layering:

Banding: oxidation banding in rock (4cm thick)

Foliation: moderate schistose foliation

Other: exterior rind with oxidation and leaching of $CaCO_3$, MnO_2 coating

Alteration: strong chloritic alteration and oxidation

Mineralization:

Deformation Features:

II. Microscopic Thin Section Description

A. Mineralogy - estimated modes (%)

		%	Alteration of:	%
Essential			kaolinite(?) & chlorite	35
			Fe_2O_3	30
			calcite	20
			quartz	10
Varietal	magnetite (skeletal outline of amphiboles)	5		
Accessory			Fe_2O_3 casts w/ calcite cores (trace)	

Plagioclase Composition:
(Michel-Lévy Method)

B. Texture and Grain Size-Shape

Essential

Varietal magnetite: very fine grain, anhedral, aligned along relict cleavage of amphibole (?)

Accessory

Alteration of:

Essential kaolinite & chlorite: very fine grain, fibrous aggregate matrix. Fe_2O_3: fine grain, amorphous. calcite & quartz: medium-very fine grain, anhedral

Varietal

Accessory

Special Textures: strong decussate-fine granulose texture, except for the magnetite, showed vague outline of large amphibole crystals, no relict metamorphic texture

Alteration: very strong complete propylitic alteration of host rock, strong oxidation, note: the kaolinite-chlorite matrix pronounced, possibly indicating abundant feldspar or amphibole in original rock

Mineralization: secondary silicification of matrix

Structures: vein structure with abundant quartz, calcite and kaolinite-chlorite, no mineralization, skeletal oxide cast of primary sulfide with secondary calcite cores (after pyrite?)

Mineral Paragenesis:

Rock Type-Name: propylitically altered rock (amphibolitic rock ?)

Geologic Occurrence: within P€$_3$ unit taken on knoll of paragneiss complex, field appearance suggested a diabasic intrusion (?)

Specimen Number AD-19-78

I. Hand Specimen Description

Color (F - fresh, W - weathered): green-black to grey-white (F), (W)

Mineralogy: quartz, feldspar, garnet, chlorite, biotite

Texture and Grain Size-Shape: fine-medium grain, anhedral schistose-lepidoblastic texture

Structures:

Layering: thin compositional layers (2mm thick)

Banding: continuous gneissic bands

Foliation: strong schistose foliation

Other: minor augen structures with garnets

Alteration: chloritic alteration

Mineralization:

Deformation Features:

II. Microscopic Thin Section Description

A. Mineralogy - estimated modes (%)

	%	Alteration of:	%
Essential			
quartz	20	kaolinite, sericite,	56
orthoclase	15	chlorite (altered	
albite (remnant)	3	matrix)	
magnetite	3		
Varietal			
garnet with inclusions of quartz	2		
Accessory biotite	1		

Plagioclase Composition: albite with albite twinning
(Michel-Lévy Method)

B. Texture and Grain Size-Shape

Essential quartz: fine grain, anhedral, granulose.
feldspar: fine grain, anhedral, granulose

Varietal garnet: medium grain, anhedral, porphyroblastic

Accessory

Alteration of:

Essential alteration matrix: very fine grain, fibrous aggregates

Varietal

Accessory

Special Textures: schistose-lepidoblastic texture with porphyroblasts of poikilitic garnet with quartz inclusions, strong kelyphytic rims around abundant garnet.

Alteration: complete sericitization-chloritization of garnet, complete argillization and weak sericitization of plagioclase

Mineralization:

Structures: moderately developed reaction rims around the garnets which are highly fractured and strongly sericitized and chloritized

Mineral Paragenesis: originally garnet-biotitic schist, then retrogressive metamorphism altered the biotite, feldspars and garnet

Rock Type-Name: garnet chlorite schist (altered)

Geologic Occurrence: within P€$_3$ unit along southern portion of major mountain ridge

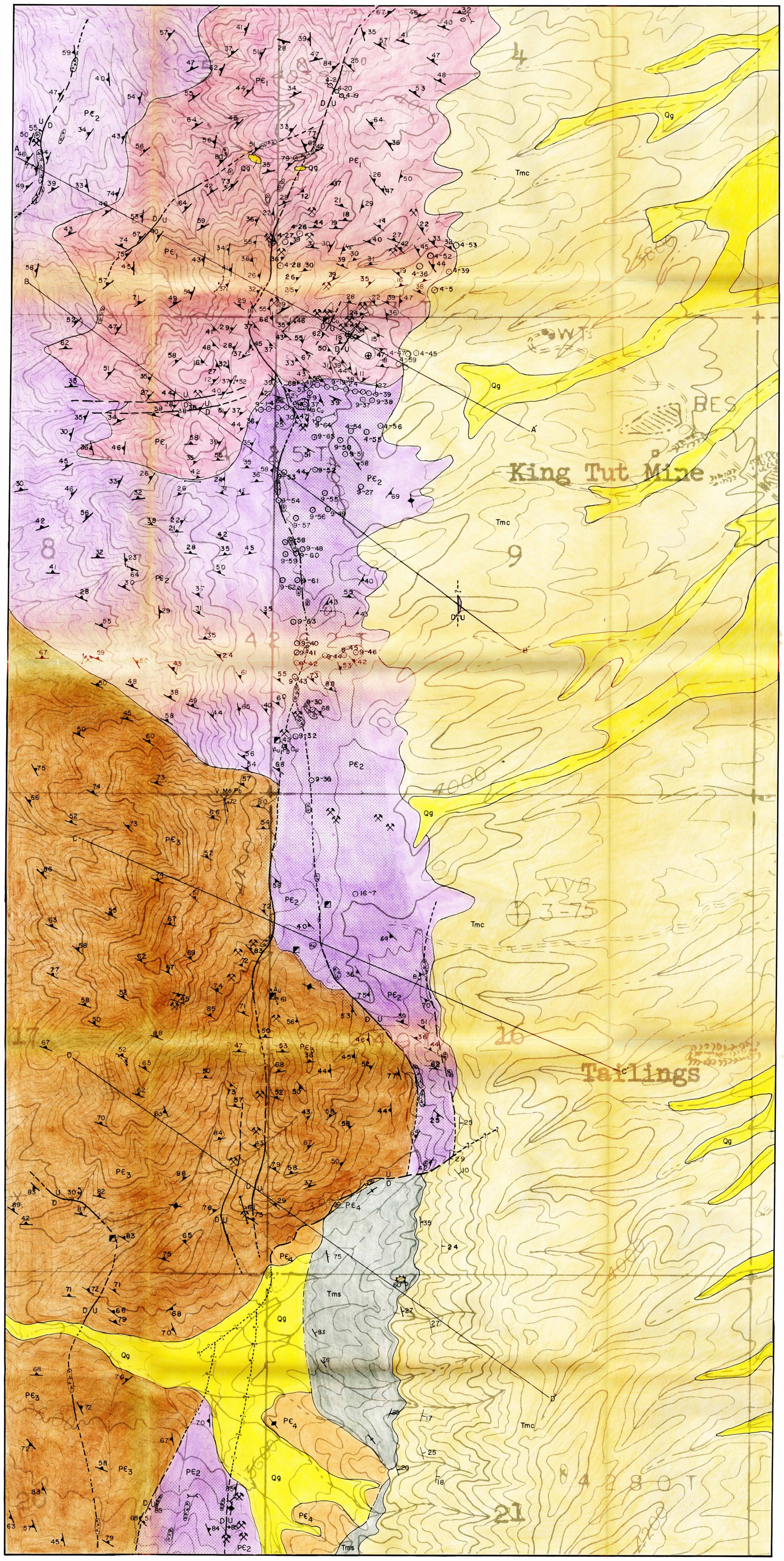

GEOLOGY BY ALFRED DEADERICK, 1978

GEOLOGIC MAP AND SECTIONS OF THE LOST BASIN PROSPECT, MOHAVE COUNTY, ARIZONA

EXPLANATION

DESCRIPTION OF MAP UNITS

QUATERNARY

Qg QUATERNARY GRAVELS STREAM GRAVEL AND ALLUVIUM DEPOSITED ALONG ACTIVE WASHES, LOCALLY INCLUDES TALUS AND COLLUVIUM

MIOCENE - PLIOCENE

Tmc FANGLOMERATE MODERATE TO WELL CONSOLIDATED ALLUVIAL FAN DEPOSITS OF THE MUDDY CREEK FORMATION, CALICHE CEMETED, WITH PREDOMINANTLY PRECAMBRIAN METAMORPHIC CLASTS, INCLUDES LENSES OF TUFFACEOUS SANDSTONE. REWORKING OF THESE DEPOSITS HAS BEEN ASSOCIATED WITH LOCAL CONCENTRATION OF DETRITAL GOLD.

UNCONFORMITY

Tms MUDFLOWS AND RHYOLITIC TUFFACEOUS SEDIMENTS STEEPLY DIPPING ALTERNATING SEQUENCE OF TUFFACEOUS MUDFLOWS WITH PREDOMINANTLY PRECAMBRIAN GRANITE MIGMATITIC CLASTS AND WATER LAID RHYOLITIC TUFFACEOUS SEDIMENTS

UNCONFORMITY

PRECAMBRIAN COMPLEX

PЄ4 GRANITIC MIGMATITE COMPLEX MAJOR BIOTITE LEPIDOBLASTIC MIGMATITE WITH CONTORTED AND TIGHTLY CRENULATED FOLIATIONS. STRONGLY DEVELOPED FELSIC LEUCOSOMES AND LARGE DISCORDANT FELSIC PEGMATITES. MIGMATITE COMPLEX INJECTED INTO PARAGNEISS COMPLEX

PЄ3 GRANODIORITE GNEISS COMPLEX SEQUENCE OF FINE TO MEDIUM GRAINED FELSIC TO QUARTZ-PLAGIOCLASE GNEISSES, MASSIVE TO THICK GNEISSIC BANDING WITH STRONG DEVELOPMENT OF PTYGMATIC FOLDING. COMPOSITIONAL BOUNDARIES ARE GRADATIONAL. LOCALLY AMPHIBOLITE GNEISSES AND THIN CHLORITIC-BIOTITE SCHISTS. SPORADIC OCCURANCES OF PEGMATITES, PREDOMINANTLY CONCORDANT TO FOLIATION TRENDS

PЄ2 PARAGNEISS COMPLEX UNDIFFERENTIATED ASSEMBLAGE OF METASEDIMENTS, ALTERNATING SEQUENCE OF THIN TO THICK LAYERED AMPHIBOLITE GNEISS, AMPHIBOLITES, QUARTZ-FELDSPAR GNEISSES, THIN MINOR BIOTITE SCHISTS AND THICK PEGMATITES STRONGLY CONCORDANT TO FOLIATION TRENDS

PЄ1 MIGMATITIC GNEISS UNDIFFERENTIATED ASSEMBLAGE OF THIN BEDDED METASEDIMENTS, DOMINANTLY FINE-MEDIUM GRAIN QUARTZ-PLAGIOCLASE GNEISS, BIOTITE-GARNET SCHISTS, AMPHIBOLITE, AMPHIBOLITE GNEISS, CALC-SILICATE GNEISS AND IRON BANDED QUARTZITE. WEAK LEPIDOBLASTIC TO NEMATOBLASTIC AND STRONG PTYGMATIC FOLDING IN QUARTZ-PLAGIOCLASE GNEISS

SYMBOLS

GEOLOGIC CONTACT, SOLID WHERE KNOWN, DASHED WHERE APPROXIMATELY LOCATED, DOTTED WHERE CONCEALED

55 U D — FAULT SHOWING DIRECTION OF DIP, SOLID WHERE KNOWN, LONG DASH WHERE APPROXIMATELY LOCATED, SHORT DASH WHERE INFERRED, DOTTED WHERE CONCEALED (U ON UPTHROWN, D ON DOWNTHROWN)

? — FAULT INFERRED FROM INDIRECT GEOLOGIC EVIDENCE

STRIKE AND DIP OF SEDIMENTARY BEDS

STRIKE AND DIP OF OVERTURNED SEDIMENTARY BEDS

STRIKE OF VERTICAL SEDIMENTARY BEDS

STRIKE AND DIP OF FOLIATION

STRIKE OF VERTICAL FOLIATION

STRIKE OF HORIZONTAL FOLIATION

STRIKE AND DIP OF JOINT

34 — STRIKE AND DIP OF QUARTZ VEIN

PROSPECT PIT, GLORY HOLE

EXCAVATION PIT

BULLDOZER CUT

MINE ADIT

MINE SHAFT

9-4 — DRILL HOLE, 9-SECTION NUMBER, 4-HOLE NUMBER

BRECCIA ZONE

ALTERED ZONE

A—A′ GEOLOGIC CROSS SECTION

Au, Ag, Cu, Mo, V, Pb — ELEMENT SYMBOLS INDICATING MINERALIZATION OBSERVED IN FIELD

SLUMP BLOCK

TN MN 15.5 MAGNETIC DECLINATION

SCALE 1:6000

0 500 1000 1500 2000 FEET

0 100 200 300 400 500 METERS

CONTOUR INTERVAL 40 FEET

BASE MAP FROM PART OF 7 1/2′ PRELIMINARY EDITION OF MT. TIPTON NW, NE, USGS TOPOGRAPHIC SHEETS

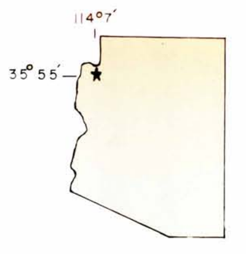

LOCATION MAP

GEOLOGIC CROSS SECTION A-A′

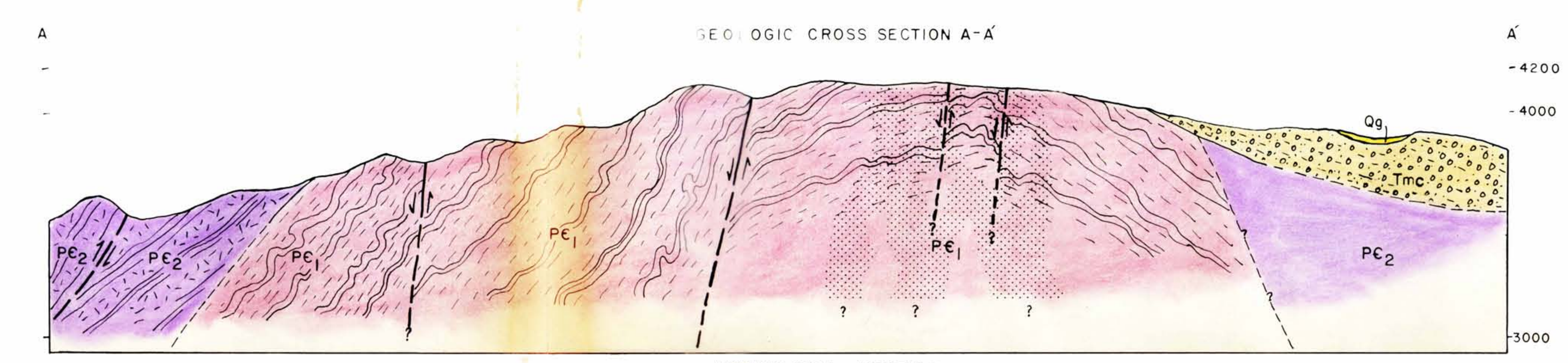

HORIZONTAL = VERTICAL

GEOLOGIC CROSS SECTION B-B′

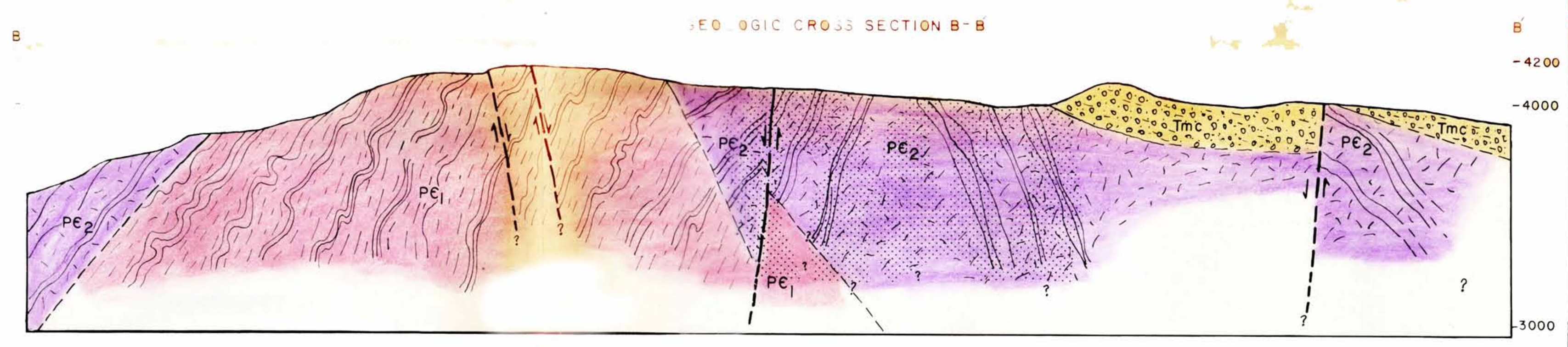

GEOLOGIC CROSS SECTION C-C′

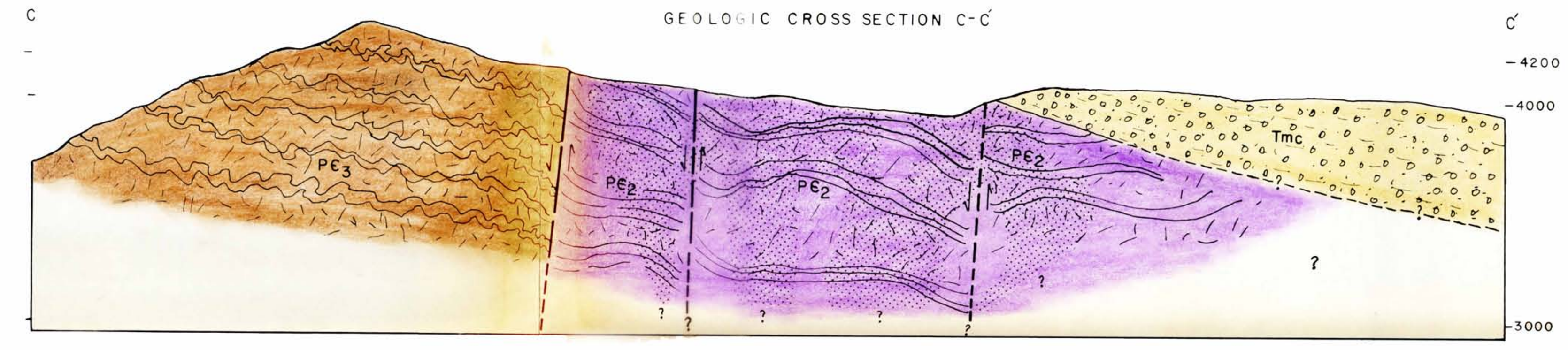

GEOLOGIC CROSS SECTION D-D′

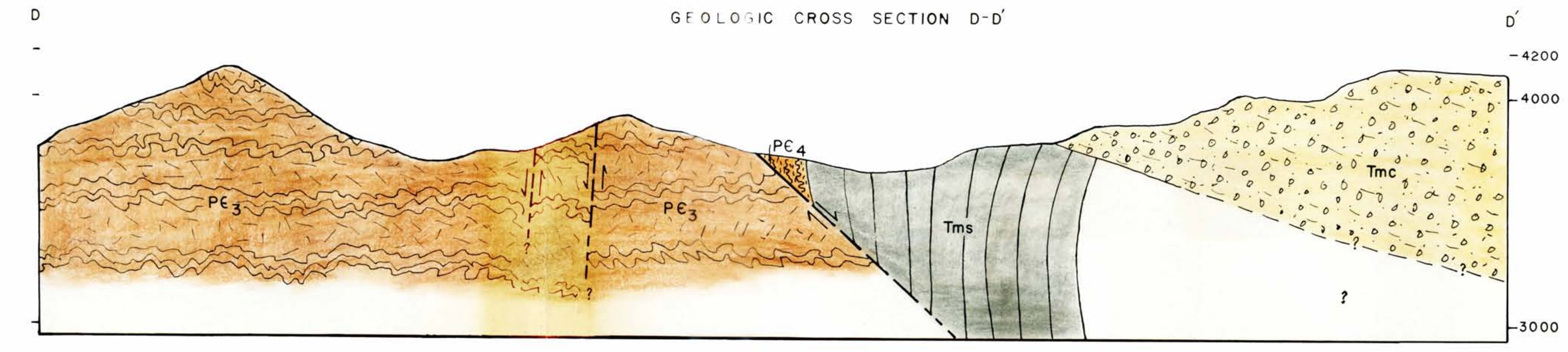

PLATE II

SAMPLE MAP AND PARTIAL STRATIGRAPHIC SECTIONS OF THE LOST BASIN PROSPECT, MOHAVE COUNTY, ARIZONA

EXPLANATION

- 4-16 DRILL HOLE, 4-SECTION NUMBER, 16-HOLE NUMBER
- BULLDOZER CUT
- GEOLOGIC SAMPLE LOCATION
  - △ - THIN SECTION
  - ∘ - GEOCHEMICAL ANALYSIS
- PROSPECT PIT, GLORY HOLE
- MINE SHAFT
- EXCAVATION PIT
- Au,Ag,Cu ELEMENT SYMBOLS INDICATING MINERALIZATION OBSERVED IN FIELD
- MINE ADIT
- A A' LOCATION AND DIRECTION OF MEASURED STRATIGRAPHIC SECTIONS

SCALE 1:6000

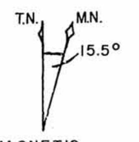

MAGNETIC DECLINATION

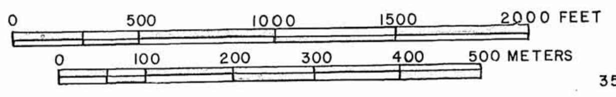

CONTOUR INTERVAL 40 FEET

BASE MAP FROM PART OF 7 1/2' PRELIMINARY EDITION OF MT. *TIPTON 1 N.W., NE.* USGS TOPOGRAPHIC SHEETS

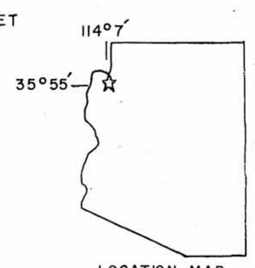

LOCATION MAP

STRATIGRAPHIC SECTION A-A'

VERTICAL SCALE 1"=10'

(w.)-weathered color

(f.)-fresh color

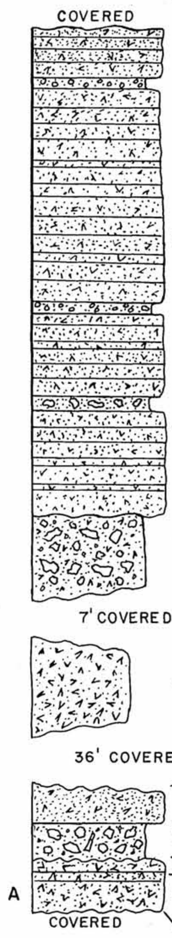

THICKNESS	STRAT. UNIT	DESCRIPTION
38'	7	TUFFACEOUS SANDSTONE, DRK. GREY WHITE(w.) TO LT. GREY WHITE(f.), MED.-FINE GRAIN, MOD. SORT., SUBANG.-SUBRND., THIN PARALLEL LAM. BEDS 3-10cm THICK, SPORADIC THIN INTERBEDDED MUDFLOWS 10-20cm THICK, JOINTING PERPENDICULAR AND PARALLEL TO BEDDING, WEATHERS TO BLOCKY RUBBLE, MOD. $CaCO_3$ CEMENT.
6'	6	MUDFLOW, LT. BROWN(w.) TO TAN(f.), COARSE GRAVEL-SILT, V. POOR SORT., TUFFACEOUS MATRIX, ANG. GRAINS, WEAKLY ORIENT., MASSIVE BEDS>1m, THIN DEFORMED BEDS DRAPED OVER CLASTS, WEATHERS TO SOIL AND COLLUVIUM OF P€ GRANITIC MIGMATITE CLASTS, POOR $CaCO_3$ CEMENT
6'	5	ANDESITIC TUFF(?), YELLOW BROWN(w.) TO LT. PURPLE BROWN, MED.-FINE GRAIN, GOOD SORT., SUBRND., HOMOGENEOUS MASSIVE BED>1m, WEATHERS TO SOIL AND FRIABLE ROUND RUBBLE, POOR FERRUGENOUS CEMENT.
2'	4	TUFFACEOUS SANDSTONE, DRK. GREY BROWN(w,f.), V. COARSE TO MED. GRAIN, POOR SORT., FINE TUFFACEOUS MATRIX, SUBRND, MOD. ORIENT., PARALLEL LAM. BEDS 3-10cm THICK, REVERSE GRADING, WEATHERS TO ROUNDED RUBBLE, PUMICE FRAGS. INTERBEDDED AND MOD. ORIENT., POOR $CaCO_3$ CEMENT.
2.8'	3	MUDFLOW, GREY BROWN(w.) TO GREY WHITE(f.), COARSE GRAVEL TO FINE GRAIN, V. POOR SORT., TUFFACEOUS MATRIX, SUBRND., MOD. ORIENT. CLASTS, MASSIVE BED>1m, NORMAL AND REVERSE GRADED BEDS, WEATHERS TO SOIL AND COLLUVIUM OF P€ GRANITIC MIGMATITE CLASTS, POOR $CaCO_3$ CEMENT.
1'	2	TUFFACEOUS SANDSTONE, TAN-BUFF WHITE(w.) TO LT. GREY WHITE(f.), V. FINE GRAIN, GOOD SORT., SUBRND., MASSIVE HOM. BEDS 10-30cm THICK, JOINTS PERPENDICULAR AND PARALLEL TO BEDS, WEATHERS TO BLOCKY RUBBLE, MOD. WELL SiO_2 CEMENT
2.5	1	TUFFACEOUS SANDSTONE, DRK. GREY WHITE(w.) TO GREY BROWN(f.), MED. TO FINE GRAIN, MOD. SORT., SUBRND., THIN HOM. LAM. BEDS 0.3-1cm THICK, WEATHERS TO ROUNDED RUBBLE, MOD. SiO_2 CEMENT.

STRATIGRAPHIC SECTION B-B'

VERTICAL SCALE 1"=10'

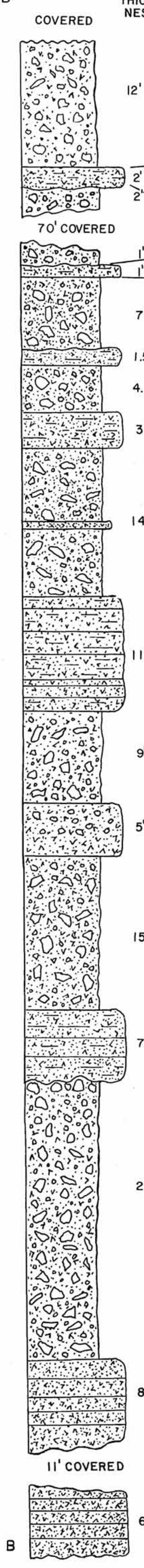

THICKNESS	STRAT. UNIT	DESCRIPTION
12'	17	MUDFLOW, TAN-LT. BROWN(w.) TO GREYBROWN-TAN(f.), COARSE GRAVEL TO FINE GRAIN, V. POOR SORT., TUFFACEOUS MATRIX, MATRIX SUPPORTED, ANG. TO SUBANG., MASSIVE BED, WEATHERS TO SOIL WITH PREDOM. P€ GRANITE MIGMATITE CLASTS FORMING COLLUVIUM, POOR $CaCO_3$ CEMENT.
2'	16	TUFFACEOUS SANDSTONE, TAN-LT. BROWN(w.) TO LT. GREY WHITE(f.), MED. TO V. FINE GRAIN., MOD. SORT WITH RELIC PUMICE FRAGS., SUBANG-SUBRND., MASSIVE WITH PARALLEL BED OF 10-30cm, JOINTS PERPENDICULAR AND PARALLEL TO BEDS, WEATHERS TO BLOCKY RUBBLE, POOR SiO_2 CEMENT.
2' / 1'	15	MUDFLOW, SIMILAR TO UNIT 17, ONLY UPPER 2' AND LOWER 1' ARE EXPOSED, REMAINING SECTION IS COVERED BY COLLUVIUM.
1'	14	TUFFACEOUS SANDSTONE, SIMILAR TO UNIT 16
7'	13	MUDFLOW, SIMILAR TO UNIT 17
1.5'	12	TUFFACEOUS SANDSTONE, SIMILAR TO UNIT 16
4.5'	11	MUDFLOW, SIMILAR TO UNIT 17
3'	10	TUFFACEOUS SANDSTONE, SIMILAR TO UNIT 8
14.5'	9	MUDFLOW, SIMILAR TO UNIT 3
11'	8	TUFFACEOUS SANDSTONE, BUFF WHITE(w.) TO LT. GREY WHITE(f.), COARSE TO FINE GRAIN, MOD. TO POOR SORT., SUBANG., ABUND. PUMICE, PARALLEL LAM. BEDS 1-3cm THICK, NORMAL AND REVERSE GRADED BEDS, JOINTS PERPENDICULAR AND PARALLEL TO BEDS, WEATHERS TO TABULAR RUBBLE, POOR $CaCO_3$ CEMENT.
9'	7	MUDFLOW, SIMILAR TO UNIT 3
5'	6	TUFFACEOUS SANDSTONE, WHITE-TAN(w.) TO GREY WHITE(f.), FINE GRAVEL TO FINE GRAIN, POOR SORT., SUBANG., ABUND. PUMICE, MASSIVE BED>1m, WEATHERS TO BLOCKY RUBBLE AND SMALL P€ GRANITE MIGMATITE CLASTS, MOD. $CaCO_3$ CEMENT.
15'	5	MUDFLOW, SIMILAR TO UNIT 3
7'	4	TUFFACEOUS SANDSTONE, WHITE-TAN(w.) TO BANDED GREY WHITE-TAN(f.), MED.-FINE GRAIN, MOD. SORT., SUBANG.-SUBRND., WEAK ORIENT. OF ELONGATE GRAINS, PARALLEL LAM. BEDS 3-10cm, DEFORMED BEDS DRAPED OVER PROTRUDING P€ CLASTS ARMOURING TOP OF MUDFLOW BENEATH THIS UNIT, JOINT PERPENDICULAR AND PARALLEL TO BEDS, WEATHERS TO BLOCKY RUBBLE, MOD. $CaCO_3$ CEMENT.
27'	3	MUDFLOW, TAN-LT. BROWN(w.) TO LT. TAN(f.), COARSE GRAVEL TO FINE GRAIN, V. POOR SORT., TUFFACEOUS MATRIX, MATRIX SUPPORTED, ANG.-SUBRND., WEAK ORIENT. OF CLASTS, MASSIVE BED>1m, WEATHERS TO SOIL WITH P€$_4$ GRANITE MIGMATITE CLASTS FORMING UNIFORM COLLUVIUM, MOD. $CaCO_3$ CEMENT.
8'	2	TUFFACEOUS SANDSTONE, LT. BROWN-TAN(w.) TO BANDED GREY WHITE(f.), COARSE TO FINE GRAIN, POOR SORT., SUBANG.-SUBRND., ABUND. PUMICE, MOD. ORIENT. INTERBEDDED SAND AND PUMICE LAYERS, PARALLEL LAM. BEDS 3-10cm, JOINTS PERPENDICULAR AND PARALLEL TO BEDS, WEATHERS TO TABULAR RUBBLE, POOR SiO_2 CEMENT.
6'	1	TUFFACEOUS SANDSTONE, SIMILAR TO UNIT 2

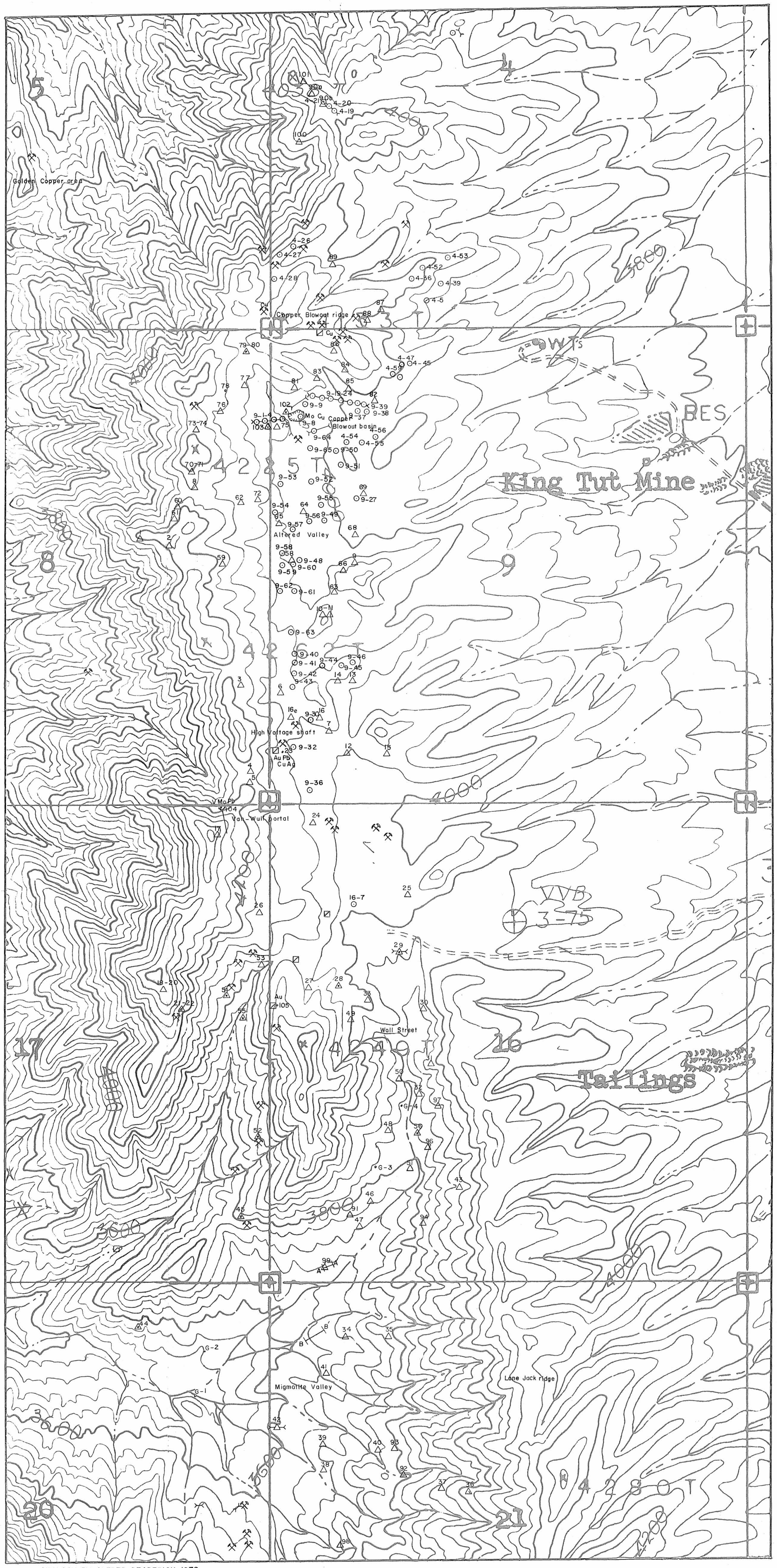

GEOLOGY BY ALFRED DEADERICK, 1978